

TA7

CG

CER 61-76

copy 2

SEP 27 1973

SSW

FOOTHILLS READING ROOM

SUMMARY PROGRESS REPORT

1 March 1959 to 1 December 1961

Prepared For: U. S. Department of Health, Education
and Welfare
Public Health Service
National Institute of Health

Grant Number: RG-6438 or AP-91
RG-6438 (C1) or AP-91 (C1)
RG-6438 (C2) or AP-91 (C2)

Title of Project: Wind Tunnel Modeling of Atmospheric
Diffusion

Principal Investigators: J. E. Cermak
L. V. Baldwin

Colorado State University
Fort Collins, Colorado

ENGINEERING RESEARCH
AUG 11 1971
FOOTHILLS READING ROOM

CER61JEC76

SUMMARY PROGRESS REPORT

1 March 1959 to 1 December 1961

Prepared For: U. S. Department of Health, Education
and Welfare
Public Health Service
National Institute of Health

Grant Number: RG-6438 or AP-91
RG-6438 (C1) or AP-91 (C1)
RG-6438 (C2) or AP-91 (C2)

Title of Project: Wind Tunnel Modeling of Atmospheric
Diffusion

Principal Investigators: J. E. Cermak
L. V. Baldwin

Colorado State University
Fort Collins, Colorado

CER61JEC76



018401 0593314

LIST OF FIGURES

<u>Figure</u>	<u>Title</u>
2 - 1	Plan of wind tunnel.
2 - 2	Test section geometry.
2 - 3	Details of source and sampling probe.
2 - 4	Feed and sampling system.
2 - 5	Plume cross section at $H = 1 \text{ in.}$, $X = 4 \text{ ft.}$
2 - 6	Vertical velocity profiles.
2 - 7	Typical temperature distribution.
2 - 8	Effect of source elevation on boundary concentrations.
2 - 9	Plume spread geometry.
2 - 10	Effect of source elevation on location of core.
2 - 11	Concentration attenuation along axis through source $Z = H$, $Y = 0$.
2 - 12	Effect of source elevation on maximum core concentration.
2 - 13	Attenuation of boundary concentrations.
2 - 14	Variation of $\bar{U}_a C_{\max}$ with distance from gas source: $\Delta T = 0$, $H = 0$.
2 - 15	Variation of σ with ambient velocity and distance from gas source: $\Delta T = 0$, $H = 0$.
2 - 16	Variation of η with ambient velocity and distance from gas source: $\Delta T = 0$, $H = 0$.
2 - 17	Concentration distribution for equivalent line source plume obtained by integrating the point source data.
3 - 1	Proposed roughness elements for studying diffusion over a rough surface.
5 - 1	New Aerodynamic Laboratory floor plan.
5 - 2	View of building of new Aerodynamic laboratory under con- struction.
5 - 3	View of steel framework being installed for new wind tunnel under construction.

TABLE OF CONTENTS

	Page
I. INTRODUCTION	1
II. DETAILED INVESTIGATIONS	2
A. Objectives.	2
B. Procedure.	2
C. Analysis	3
1. First Phase of Experimental Study	4
(a) Boundary Concentration Attenuation	4
(b) Plume Geometry	5
(c) Location of the Core Zone.	6
(d) Concentration Attenuation	6
(e) Maximum Core Concentration	7
(f) Comparison with Theoretical Solutions of Yih and Sutton	7
(g) Evaluation of Diffusivities.	7
2. Second Phase of Experimental Study	8
III. REMAINING PROGRAM.	10
IV. PERSONNEL	11
V. FUTURE RESEARCH.	12

I. INTRODUCTION

This report summarizes progress on "The Wind Tunnel Modeling of Atmospheric Diffusion" for the period 1 March 1959 to 1 December 1961. The report supplements the previous progress reports dated 15 December 1959 and 16 December 1960; it is submitted in conjunction with the application for research grant (AP-91-C-3) dated October 28, 1961.

II. DETAILED INVESTIGATIONS

A. Objectives

During the period of this research grant, the experimental study of diffusion from a point source in a turbulent boundary layer has been conducted in two phases.

The first phase pertained to the effect of source elevation on the downwind plume geometry and concentration distributions for a smooth, isothermal boundary layer flow at one Reynolds number. The basic objectives during this part of the work was to map the diffusion field for various source elevations. The data obtained was semi-empirically analyzed to show the effect of the changing variable, i. e. the source elevation. The basic data obtained also was used to check theoretical models of diffusion and related mathematical formulations in the light of different hypotheses.

The second phase of the experimental study performed during this grant period was a study of the effect of varying the flow Reynolds number and the plate-ambient air temperature difference on the concentration field downwind of a point source located on the boundary. The immediate objectives were the measurement of the mean concentration distribution, the mean velocity distribution, the mean temperature distribution and the distribution of the heat flux through the heated plate for various flow conditions. The data obtained are being analyzed now.

B. Procedure

The studies to date have all been conducted in a low velocity recirculating wind tunnel having a 6 x 6 ft. by 28 ft. long test section. The physical features of the wind tunnel used are outlined in Fig. 2-1. The wind tunnel had an air-drive system capable of varying the ambient air speeds over a range of 1 - 60 ft. per sec. This permitted the variation

of flow Reynolds number over a wide range.

The test-section geometry and boundary features are shown schematically in Fig. 2-2. The boundary consisted of a 1/2 in. thick aluminum plate mounted flush with the floor of the tunnel. This plate could be heated by means of nichrome heating coils mounted directly below the plate and running across the full width of the tunnel. With this arrangement thermal stratifications of the flowing air, for a wide range of stability, could be attained.

Anhydrous ammonia gas was emitted from a source, shown in Fig. 2-3, located within the artificially stimulated boundary layer generated on the floor of the tunnel. Downstream concentrations were measured by obtaining samples of the air-gas mixture and determining the amount of ammonia present by colorimetric analysis. The sampling system is shown schematically in Fig. 2-4.

The mean velocity distributions were measured using a constant-temperature mean velocity hot-wire anemometer. The sensing element consisted of a 0.4 inch length of a 0.001 inch diameter platinum wire.

The mean temperature of the air was measured with a copper-constantan thermocouple 0.001 inch in diameter. The temperature was read on a single-point strip chart recorder.

The heat flux through the plate was estimated by measuring the current through and the voltage across each of the nichrome heating coils.

A typical gas plume cross-section, mean velocity and mean temperature profile are shown in Figs. 2-5, 2-6 and 2-7 respectively. These figures define some of the nomenclature to be used throughout this discussion.

C. Analysis

In this section the significant conclusions of the first phase of this experimental study are discussed and summarized (details are reported in the Ph.D. dissertation of Mr. K. S. Davar, Ref. 2-1). The results of the

preliminary analysis of the data obtained during the second phase of this study are also presented.

1. First Phase of Experimental Study:

The first phase of the study was conducted at an ambient velocity of 6 fps over a smooth unheated boundary. The depth of the boundary layer at the source was 3 in.; the height of the point source was varied from $H = 1/16$ in. to 5 in.

The analytical objectives of the first phase of the experimental study can be divided as follows:

- 1) To establish an empirical law for describing the build-up and attenuation of downwind concentrations on the boundary for varying source elevations.
- 2) To study the effect of source elevation on the plume spread geometry, on the location of the core zone of the diffusing plume, on the concentration attenuation along an axis through the source and on the maximum core concentration.
- 3) To check the theoretical models of diffusion of Yih (Ref. 2-2) and Sutton (Ref. 2-3) by means of the data obtained during this study.
- 4) To determine the form and the magnitude of the diffusivities from the turbulent diffusion equation assuming the eddy diffusivity model in analogy with heat conduction.

(a) Boundary Concentration Attenuation

The experimental equation for attenuation of boundary concentrations (smooth, isothermal boundary layer) was obtained as $C \sim X^{-1.47}$ for $H = 0$. Up to $H/\delta_f = 0.167$ the equation of attenuation was nearly the same, but concentrations were lower. For $H/\delta_f \geq 0.33$ the concentrations are considerably lower than for a ground level source for short distances; they rise to a peak value and then decrease with a trend which appeared the same as for $H/\delta_f = 0.167$. No data was obtained

to conclusively verify this trend due to the short length of the test-section. Nevertheless Fig. 2-8 shows that at least up to $H/\delta_f = 0.33$ the ground concentration asymptotically approaches the curve for $H=0$ for large distances.

(b) Plume Spread Geometry

Fig. 2-9 shows some typical curves for the maximum plume spread in the lateral direction and in the vertical plane through the center line for various vertical sections normal to the mean flow direction.

An examination of the vertical spread profiles indicates that the vertical plume geometry can be generally divided into three distinct regions, irrespective of source elevation within the boundary layer. These regions are approximately

- a) X/δ_f from 0 to 4 ($X = 0$ to 1 ft.) - nearly linear spread regime,
- b) X/δ_f from 4 to 16 ($X = 1$ to 4 ft.) - transition regime,
- c) $X/\delta_f > 16$ ($X > 4$ ft.) - established approximately asymptotic spread regime.

The plume spread in the vertical direction results from various factors. These are: 1) convective deformation due to the mean-velocity gradient; 2) transverse diffusion by turbulence; 3) the boundary acting as an impermeable barrier below the plume; 4) the intermittency effect at the upper part of the boundary layer; and 5) molecular effects very close to the boundary.

The various regimes of the spread are caused by one or more of the above factors being more pronounced than others. For regime (a) neither the effects of convective deformation nor those due to anisotropic diffusion are significant because the time for spread is relatively small. For regime (b) the combined effects of convective shear deformation and turbulent diffusion are very pronounced. For lower elevations the effect of boundary interference with plume spread are evident, and for the higher elevations, deformation is influenced due to the presence of the free boundary

of the boundary layer. For regime (c), the effects of convective deformation and turbulent diffusion are gradual, and an asymptotic rate of plume growth appears to have been achieved, except when the growing plume encounters the free boundary of the boundary layer.

(c) Location of the Core Zone

The vertical movement of the core zone of the plume, with respect to the source elevation, is presented in Fig. 2-10; here, Z_* is measured to the center of the zone of maximum concentrations, in vertical cross-sections normal to the mean flow direction.

The downward drift of the core zone for H/δ_f up to 0.33, as indicated in Fig. 2-10, is due primarily to the strong shearing-deformation action of the gradient of mean velocities. With the source located at $H/\delta_f = 0.116$ the core zone is close to the boundary and expanding; thus Z_* has necessarily to increase with the enlargement of the core. The same observations hold for $H/\delta_f = 0.33$ after the core encounters the boundary. For $\delta_f/3 < H < \delta_f$, the effect of shear deformation is diminishing, and turbulence is approaching isotropy; the plume core tends to expand uniformly and $Z_* = H$. When $H/\delta_f = 1.0$, the plume enters the zone of intermittency and tends to be lifted up, probably due to large eddies intermittently breaking away upward from the outer edge of the boundary layer.

Thus it may be concluded that by keeping the source elevation above $H/\delta_f = 0.33$, it should be possible to greatly delay the spread of the plume towards the boundary.

(d) Concentration Attenuation Along Axis Through Source

For elevated sources, it is sometimes necessary to know the equation of attenuation for concentrations along an axis through the source ($Z = H, Y = 0$). This comparison is made in Fig. 2-11. For $H = 0, 1/2, 1, 2, \text{ and } 3 \text{ in.}$, the rate of attenuation is nearly the same, except close to the source.

(e) Maximum Core Concentration

Fig. 2-12 shows the effect of the source elevation on the maximum core concentrations. The maximum concentration C_{\max} is very sensitive to the parameter H/δ_f for small distances ($X/\delta_f = 4$). As long as $H/\delta_f < 1$ the variation of C_{\max} with H/δ_f becomes insignificant for large distances ($X/\delta_f > 30$). Thus it may be concluded that the gas 'forgets' its initial distribution as it is swept downwind.

(f) Comparison with the Theoretical Solutions of Yih and Sutton

Fig. 2-13 compares the experimental data of boundary concentration attenuation (source at boundary) to the theoretical laws obtained by Yih and Sutton. All three curves are in the form of power laws although the exponents are quite different -- $C \sim X^{-1.9}$ for Yih's solution, $C \sim X^{-1.39}$ for Sutton's solution and $C \sim X^{-1.47}$ for the experimental law obtained in this study.

(g) Evaluation of Diffusivities

An attempt was made to evaluate the lateral diffusivities (A_l) by numerically integrating the diffusion equation

$$\bar{U}_1 \frac{\partial \bar{C}}{\partial X_1} + \bar{U}_3 \frac{\partial \bar{C}}{\partial X_3} = \frac{\partial}{\partial X_1} \left[A_X \frac{\partial \bar{C}}{\partial X_1} \right] + \frac{\partial}{\partial X_2} \left[A_l \frac{\partial \bar{C}}{\partial X_2} \right] + \frac{\partial}{\partial X_3} \left[A_V \frac{\partial \bar{C}}{\partial X_3} \right]$$

with the following assumptions:

a) $\bar{U}_3 \frac{\partial \bar{C}}{\partial X_3}$ negligible compared to $\bar{U}_1 \frac{\partial \bar{C}}{\partial X_1}$.

b) $\frac{\partial}{\partial X_1} \left[A_X \frac{\partial \bar{C}}{\partial X_1} \right]$ negligible compared to the other terms of the

left hand side of the above equation.

c) The variation of A_V identical in distribution and magnitude to that of E_m (eddy viscosity) obtained through turbulence measurements.

The computed A_Z was found to be 10 to 12 times larger than the measured E_m for the same $\frac{Z}{\delta}$. These results do not appear reasonable, and suggest that:

- a) the model of turbulent diffusion represented by the diffusion equation may not completely represent the actual process;
- b) the assumed relationship $A_Z = E_m$ may not be valid for three-dimensional diffusion of mass in a two-dimensional flow field. More work along these lines is now underway. A summary of the work described above is now being prepared for publication.

2. Second Phase of Experimental Study:

During the second phase of the experimental program the following factors were studied:

- 1) The effect of the variation of mean ambient velocity (flow Reynolds number) on the boundary concentration attenuation for gas discharging from a boundary source into a smooth, isothermal boundary layer flow.
- 2) The effect of the mean ambient velocity on the maximum horizontal and vertical spread of the diffusing plume.
- 3) The effect of unstable thermal stratification on the downwind plume geometry and concentration distributions.

The diffusion field was mapped for flow velocities of 6 and 9 ft/sec and plate-ambient air temperature differences of 0°, 100° F and 200° F. The boundary concentration profiles were also obtained for ambient velocities of 15, 25 and 57 ft/sec for the isothermal case.

Figs. 2-14, 2-15, and 2-16 show the experimental plots for the effect of ambient velocity on ground concentration and the maximum vertical and horizontal spread. Fig. 2-14 shows that the maximum ground concentration is universally proportional to the ambient velocity but that the equation of attenuation is independent of the velocity, i. e.

$$C_{\max} = \frac{\text{const}}{\bar{U}_a} X^{-1.47}$$

Figs. 2 - 15 and 2-16 show the maximum horizontal and vertical spread of the diffusing plume. The rate of spread is the same for both the vertical and horizontal directions, although the horizontal spread is larger in magnitude. Thus

$$\sigma = \text{Const.} \frac{X}{(\bar{U}_a X/\nu)^{0.25}},$$

$$\eta = \text{Const.} \frac{X}{(\bar{U}_a X/\nu)^{0.25}},$$

and $\sigma = \text{Const.} \eta$,

where σ and η are the horizontal and vertical scales of the diffusion plume.

The above figures indicate an interesting finding in the sense that both the horizontal and vertical characteristic scales of the diffusion plume are independent of the ambient velocity (at least for the range of these experiments).

The point source data for the isothermal case were integrated to obtain equivalent line source distributions of concentration. This integration was carried out by assuming a Gaussian distribution of concentration in the horizontal for each elevation and distance from the source. The distributions thus obtained were compared with actual line source data gathered in another wind tunnel at Colorado State University and found to be very similar. Fig. 2-17 shows a typical distribution of concentration for the equivalent line source.

Further analysis of the data for the second phase of the program is in progress and will soon be summarized in a Ph.D. dissertation by Mr. R. C. Malhotra.

References:

- 2-1. Davar, K. S. Diffusion from a point source within a turbulent boundary layer. Ph.D. dissertation. Colorado State University, Fort Collins, Colorado. July 1961.

- 2-2. Yih, C. S. Similarity solution of a specialized diffusion equation. Transactions, American Geophysical Union, 33: 356-360, 1952.
- 2-3. Sutton, O. G. Micrometeorology. McGraw-Hill, New York. 1953, 333 p.

III. REMAINING PROGRAM

(December 1, 1961 to March 31, 1962)

Aerodynamically smooth surfaces rarely occur in natural terrain, so in order to obtain quantitative data on the effect of surface roughness, the third phase of the experimental program by Mr. S. Bhaduri has been underway for two months. This program will continue throughout the current contract period.

Very little, if any, experimental work of mass diffusion in turbulent boundary layers flowing over rough surfaces has been published. However, many studies are available on the momentum transfer or drag characteristics of turbulent boundary layers on rough surfaces. This work is summarized by Schlichting (Ref. 3-1), Hama (Ref. 3-2), and Clauser (Ref. 3-3). A study of these summaries led to the choice of two dimensional roughness elements consisting of circular rods fixed on the tunnel floor and placed transverse to the flow. The mean concentration field downstream of the gas source at the surface will be measured for the experimental conditions outlined in Fig. 3-1. These results will be compared with the data of the second phase discussed earlier, where the experimental conditions were similar except for the roughness elements. The mass diffusion data will be correlated in terms of the standard roughness parameters which have been developed for the turbulent momentum boundary layer. If successful, this procedure should enable one to use these wind tunnel data for the prediction of certain aspects of atmospheric mass diffusion within the earth's surface layer under neutrally stable conditions, because micrometeorological data on momentum transfer over rough terrain has usually been correlated in terms of nondimen-

sional roughness parameters developed in laboratory research (e. g. , Ref. 3-4).

References:

- 3-1 Schlichting, H. Boundary layer theory. 4th Ed. , McGraw-Hill, 1960.
- 3-2 Hama, F. R. Boundary layer characteristics for smooth and rough surfaces. Trans. Soc. Naval Architects Marine Engrs. , 62, 333 - 358 (1954).
- 3-3 Clauser, F. H. The turbulent boundary layer. "Advances in Applied Mechanics," Vol. 4, Academic Press (1956).
- 3-4 Panofsky, H. A. and Deland, R. J. Spectra of turbulence in lowest 100 meters. "Advances in Geophysics," Vol. 6, p. 61, Academic Press (1959).

IV. PERSONNEL

In addition to the permanent research staff whose biographical sketches are included in the contract proposal (AP91-C-3), the N.I.H. research grants have supported the following students in their graduate research.

Kersi Davar - Dr. Davar came to us from Bombay, India, and held a Bachelor of Engineering degree from the College of Engineering, Poona, India. From 1956 to 1961, he was a research assistant at Colorado State University where he obtained his M. S. and Ph.D. degrees. He is currently Assistant Professor of Civil Engineering at the University of New Brunswick, Canada.

R. C. Malhotra - Mr. Malhotra has a M. S. degree from Colorado State University and a B. S. degree in Civil Engineering from Oregon State College. He has worked in hydraulic and fluid mechanics research since 1956 as a Graduate Research Assistant at Colorado State University.

S. Bhaduri - Mr. Bhaduri attended the Calcutta University, India, and in addition holds Bachelor of Mechanical Engineering and Bachelor of Commerce degrees from the Jadavpur University in Calcutta. His work experience in India includes a year of industrial engineering and seven years

as instructor and lecturer in technical universities. He has been in university research in this country since 1954, and has Master of Science degrees in Mechanical Engineering from State University of Iowa and in Engineering Science in Fluid Mechanics from Johns Hopkins University.

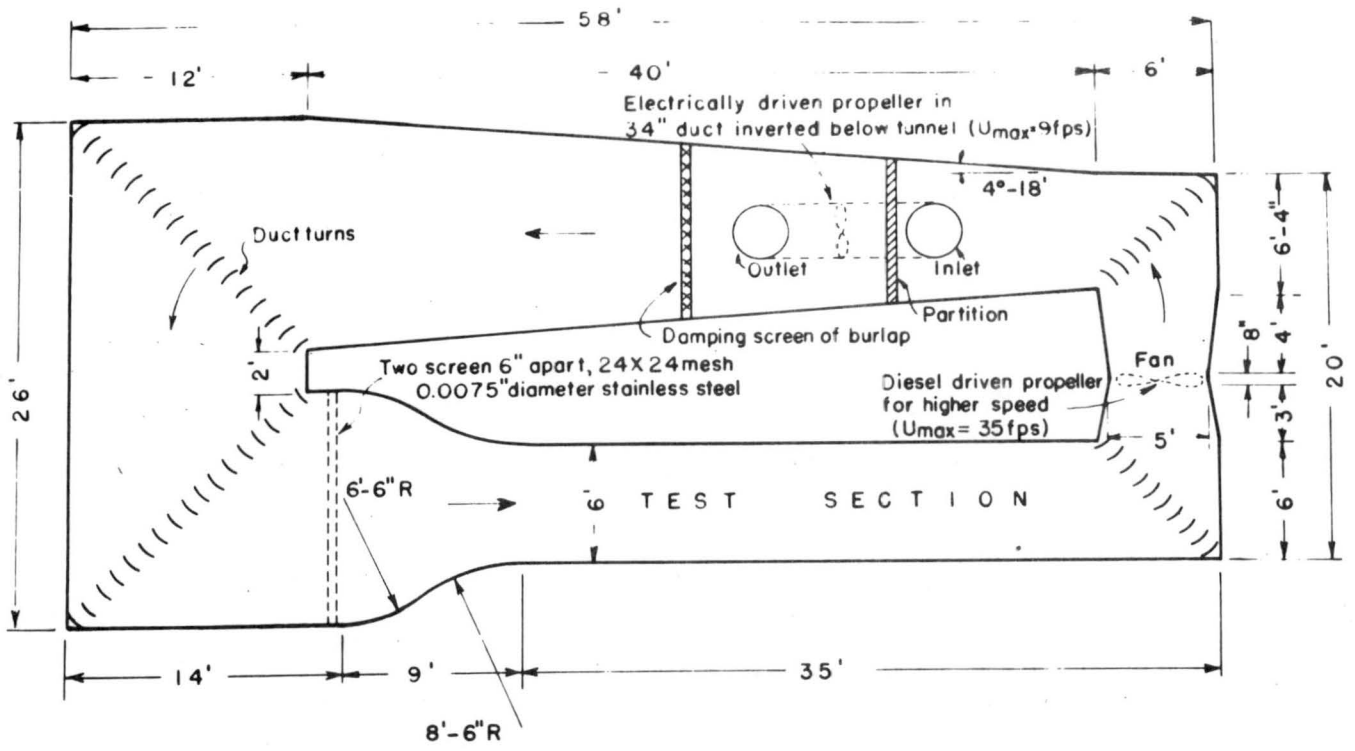
V. FUTURE RESEARCH

Two factors which are important to future progress on the wind tunnel modeling of atmospheric diffusion will be discussed here. Each item is a significant factor in future research capability, although no direct cost to the current N.I.H. contract has been involved.

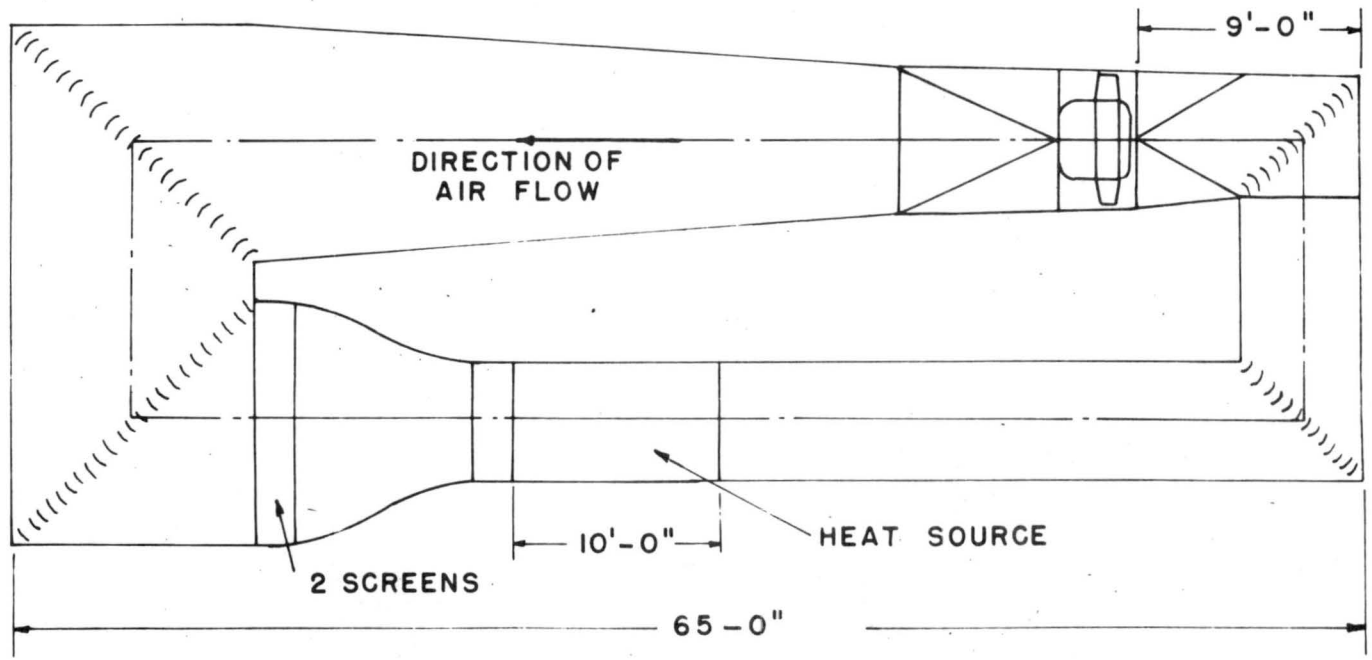
The large wind tunnel facility described on pages 7 and 9 of application AP-91 (C3) is nearing completion. Fig. 5-1 shows a plan view of new Aeromechanics Laboratory Building with two wind tunnels installed. The smaller tunnel has been used in the research to date and it is scheduled for installation in the new building before June 1962. This small tunnel will be modified by the addition of a new drive unit to increase the wind velocity range to 3 to 150 ft/sec. The larger wind tunnel construction has been almost completed in the civil engineering shops and it will be installed by September 1962, and operational by January 1962. Figs. 5-2 and 5-3 show the building and the steel frame support construction now in progress prior to the assembling of the large wind tunnel. This progress on the improvement of physical research facilities, and associated instrumentation discussed in AP-91 (C3), will materially aid the proposed research program.

The second factor is the extension of the original research goals to include some new aspects of wind tunnel modeling which have evolved recently from the statistical theory of turbulence diffusion. This new approach (discussed briefly on page 8 of AP-91 (C3)) will supplement the current program. The work to date seeks to model the turbulent diffusion by controlling the external boundary conditions of the flow which influence the turbulent field, e. g. , the surface temperature gradient and surface roughness.

The application of model data to field conditions using this approach would follow from dimensionless data correlations involving not only the two effects mentioned above, but also parameters related to aerodynamic similarity such as a turbulent Reynold's number. Work along these lines will continue. In addition the new approach will be taken to relate the turbulent diffusion of heat and mass to the turbulent statistical properties which can be measured by hot-wire anemometers in the laboratory. Then, using similar anemometer data from published field studies, the diffusive characteristics of atmospheric turbulence might be predicted. For homogeneous turbulent flow fields, this approach has been successful. The enclosed preprint of the technical paper entitled "The Experimental Relation Between Turbulent Diffusion and Hot-Wire Anemometer Measurements" discusses this procedure in detail. The extension of these empirical relations between Eulerian and Lagrangian statistical properties of turbulence to shear flows will be a long range goal of the proposed research. Some hint that this extension might be successful is provided by the work of F. H. Clauser, who was able to describe much of the turbulent momentum boundary layer by using the concept of an eddy diffusivity.



PRESENT SMALL WIND TUNNEL



FUTURE SMALL WIND TUNNEL

FIG. 2-1 SMALL WIND TUNNEL LAYOUT

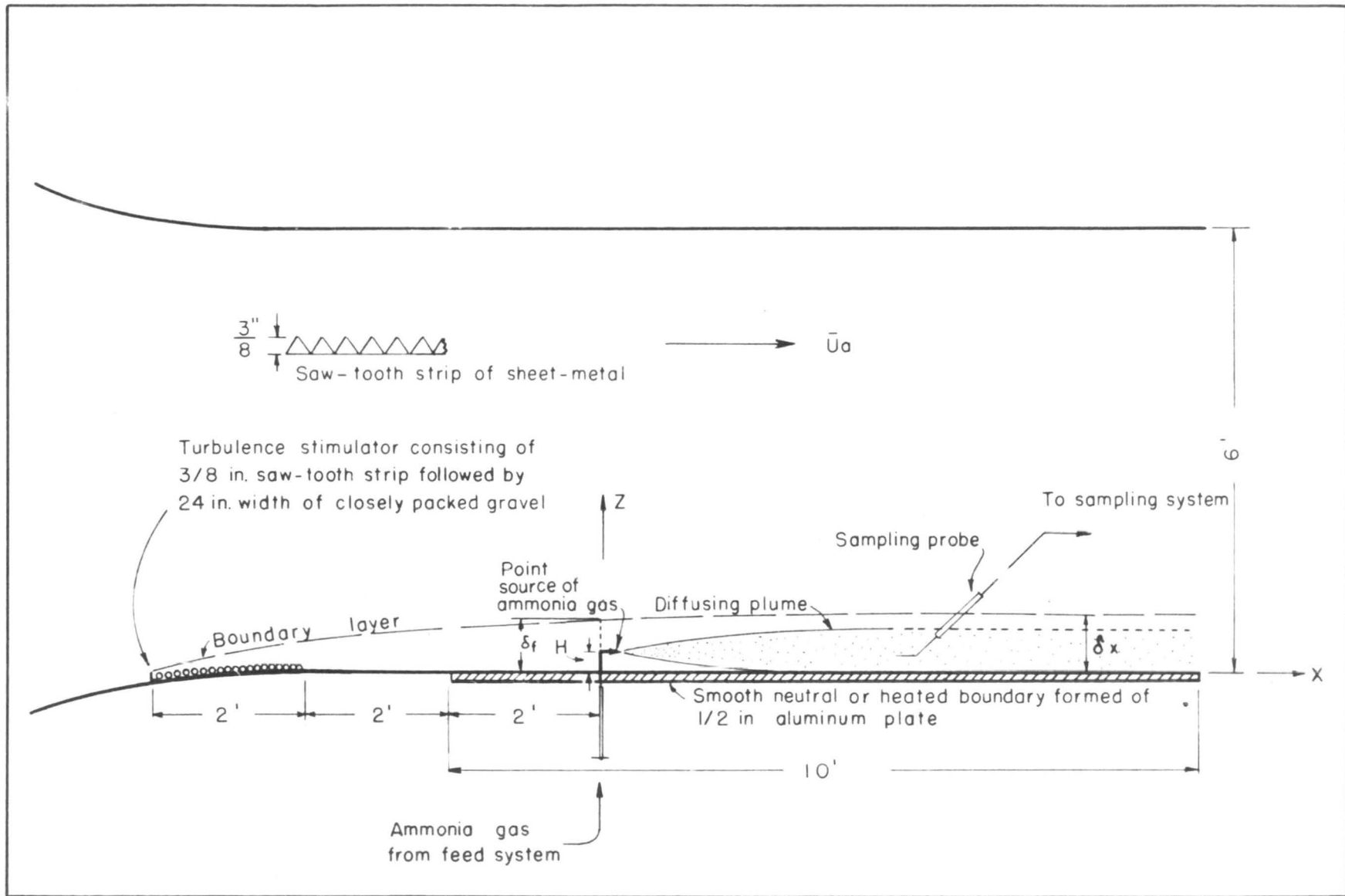
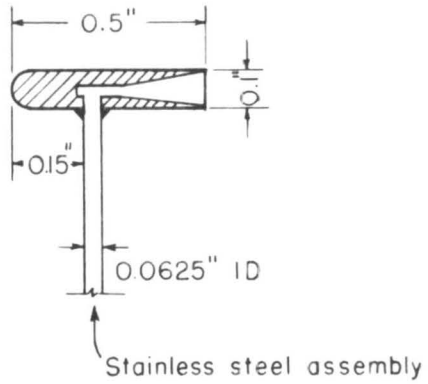
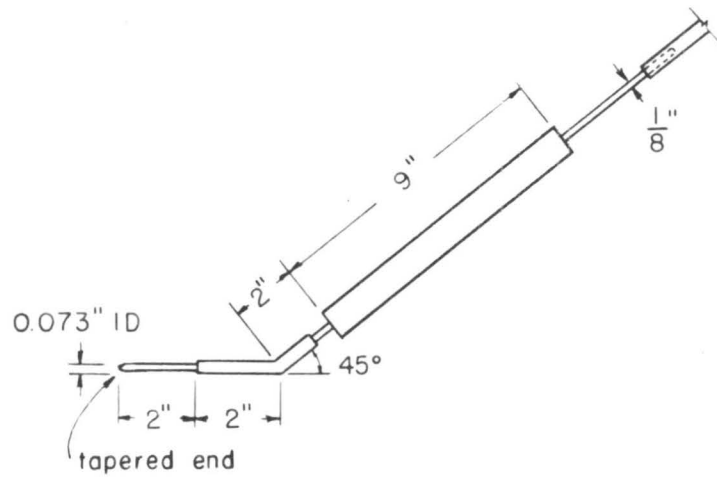


FIG. 2-2 TEST SECTION GEOMETRY



(a) SOURCE



(b) SAMPLING PROBE

FIG. 2-3 DETAILS OF SOURCE AND SAMPLING PROBE

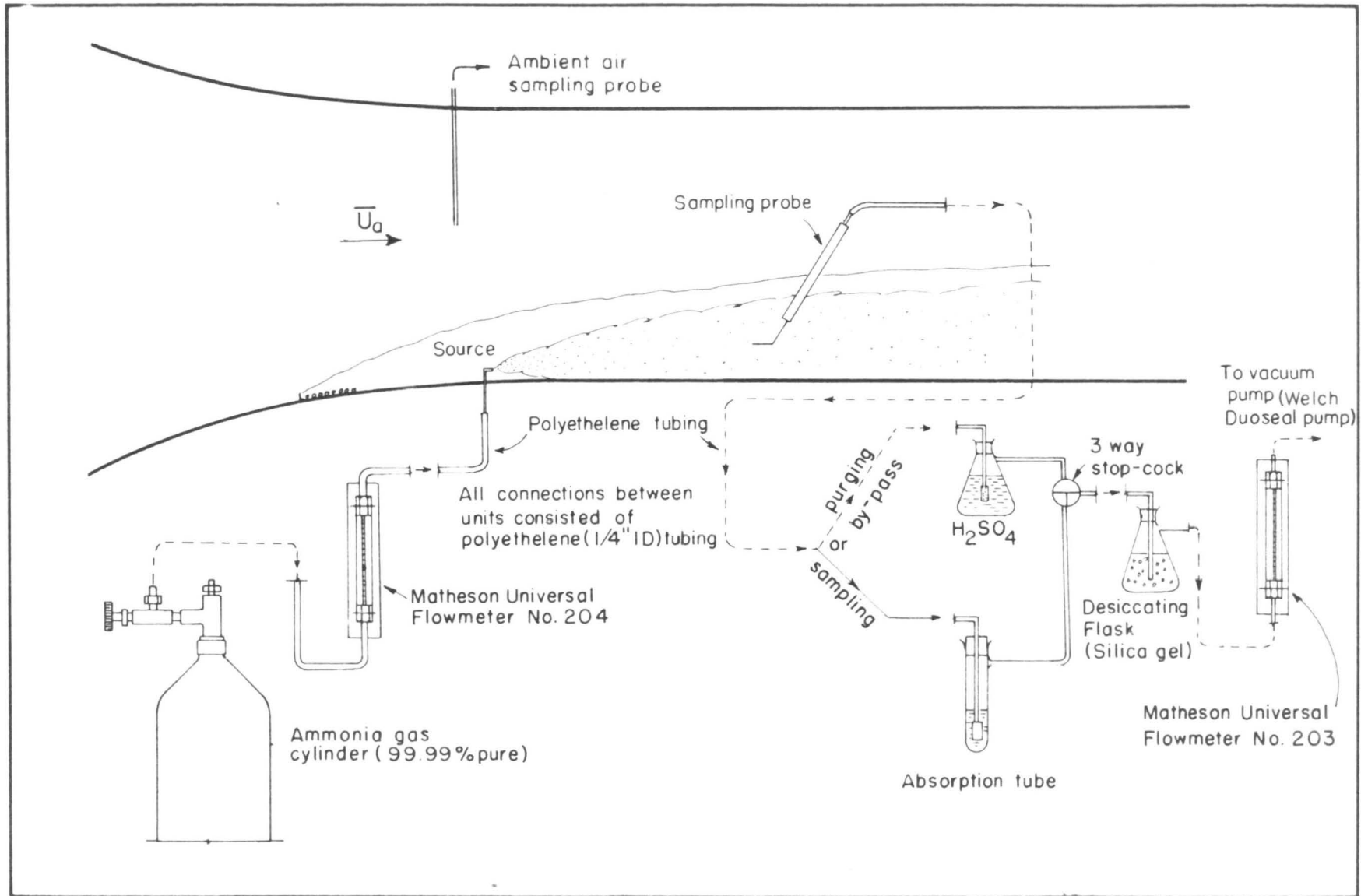


FIG. 2-4 FEED AND SAMPLING SYSTEM

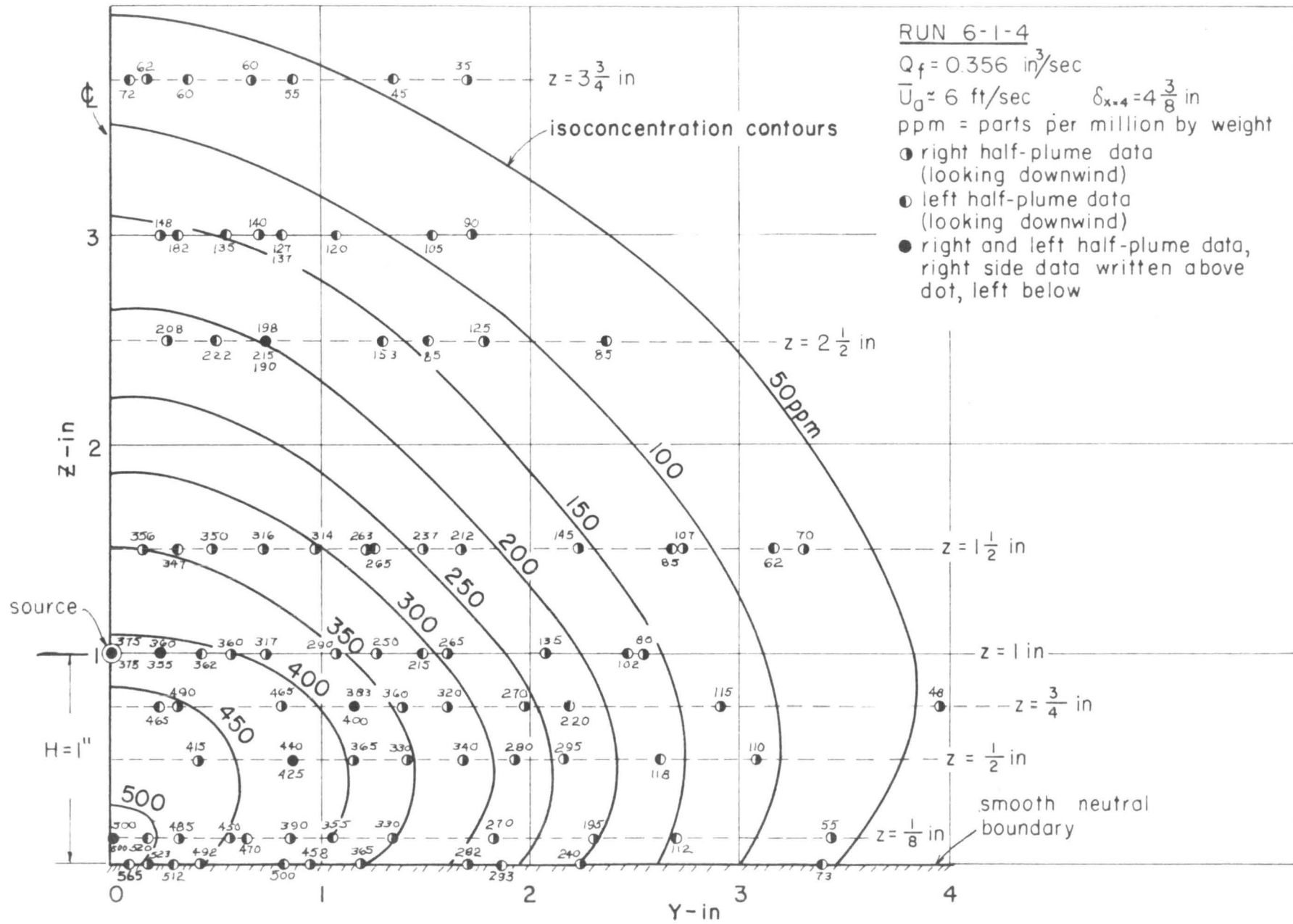


FIG. 2-5 PLUME CROSS SECTION AT H=1 in, X=4 ft

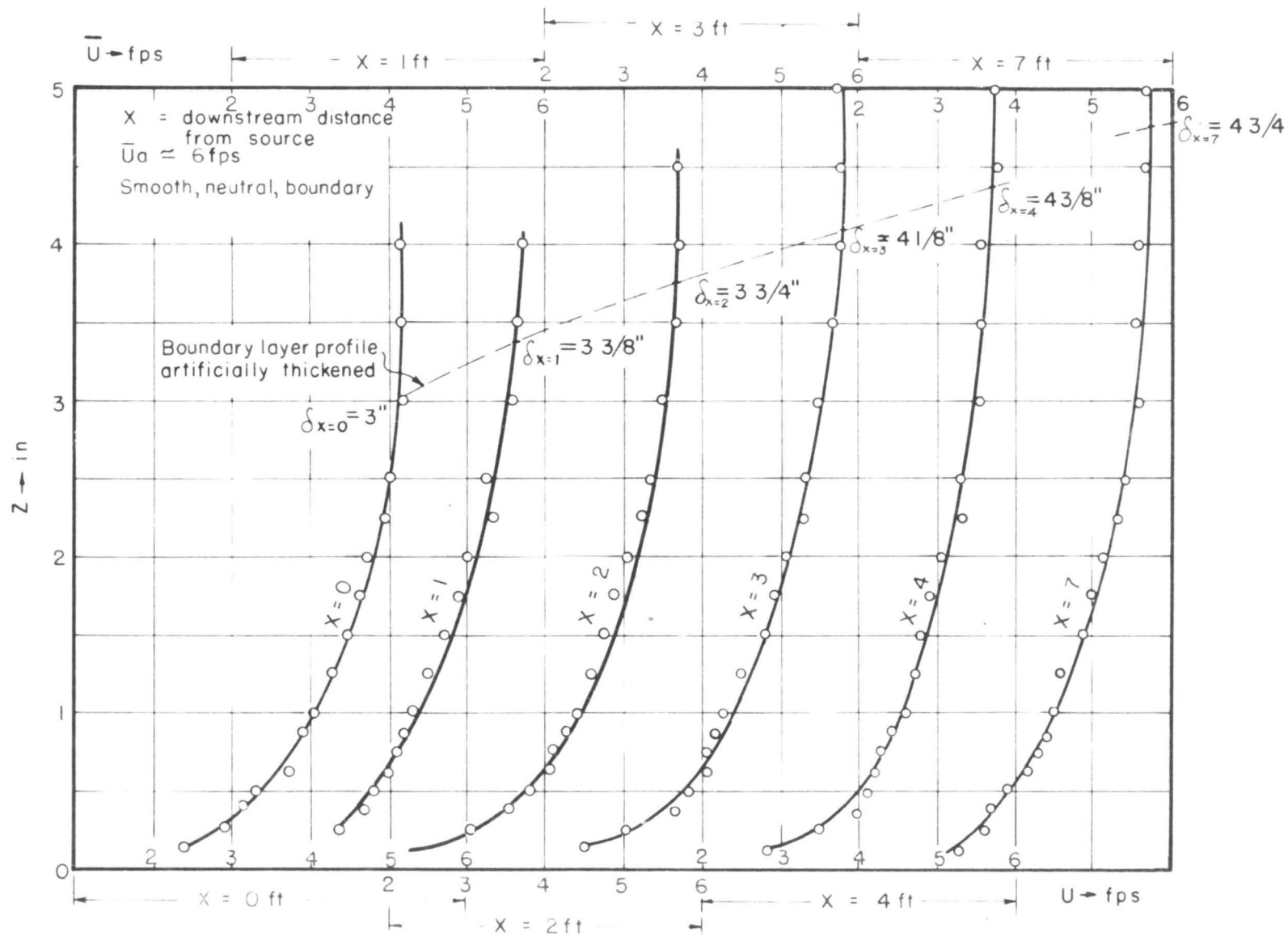


FIG. 2-6 VERTICAL VELOCITY PROFILES ($X = 0, 1, 2, 3, 4, 7$ ft)

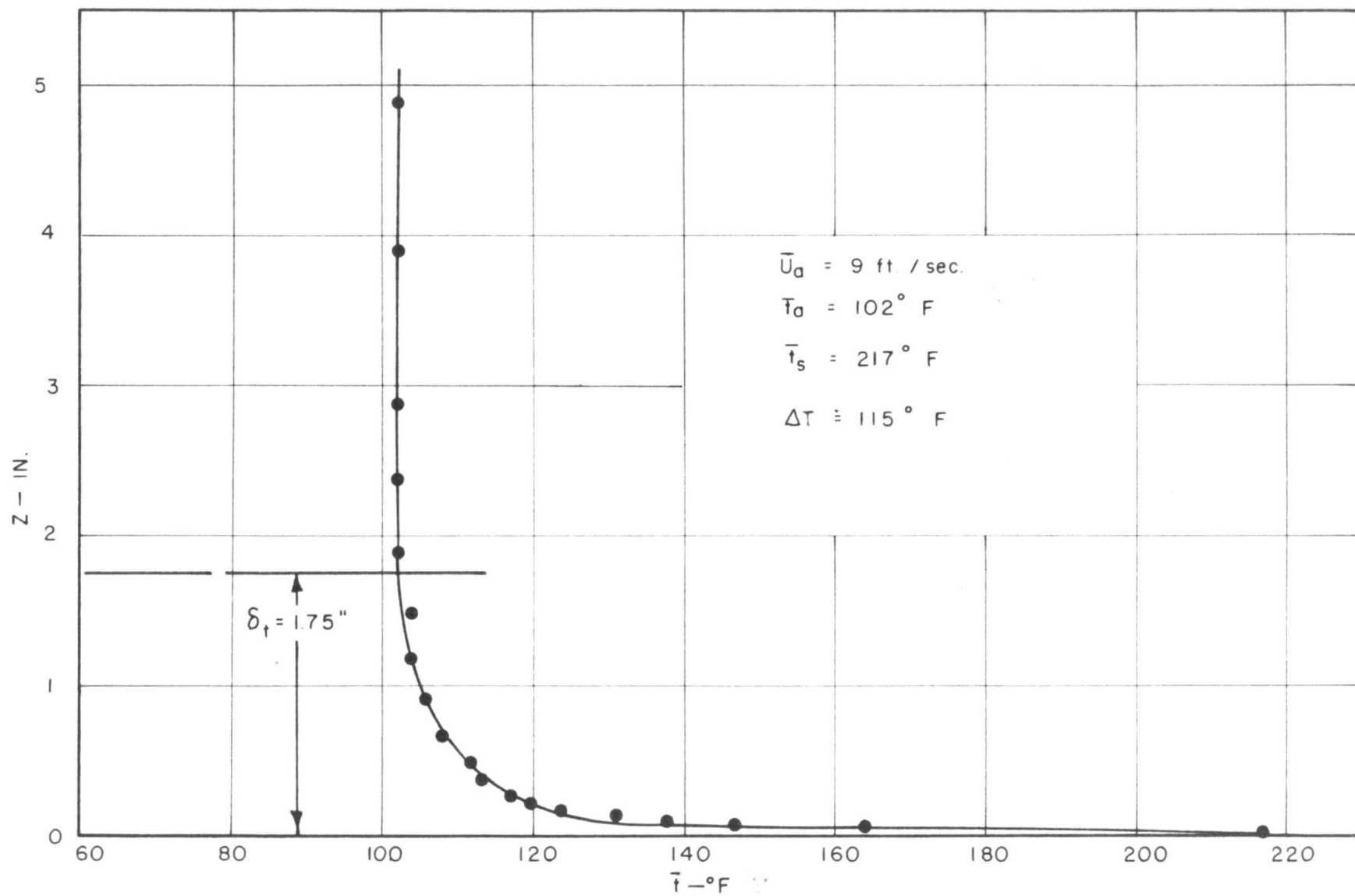


FIG. 2-7 TYPICAL TEMPERATURE DISTRIBUTION — $\Delta T = 115^\circ \text{ F}$
 (AT LOCATION OF GAS SOURCE)

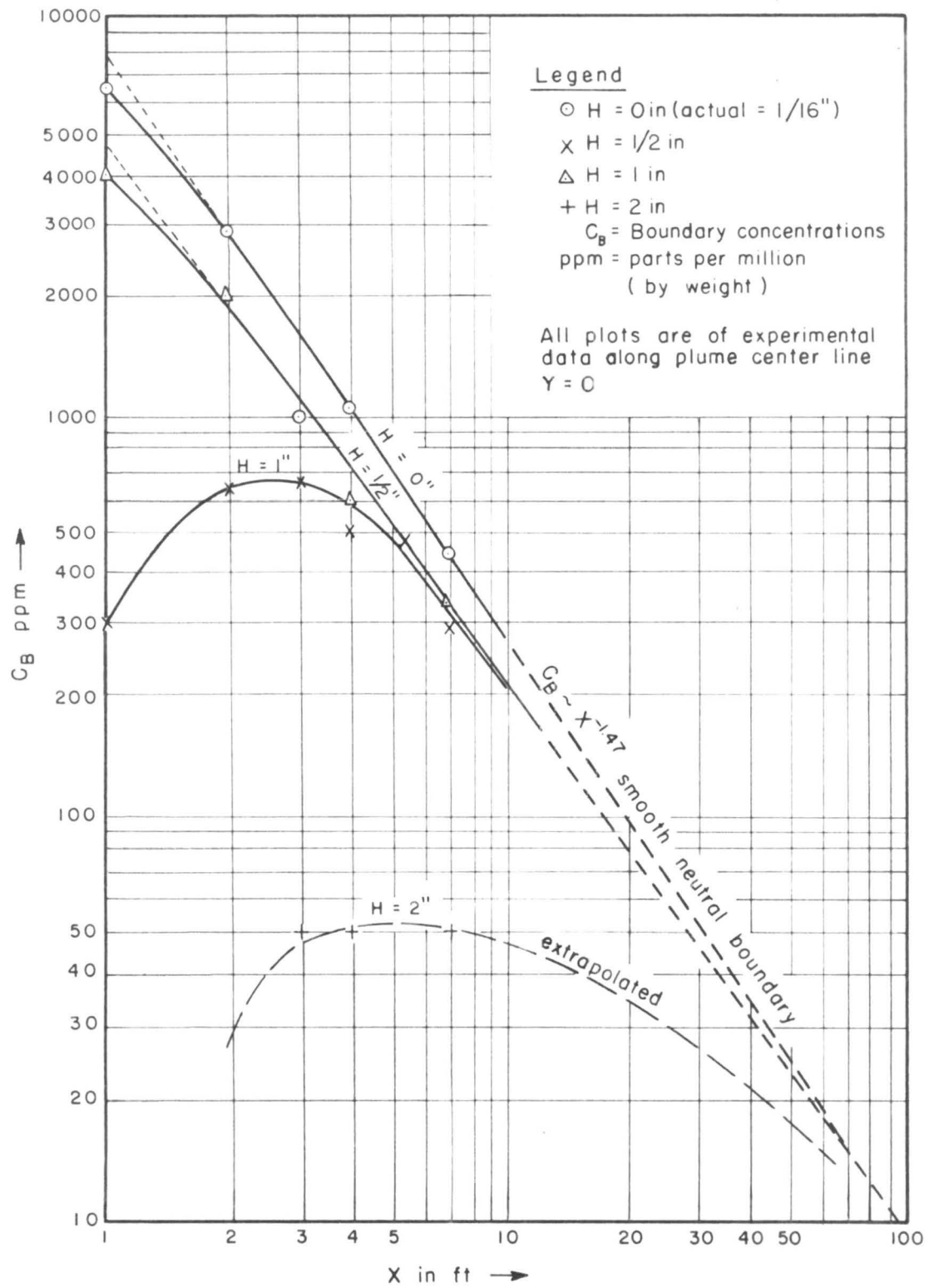


FIG.2-8 EFFECT OF SOURCE ELEVATION ON BOUNDARY CONCENTRATIONS

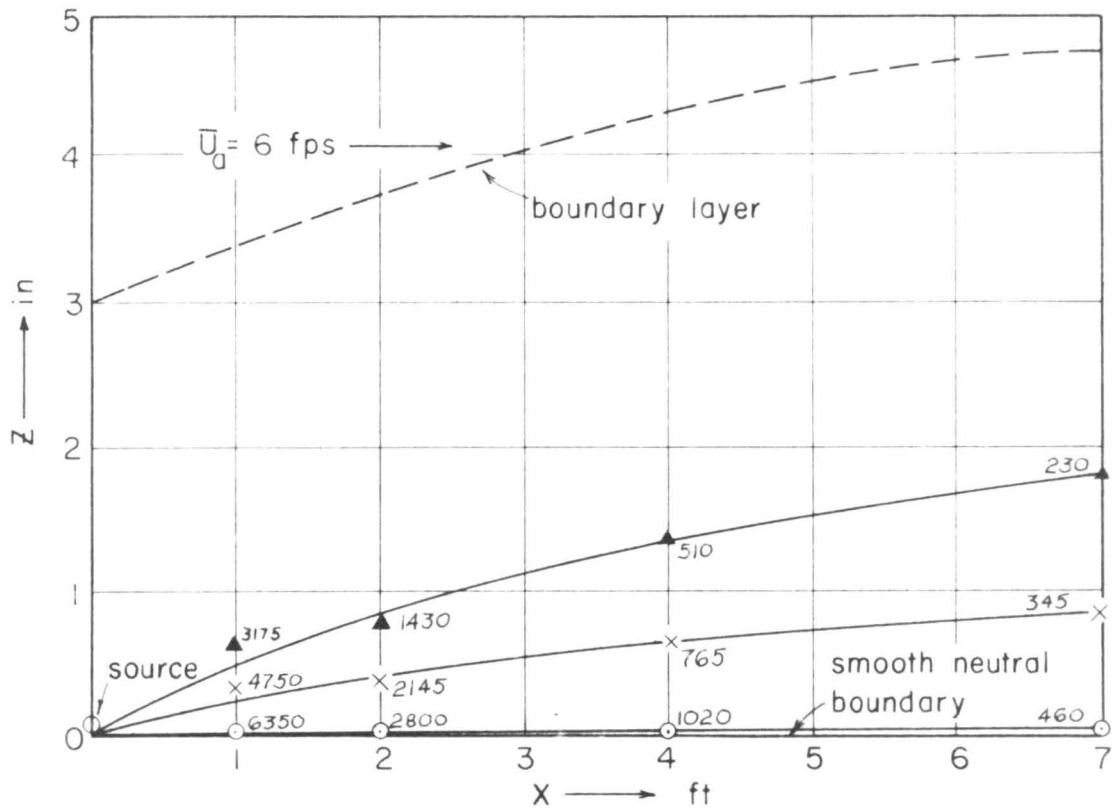
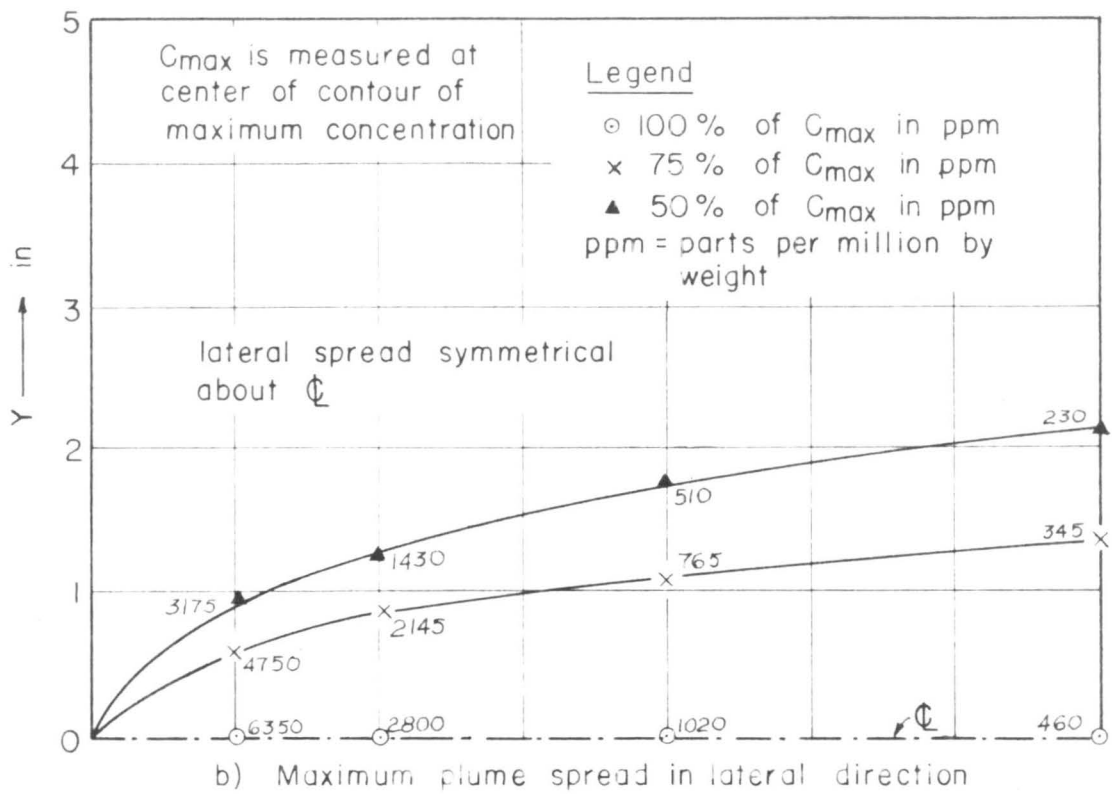


FIG. 2-9(i) PLUME SPREAD GEOMETRY, $H = 0$ in

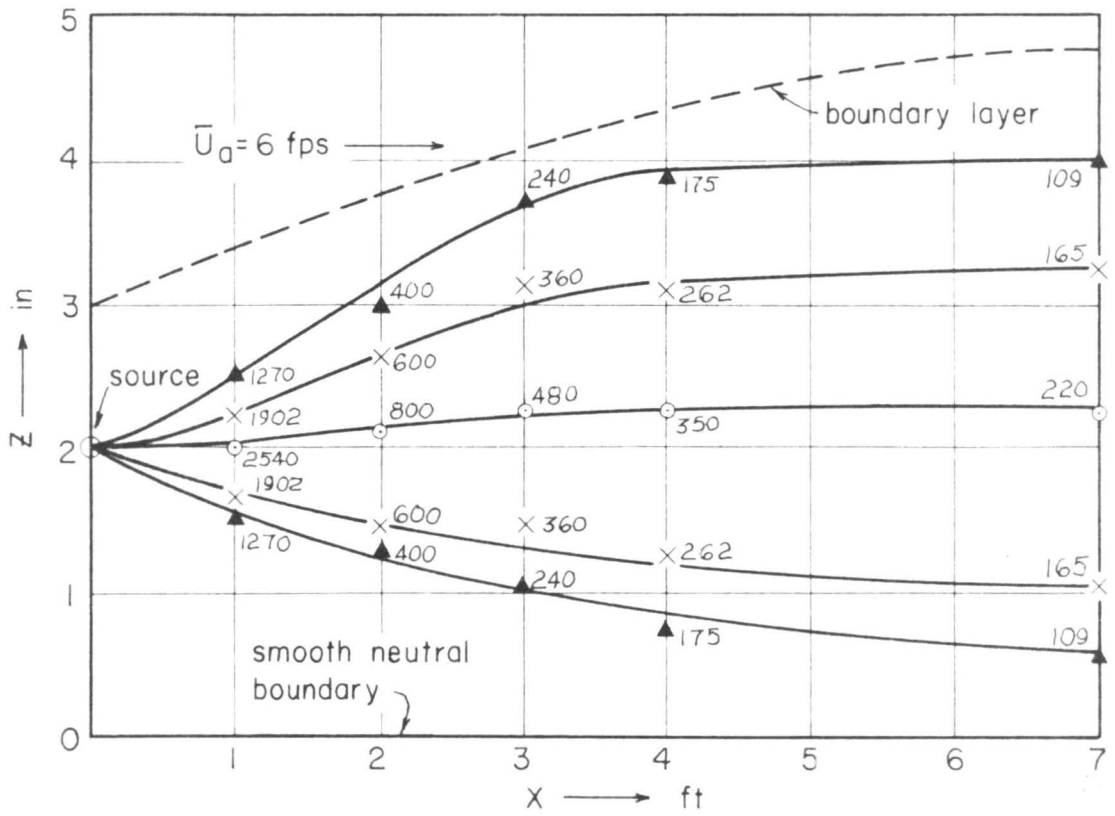
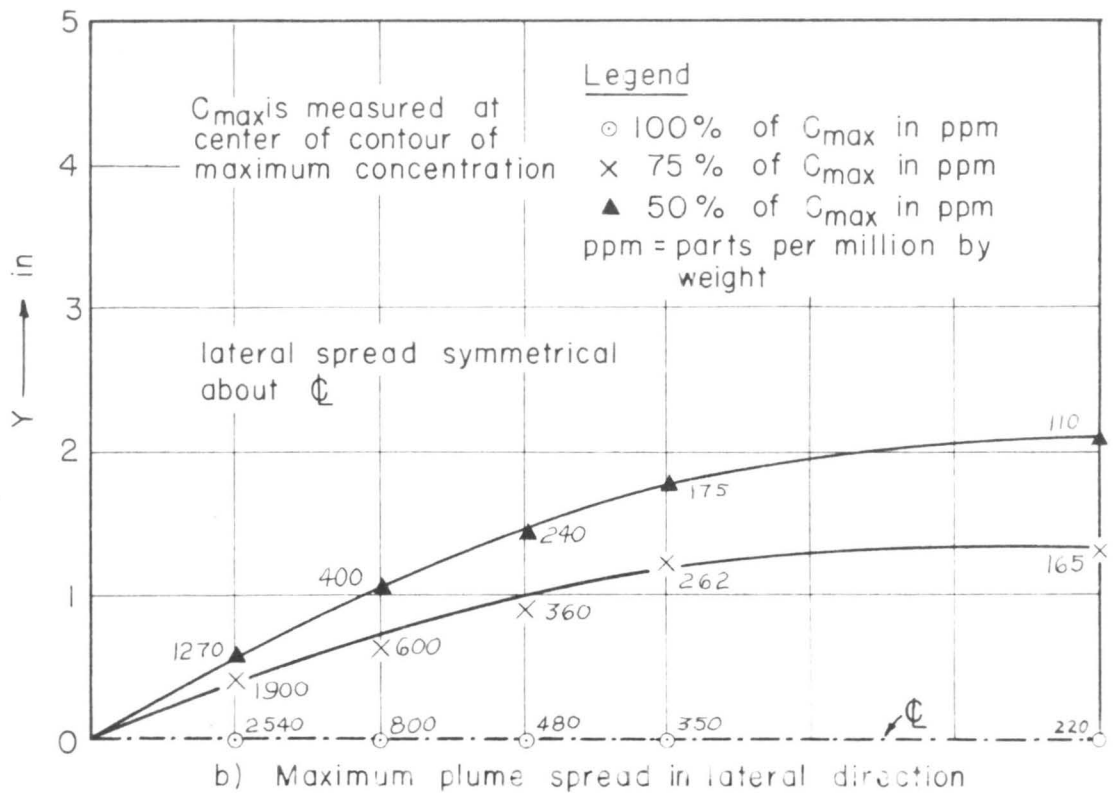
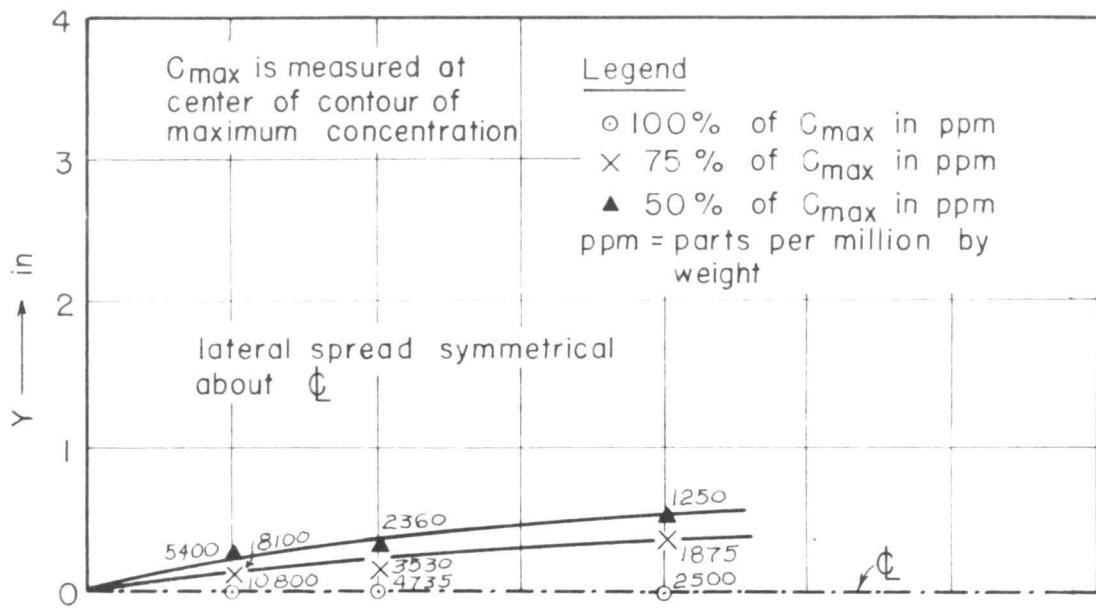
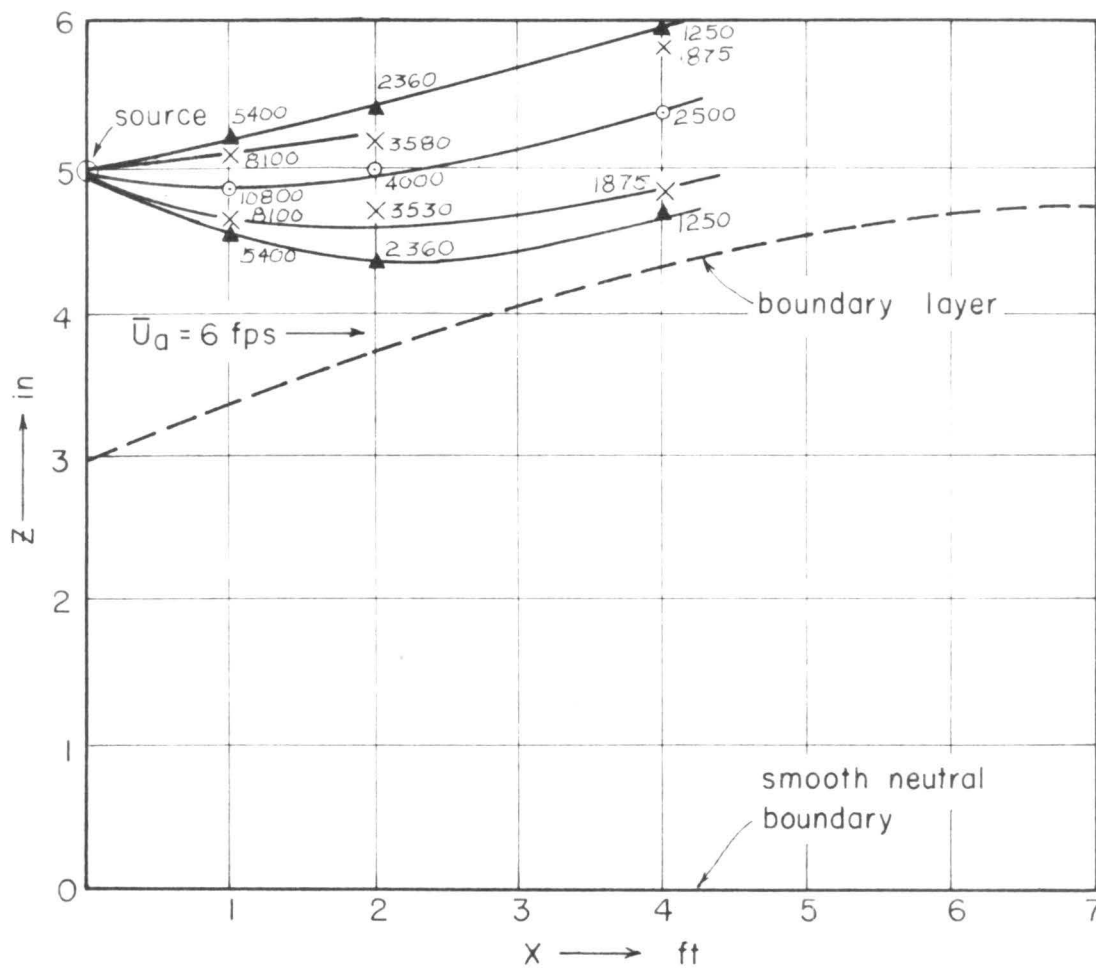


FIG. 2-9(ii) PLUME SPREAD GEOMETRY, $H = 2 \text{ in}$



b) Maximum plume spread in lateral direction



a) Plume spread in vertical plane through center line

FIG. 2-9(iii) PLUME SPREAD GEOMETRY, $H = 5$ in

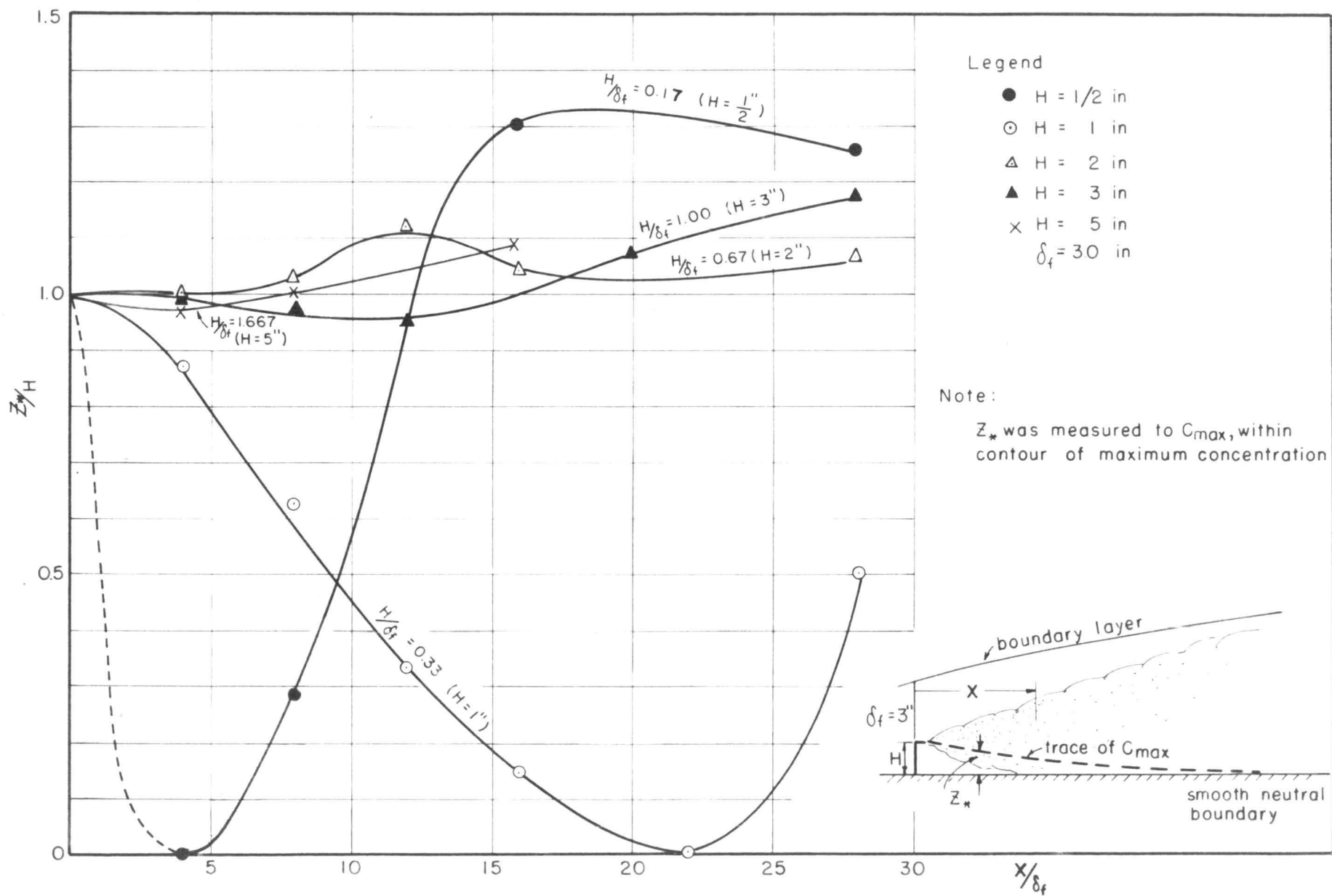


FIG. 2-10 EFFECT OF SOURCE ELEVATION ON LOCATION OF CORE

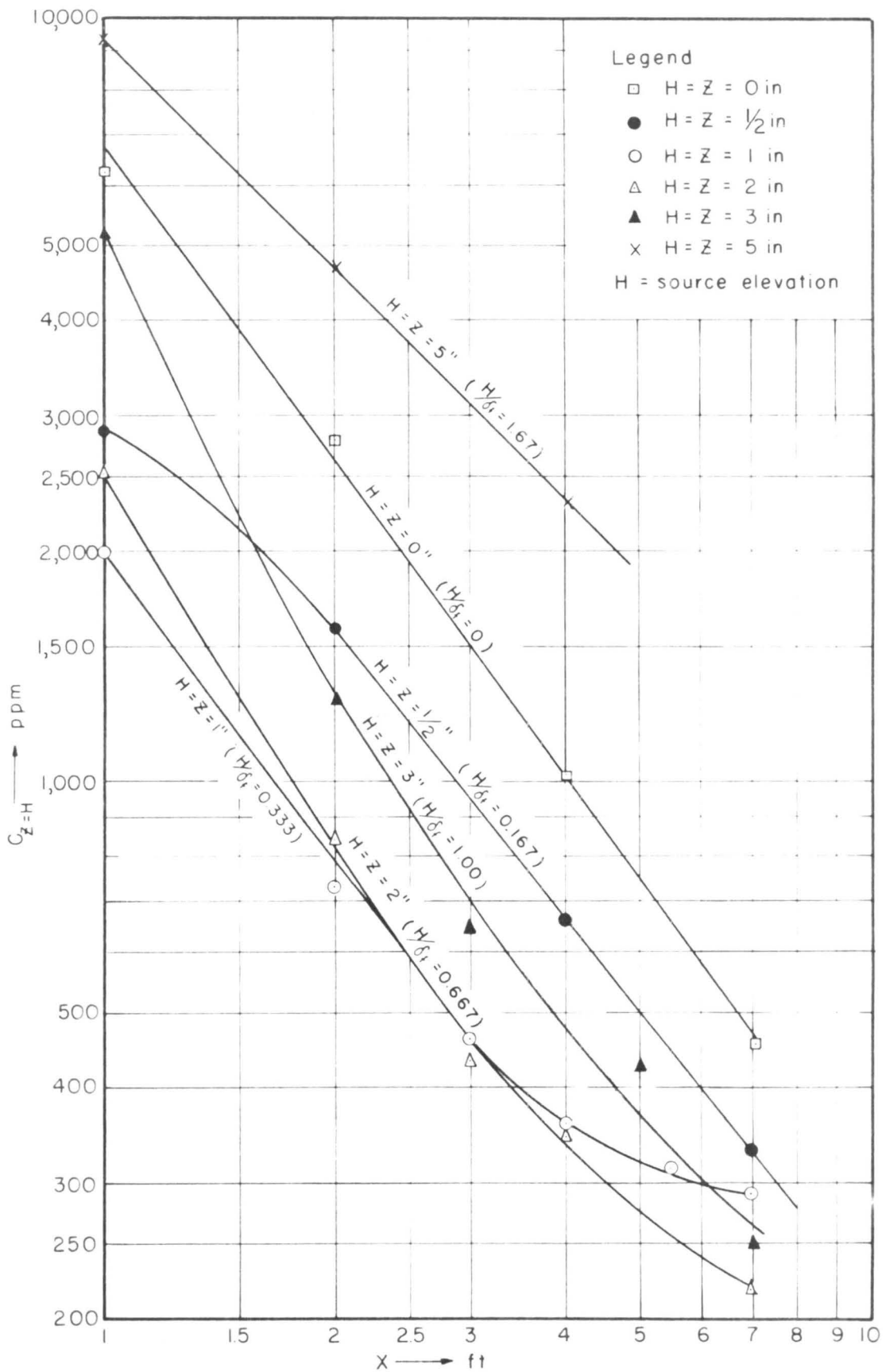


FIG. 2 -II CONCENTRATION ATTENUATION ALONG AXIS THROUGH SOURCE $Z=H$, $Y=0$

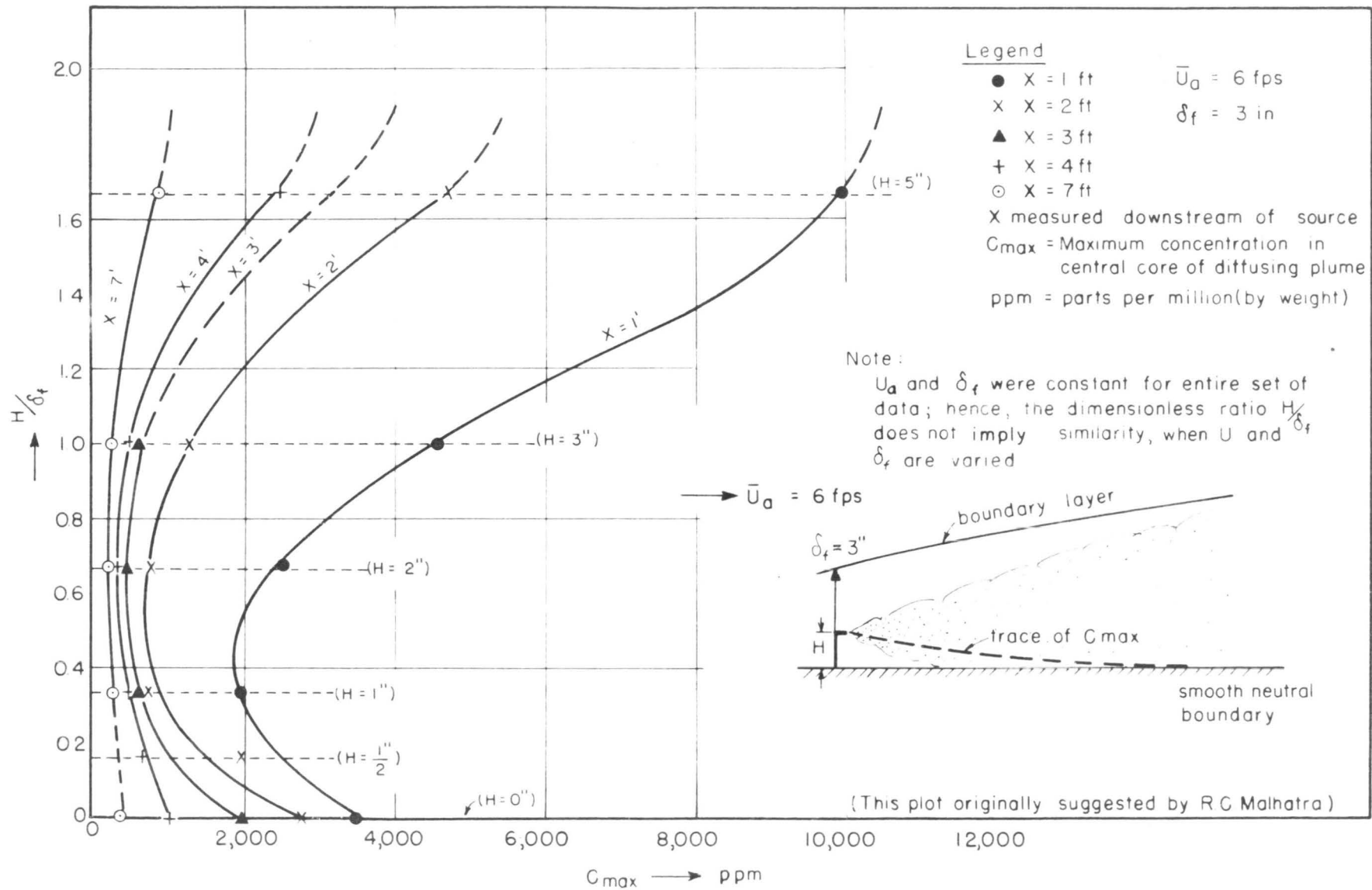


FIG 2-12 EFFECT OF SOURCE ELEVATION ON MAXIMUM CORE CONCENTRATION

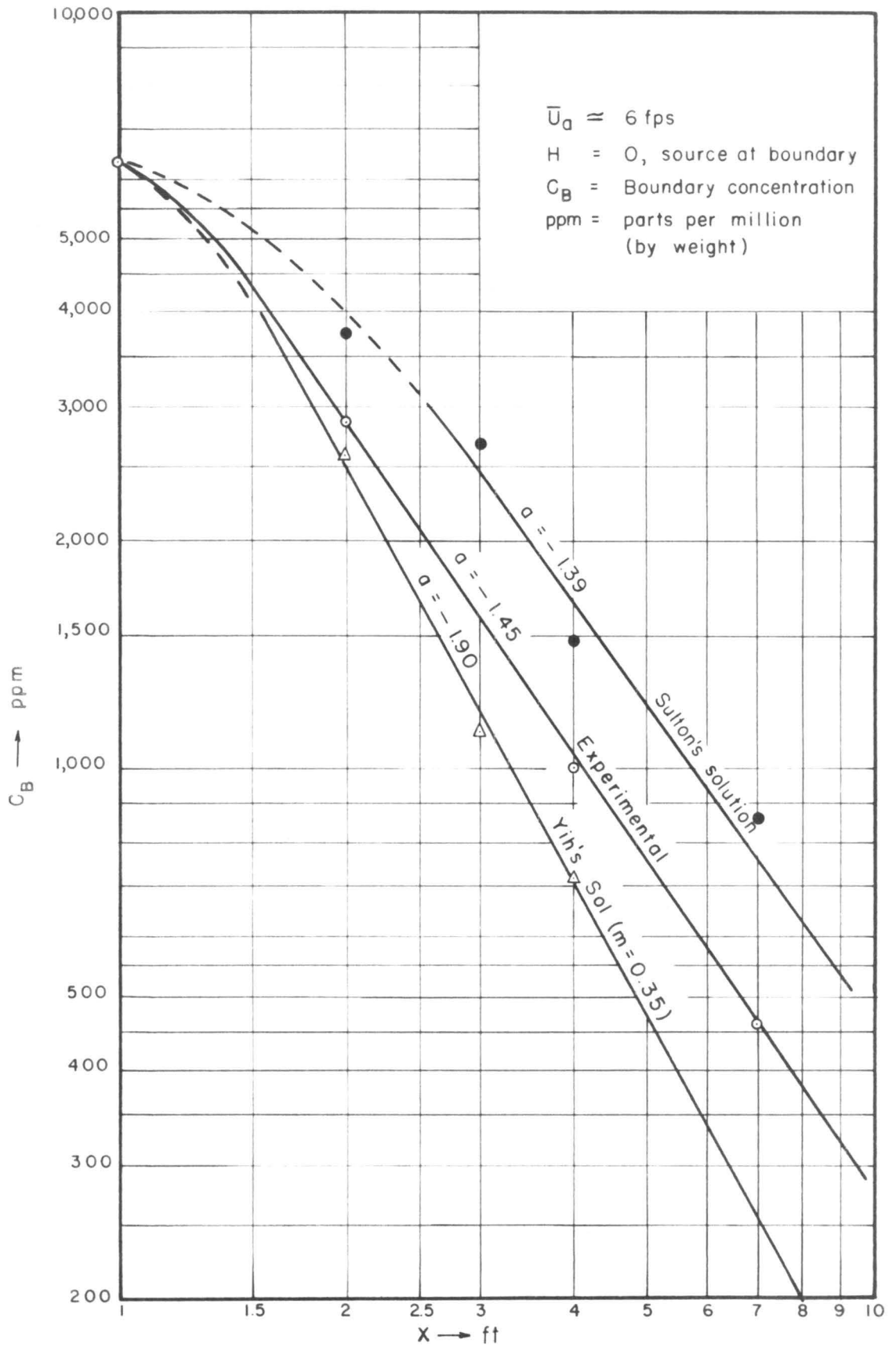


FIG. 2-13 ATTENUATION OF BOUNDARY CONCENTRATIONS

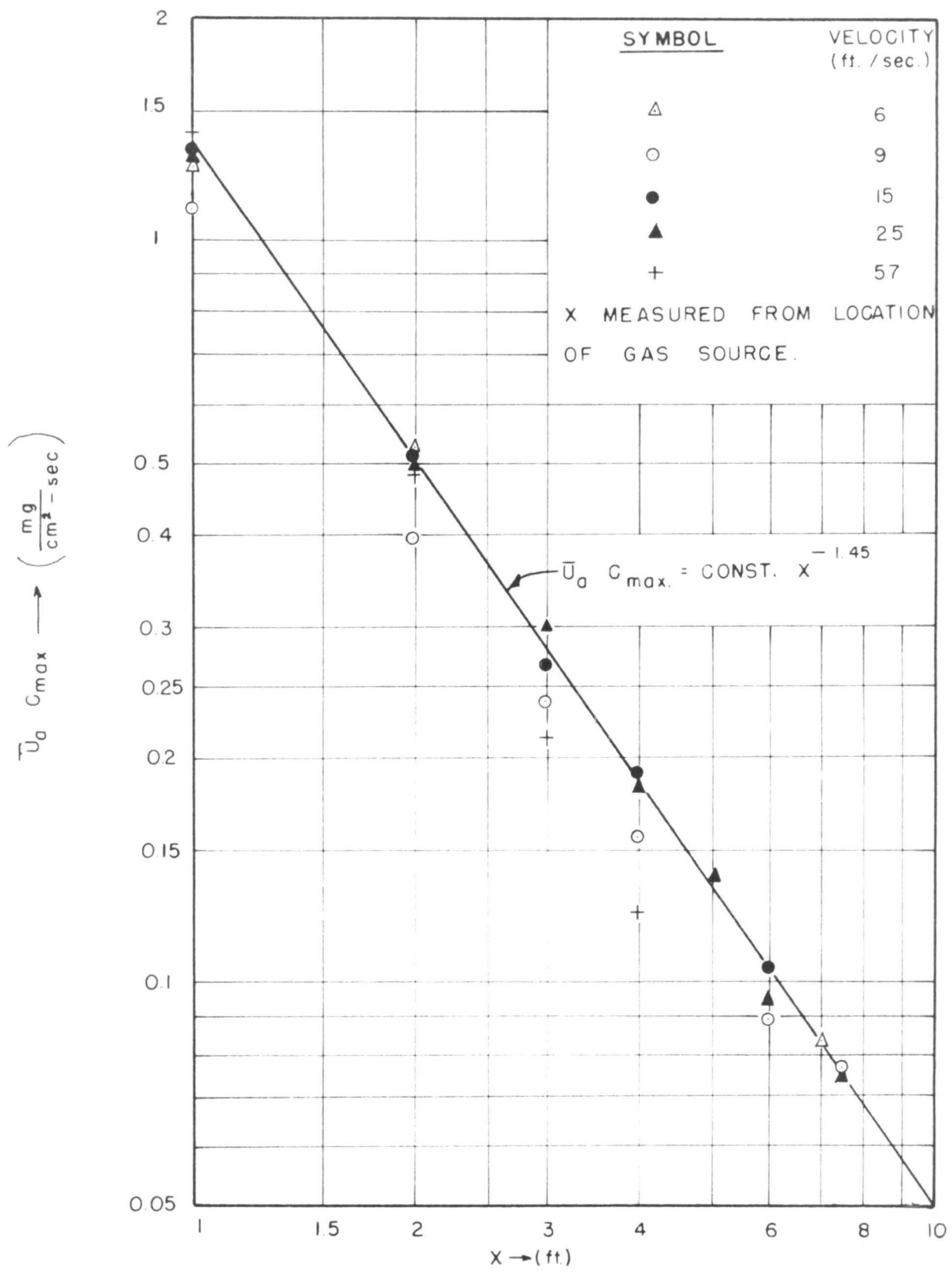


FIG. 2-14 VARIATION OF $\bar{U}_a C_{max}$ WITH DISTANCE FROM GAS SOURCE: $T = 0$, $H = 0$.

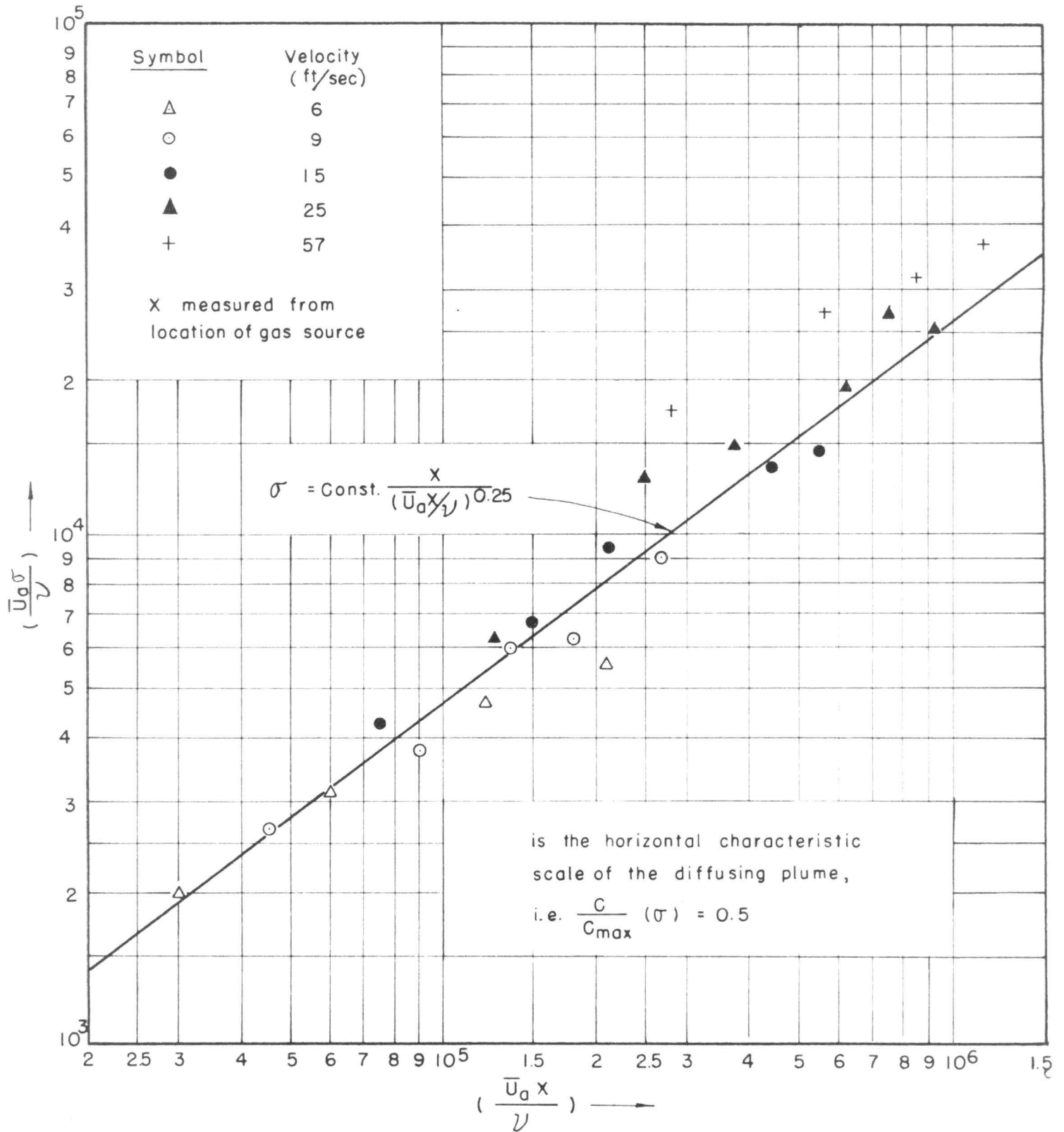


FIG. 2-15 VARIATION OF WITH AMBIENT VELOCITY AND DISTANCE FROM GAS SOURCE: $\Delta T = 0$, $H = 0$.

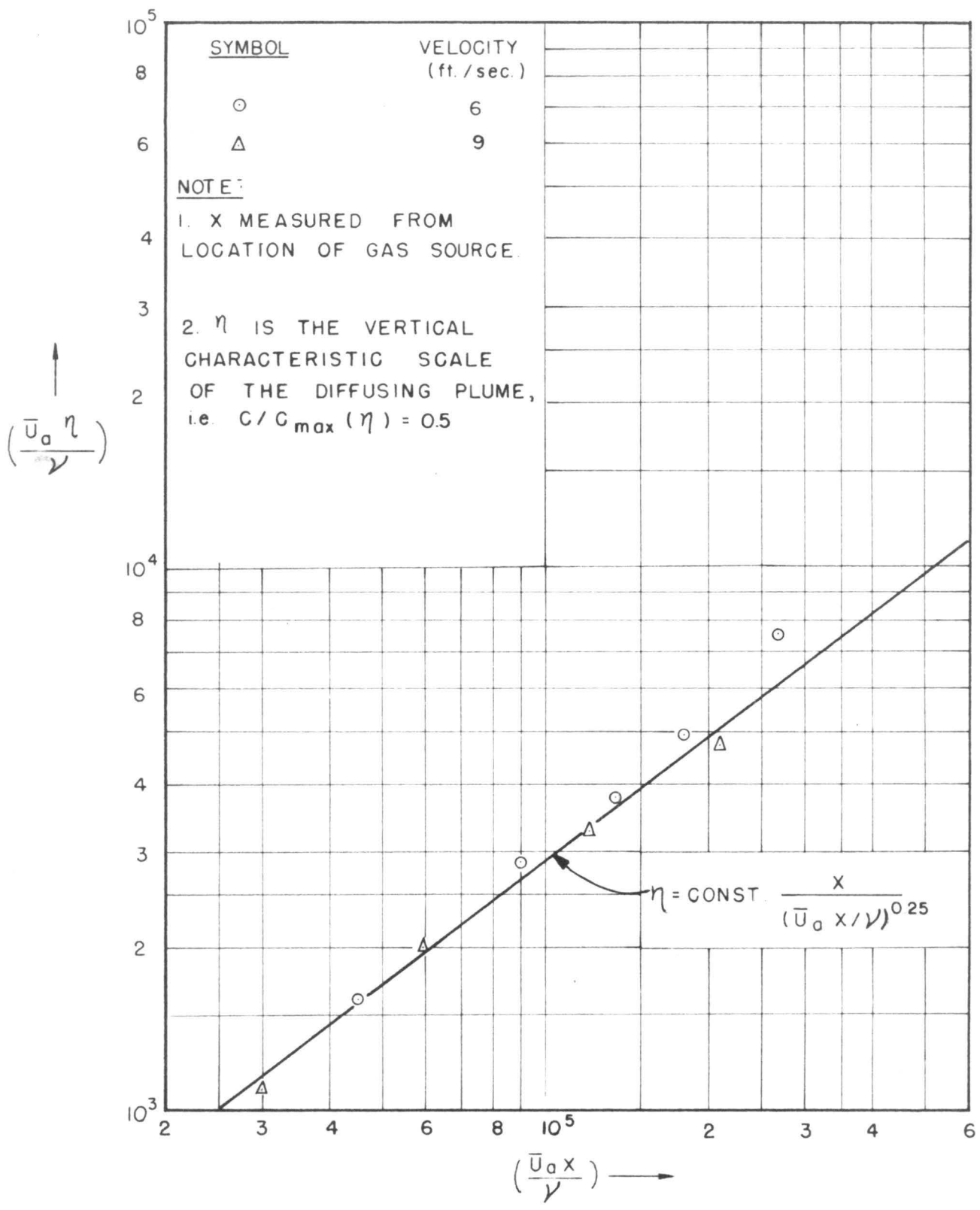


FIG. 2-16 VARIATION OF η WITH AMBIENT VELOCITY AND DISTANCE FROM GAS SOURCE:
 $T = 0, H = 0.$

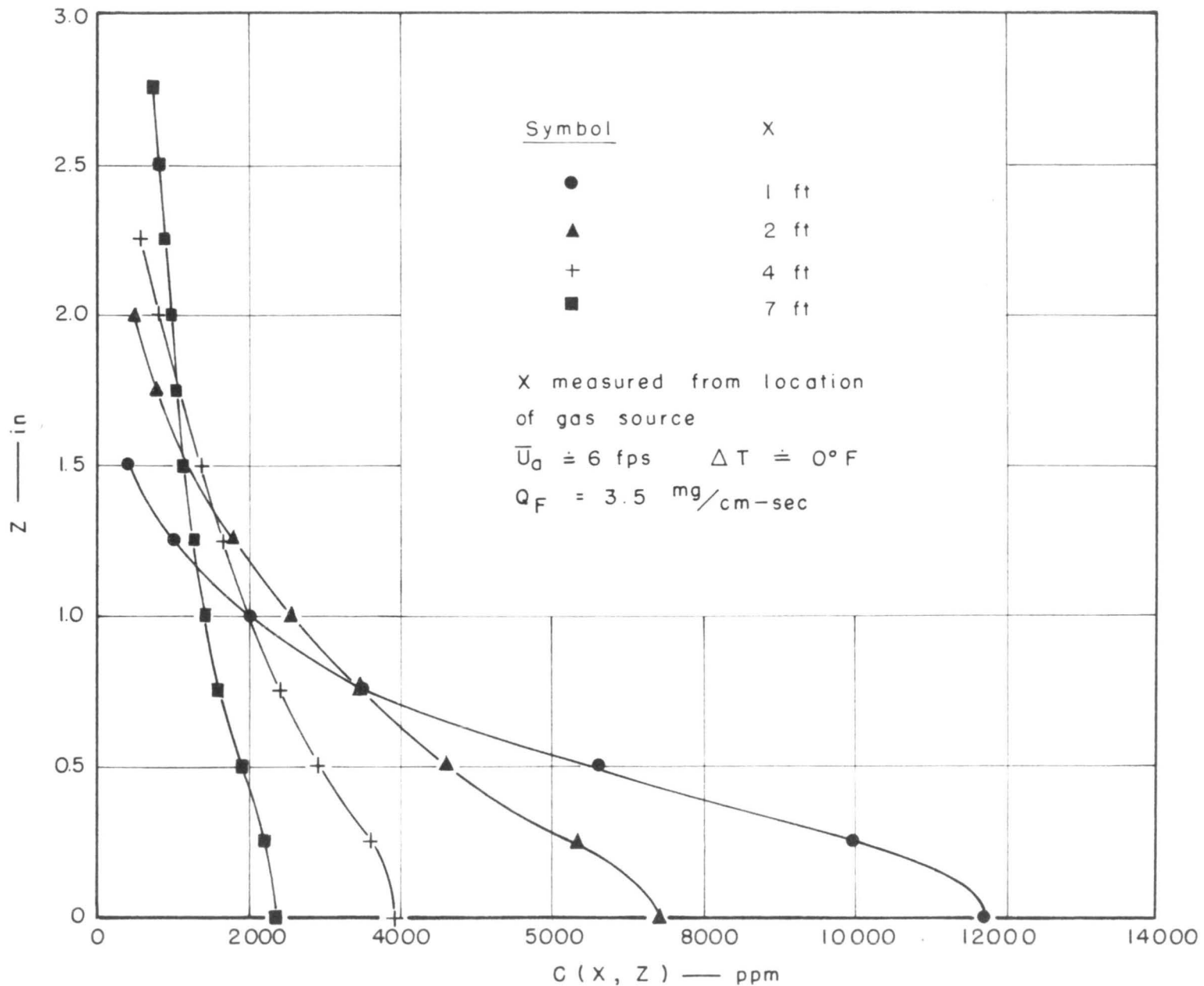


FIG. 2-17 CONCENTRATION DISTRIBUTION FOR EQUIVALENT LINE SOURCE PLUME OBTAINED BY INTERGRATING THE POINT SOURCE DATA

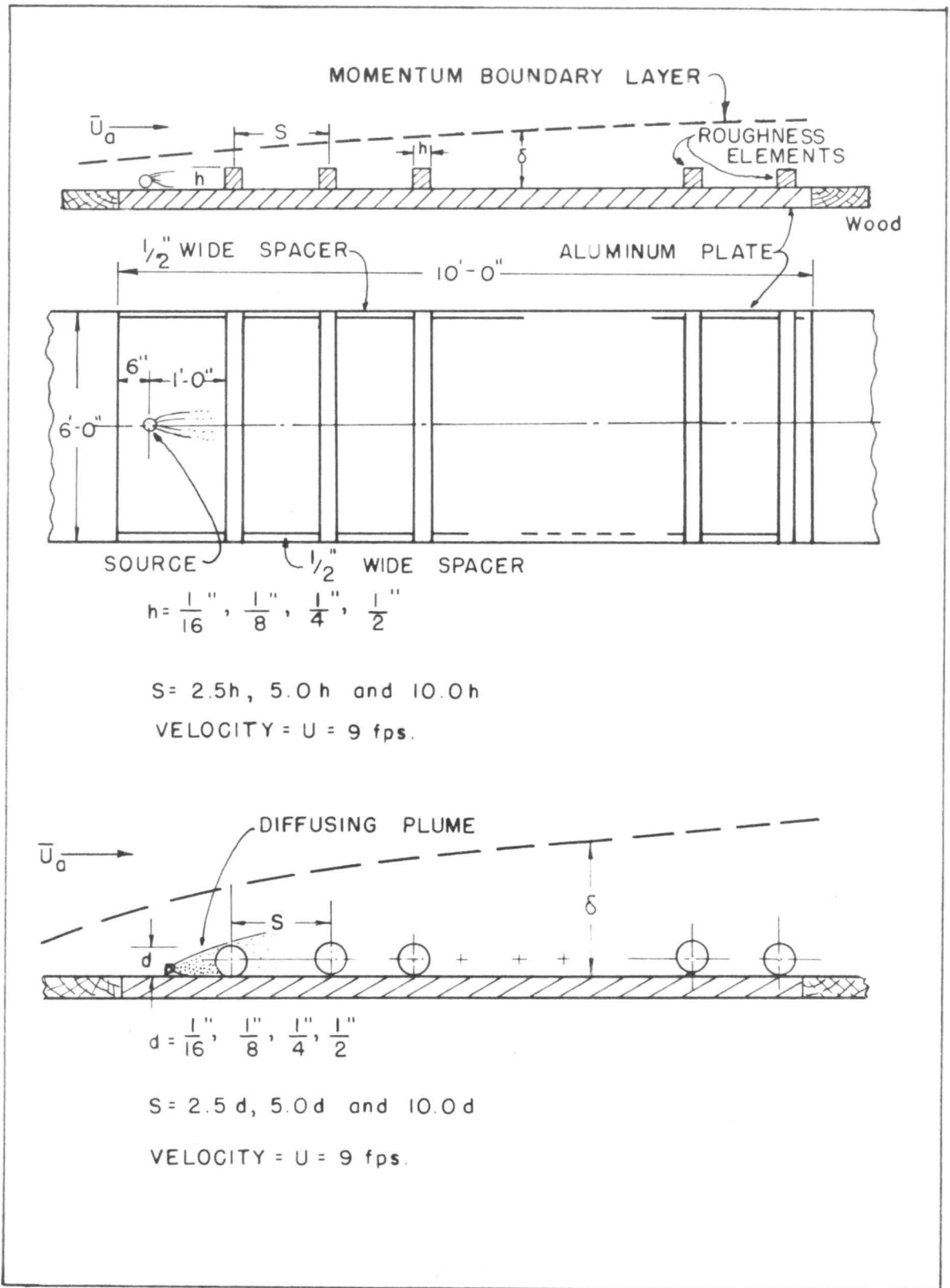


FIG. 3-1 PROPOSED ROUGHNESS ELEMENTS FOR STUDYING DIFFUSION OVER A ROUGH SURFACE.

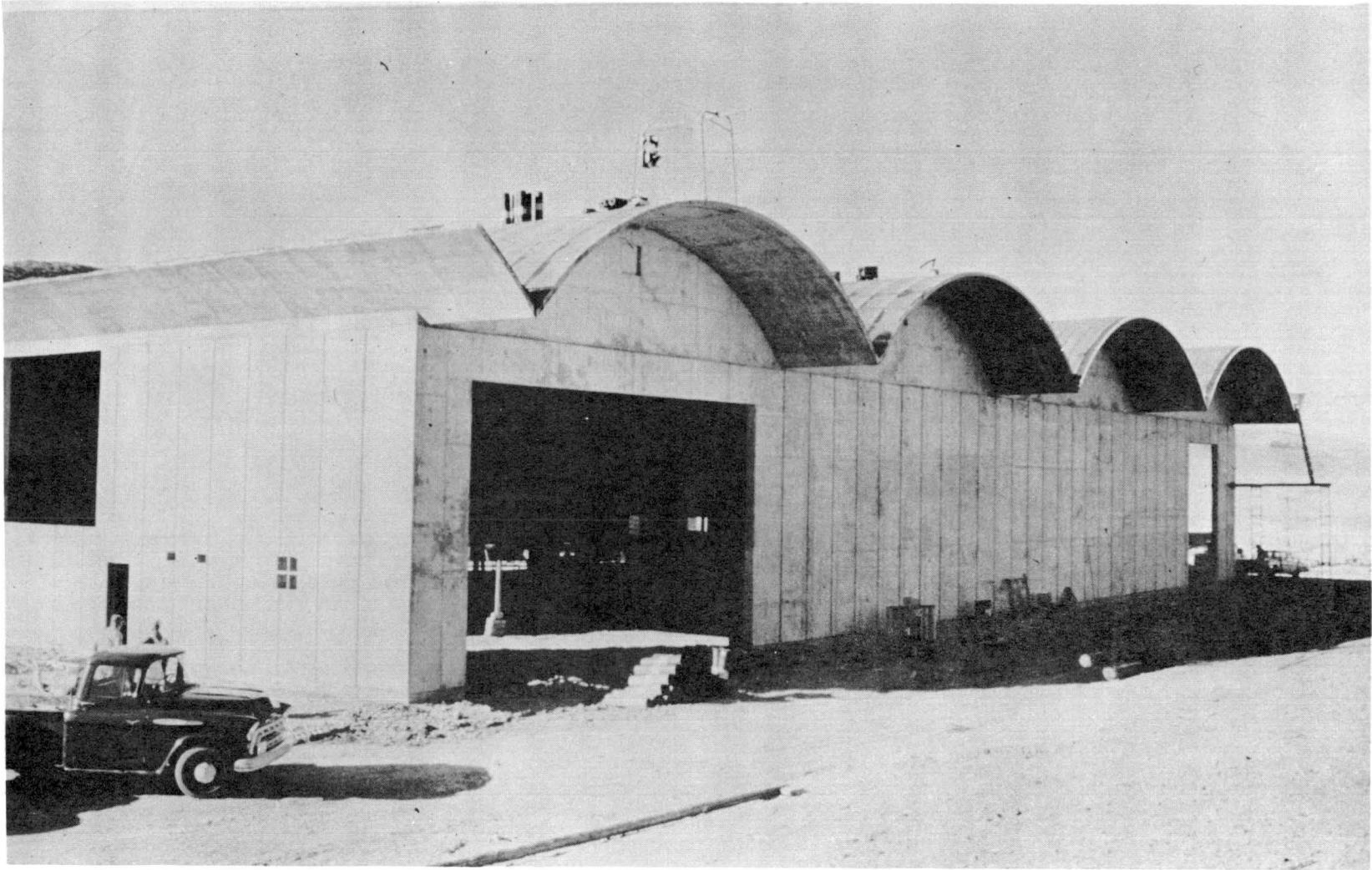


FIG. 5 - 2 VIEW OF BUILDING OF NEW AERODYNAMICS LABORATORY
 UNDER CONSTRUCTION

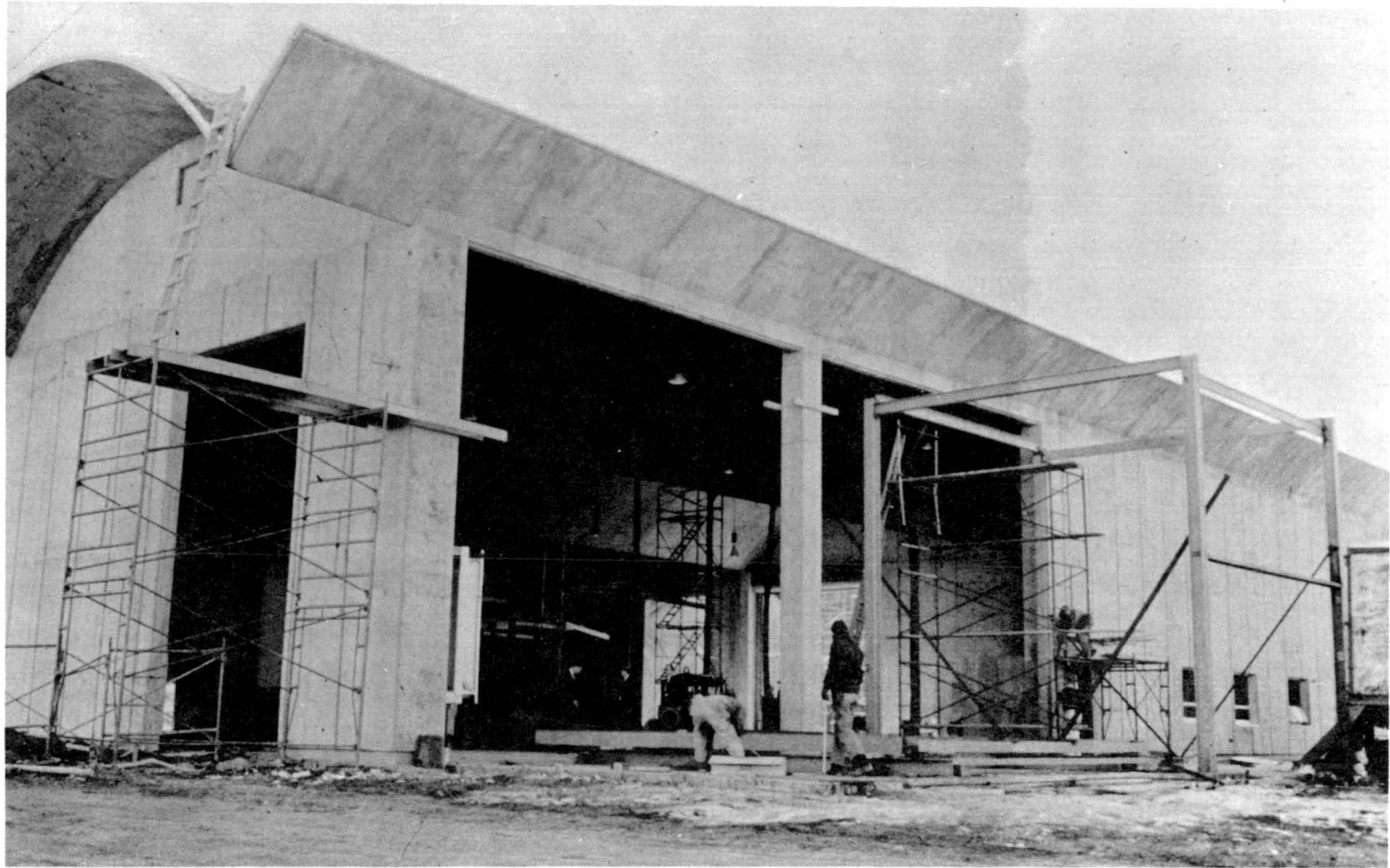


FIG. 5-3 VIEW OF STEEL FRAME WORK BEING INSTALLED FOR NEW WIND TUNNEL UNDER CONSTRUCTION.

paper accepted by the Committee on Fluid
Dynamics of the Engineering Mechanics
Division for the American Society of Civil
Engineers annual convention to be held in
New York City, Oct., 1961

THE EXPERIMENTAL RELATION BETWEEN TURBULENT DIFFUSION

HOT-WIRE ANEMOMETER MEASUREMENTS

Lionel V. Baldwin* and William R. Mickelsen**
Lewis Research Center
National Aeronautics and Space Administration
Cleveland, Ohio

ABSTRACT

Theoretical prediction of diffusion in homogeneous turbulent fields from the Taylor theory of diffusion by continuous movements requires knowledge of the Lagrangian turbulent velocity correlation coefficient. Although a direct theoretical connection between the Lagrangian and Eulerian correlation coefficients has not been found, it is shown that an empirical relation can be established. Eulerian correlation coefficients from hot-wire anemometer measurements are compared with Lagrangian correlation coefficients derived from diffusion measurements in a homogeneous turbulent flow. From this comparison, a relation is found which permits a direct prediction of turbulent diffusion from hot-wire (Eulerian) measurements of the turbulent field.

Some measurements of a mixed space-time Eulerian correlation coefficient are described, and a possible direction of further research is discussed.

INTRODUCTION

One of the most familiar aspects of turbulent fluid motion is its dispersive property. The rapid spread of smoke from chimneys and of

*Presently Associate Professor, Colorado State University, Fort Collins, Colorado.

**Head, Electrostatic Propulsion Components Section, NASA-Lewis Research Center.

the vapor trails of high-altitude jet planes are examples that fascinate even the casual observer. Few physical phenomena have attracted research from the scientific and engineering community with such disregard for speciality. This attests to the general occurrence and importance of turbulent diffusion. But, like all aspects of turbulent fluid motion, the problems are notorious, and a great deal of work has yielded only a little understanding.

In order to gain an insight into turbulent motion, Taylor¹ proposed his statistical theory for isotropic, homogeneous turbulence. The simplifications introduced by the assumptions of isotropy and homogeneity opened the way to theoretical development; and much experimental work was devoted to the closest real analog available, grid-produced wind tunnel turbulence. Batchelor² summarizes that work in his book. The theory was formulated for a "box" of turbulence, and the transformation to the wind tunnel was made by assuming that the "box" moved with the mean stream velocity U . Thus, the predicted decay of the turbulence at time t , after the grid was inserted, was related to the flowing system at an axial station X , where $X = Ut$. A more subtle problem was resolved by "Taylor's hypothesis," which related approximately the measured spectrum of an anemometer fixed in the flow to the theoretically more convenient spectrum in wave-number space. But, aside from these examples, the development of the statistical theory of turbulence retained an Eulerian viewpoint. The statistical description of the flow in these terms (spectrum or Eulerian autocorrelations,

two-point correlations, velocity variance or intensity) has not been related theoretically to the dispersive characteristics of even homogeneous turbulence. The reason is that the derivation of transport coefficients for conserved quantities like heat and mass requires a Lagrangian description of fluid-particle motion. A theoretical development along these lines was published by Taylor in his theory of diffusion by continuous movements.³ Recent reviews of this theory and some subsequent experimental work are available.^{4,5} Nevertheless, since we will have to examine some of the fundamental assumptions of this theory in detail to interpret our experimental results, a brief summary of the Lagrangian description of diffusion is included in the next section.

The objective of this paper is to summarize the results of an experimental program in which empirical relations were sought between the anemometer (Eulerian) specification of turbulence and the Lagrangian statistical properties that determine diffusion. Such empirical relations would have engineering utility because anemometer measurements are readily made and therefore are more available than tagged particle data. Furthermore, by choosing a nearly homogeneous, isotropic flow that was stationary in time, we hoped that these empirical relations might serve as the basis for new theoretical approaches by supplying working approximations to make the problem tractable.

REVIEW OF THE THEORY OF DIFFUSION BY CONTINUOUS MOVEMENTS

Imagine that a fluid element having negligible molecular diffusivity is tagged at the origin of the x -, y -, z -coordinates at some

time $t = 0$ in a box of stationary turbulence. Then this fluid element at some dispersion time t later has moved to a point $P(X,Y,Z)$, whose coordinates are equal to:

$$X = \int_0^t u_{La}(t') dt' \quad Y = \int_0^t v_{La}(t') dt' \quad Z = \int_0^t w_{La}(t') dt' \quad (1)$$

where u_{La} , v_{La} , and w_{La} are the velocity components of the fluid particle. Since the fluid is at rest except for the turbulence, the time mean displacements over all the particles have the same properties as the mean turbulent velocity; that is, $\bar{X} = \bar{Y} = \bar{Z} = \bar{0}$. However, the displacement variances will depend on the dispersion time. For example, in the y-direction (since $dY/dt = v_{La}(t)$),

$$\overline{\frac{dY}{dt} Y} = v_{La}(t) \int_0^t \overline{v_{La}(\tau)} d\tau \quad (2)$$

where $0 \leq \tau \leq t$. Here, the superscript bar indicates an average (over many particles) of individual particle histories. But $v_{La}(t)$ is not a function of τ , and, since $\overline{Y \frac{dY}{dt}} = \frac{d\overline{Y^2}}{2dt}$,

$$\frac{1}{2} \frac{d\overline{Y^2}}{dt} = \int_0^t \overline{v_{La}(t)v_{La}(\tau)} d\tau \quad (3)$$

When the average motion of a great many fluid particles (tagged at $t = 0$ at the origin) is considered, the mean velocity product may be written in terms of the Lagrangian correlation coefficient:

$$\mathcal{R}(\tau) = \frac{\overline{v_{La}(t)v_{La}(\tau)}}{\overline{v_{La}^2}}$$

$$\frac{1}{2} \frac{d\overline{Y^2}}{dt} = \overline{v_{La}^2} \int_0^t \mathcal{R}(\tau) d\tau \quad (4)$$

Finally, the desired equation for the variance $\overline{Y^2}$ is

$$\frac{1}{2} \overline{Y^2} = \overline{v_{La}^2} \int_0^t \left[\int_0^{t'} \mathcal{R}(\tau) d\tau \right] dt' \quad (5)$$

where the prime and τ notation merely distinguishes between the variable and the limit in each integration. Owing to the isotropy of the motion,

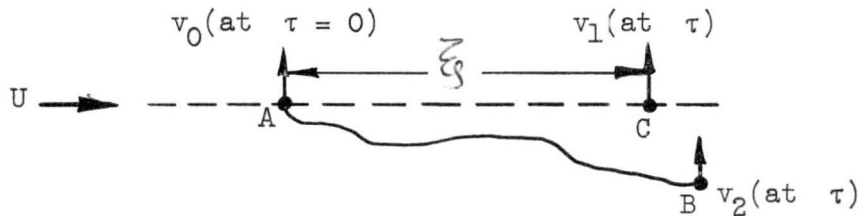
$$\overline{Y^2} = \overline{X^2} = \overline{Z^2}$$

Of course, the specification of the mean concentration distribution in space and time that is produced by the turbulent motion is the objective of an ordinary diffusion analysis. The dispersion of the particles tagged at the origin at $t = 0$ is assumed to be a three-dimensional Gaussian function (Batchelor⁷ and Frenkiel⁴ point out that, if the velocity distribution is Gaussian, then the dispersion would also be expected to be Gaussian):

$$c(x,y,z,t) = \frac{1}{(2\pi\overline{Y^2})^{3/2}} \cdot \exp\left(-\frac{x^2 + y^2 + z^2}{2\overline{Y^2}}\right) \quad (6)$$

The concentration c is defined here as the fraction of the total number of particles tagged, which at some time t later are at the point x,y,z . The mean concentration at a point depends on the variance $\overline{Y^2}$ and its functional relation with the dispersion time t . Equation (5) shows that $\overline{Y^2}$ is given in terms of the Lagrangian correlation coefficient $\mathcal{R}(\tau)$ and the Lagrangian velocity variance $\overline{v_{La}^2}$. Thus, the prediction of the mean concentration in turbulent diffusion

depends on the characterization of the turbulent motion by these two Lagrangian statistical properties. Conversely, the Lagrangian statistical properties must be inferred from concentration measurements if the individual fluid-particle velocities cannot be measured. This situation is illustrated in the following sketch:



A fluid particle leaving point A at time $\tau = 0$ will transverse the path shown to point B where it will have the velocity v_2 at time τ . The lateral velocities at points A and C can be measured with hot-wire anemometer probes, and the "signals" from the probe at C could be delayed by a time $\tau = \xi/v$ to obtain a correlation $\overline{v_0(0)v_1(\tau)}$ which would be a "mixed correlation," that is, an Eulerian correlation between two points, with an artificial time delay. It is evident from the sketch that the Lagrangian correlation $\overline{v_0v_2}$ will not be identical to the Eulerian autocorrelation $\overline{v_0v_1}$ because of the displacement of point B from point C.

The extension of the Taylor theory to a variety of initial and boundary conditions has been published by Frenkiel⁴ and Mickelsen.⁶

POSSIBLE INTERACTION BETWEEN TURBULENT AND MOLECULAR DIFFUSION

The preceding derivation assumed that the fluid particle had negligible molecular diffusivity. A "particle" of a real fluid will

have continuum properties only if its volume is large enough so that the net molecular motion within its volume converges to an average (the fluid velocity). The position of a tiny fluid particle could then be determined from the location of the centroid of the tagged molecules. These molecules would be meandering because of turbulent motion, and also spreading relative to the particle centroid because of molecular motion. If the dimensions of this single particle were small compared with the smallest scale of the turbulent motion, then these two dispersion mechanisms would occur independently. The total dispersive spread $\overline{D^2}$ (for the average over a great many particles) is the sum of each average contribution:

$$\overline{D^2} = \overline{Y^2} + 2\alpha t \quad (7)$$

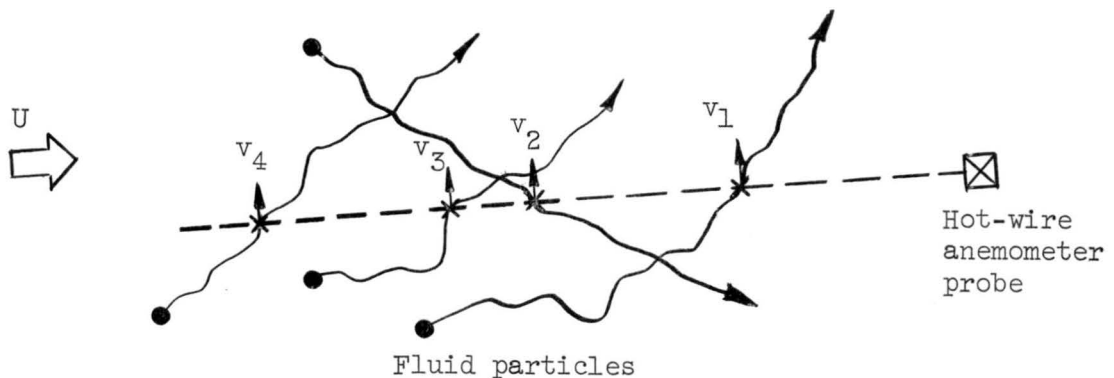
Townsend^{6,7} has postulated that the turbulent motion accelerates the molecular diffusion by rotating and straining the instantaneous diffusion wake. He evaluated this coupling in terms of the ~~velocity~~ ^{vorticity} ω of the turbulent motion:

$$\overline{D^2} = \overline{Y^2} + 2\alpha t \left(1 + \frac{14}{45} \overline{\omega^2} t^2 + \text{higher terms} \right) \quad (8)$$

Townsend developed this model to account for diffusion of hot-air "spots" downstream of a pulsating heated wire. He observed that near the source the initial total spread of the spot was greater than predicted by Taylor's theory. In this initial dispersion, the Lagrangian correlation coefficient (Eq. (4)) does not differ greatly from unity, so $\overline{Y^2}$ can be calculated from Eq. (5) and, if there were no coupling,

$$\overline{D^2} = 2\overline{v_{La}^2} t^2 + 2\alpha t \quad (t \rightarrow 0) \quad (9)$$

A hot-wire anemometer operated at several angles of attack to the mean flow can be used to determine $\overline{v^2}$ at a fixed point. It is customary to assume that this Eulerian velocity variance $\overline{v^2}$ (fixed point, time average over many different particles that pass by) is identical with the Lagrangian variance (single-particle velocities measured along their trajectories and averaged over many particle histories). The only (indirect) experimental evidence which shows that these quantities may be equal was obtained by Batchelor⁸ using small solid tracers. The question of equivalence of $\overline{v^2}$ and $\overline{v_{La}^2}$ may be illustrated in the following sketch:



The individual fluid-particle trajectories are shown, and the locus of points on those trajectories that will encounter the probe is shown as a dashed line. The probe will then measure the turbulent velocity at some one point in each individual trajectory. The variance of these discrete samples of the turbulent velocities v_i is determined by auxiliary instrumentation to form the Eulerian variance $\overline{v^2}$. The

question is whether this discrete sampling process will result in a variance $\overline{v^2}$ equal to the variance $\overline{v_{La}^2}$ of the turbulent velocity along the trajectory of an individual fluid particle. Since the turbulent velocities of adjacent fluid particles are correlated to some degree, the sampling process shown above is not strictly random; but, if enough samples are taken by the probe, it does seem that the Eulerian and Lagrangian variances would be equal. Assuming $\overline{v_{La}^2} = \overline{v^2}$ and setting $t = X/U$, Townsend found that $\overline{D^2}$ calculated from Eq. (7) was smaller than the measured total spread at X . Similar results for steady hot-air wakes in grid turbulence were noted by Schubauer,⁹ who found about 25 percent greater total spread than predicted, and by Uberoi and Corrsin.¹⁰

The implications of Townsend's theory of accelerated diffusion led Batchelor and Townsend⁷ to predict that the contribution to total dispersion by accelerated diffusion would increase rapidly with distance (i.e., time) downstream from the source. To test this prediction, Mickelsen¹¹ measured the dispersion of two different gases from the same source in a turbulent airstream. Equation (8) predicts that gases having different molecular diffusivities α (e.g., He and CO₂) injected into the same turbulent airflow would spread at markedly different rates. However, the data of Ref. 11 showed that, for long diffusion times, accelerated molecular diffusion was negligible, so that molecular diffusion made only an independent contribution to the total dispersion of helium and carbon dioxide, as predicted by Eq. (7).

These results led Saffman¹² to reexamine Townsend's derivation in some detail. Saffman makes a distinction between the Lagrangian single-particle correlation introduced by Taylor and a "substance" autocorrelation coefficient which relates "the fluid velocity at two points that lie on the trajectory of a molecule." He deduces that the interaction in the initial period is

$$\overline{D^2} = \overline{Y^2} + 2\alpha t \left(1 - \frac{1}{18} \overline{\omega^2 t^2} \right) \quad (10)$$

so that the interaction decreases the spread. But a corollary of Saffman's argument is that the centroid of an injected heat spot will lag behind, on the average, the fluid particle released at the same instant; that is, $t \neq X/U$. He concludes that the average displacement of the instantaneous centroid of the tagged particles is less than that of the fluid particles by an amount which more than compensates for the increase in the instantaneous wake width due to the interaction (Townsend's analysis).

The concept used by Saffman is difficult to follow. The problem stems from the vague notion of a "fluid particle." It apparently has meant different things to different people. (To cite an extreme, L. F. Richardson once contended that it would not be nonsensical to deny that an average called the velocity of a gas can be defined at all.)^{13,14} At any rate, the discussion in Ref. 7 concerning the pitfalls of interpreting diffusion wake data in terms of single-particle correlation coefficients was perhaps too emphatic. The debate on this point

will probably continue; but, for the work to be described herein, the uncoupled form of the total displacement equation (Eq. (7)) has been used to calculate $\overline{Y^2}$ from measured $\overline{D^2}$. In a sense, the definition of a fluid particle has been chosen to make Eq. (7) true.

EXPERIMENTAL PROGRAM

Apparatus and Procedure

The axial core of a fully developed pipe flow was the turbulent flow field used. All the hot-wire anemometer and diffusion results were obtained within a 2-in.-radius core of ambient air flowing through a commercial 8-in. diameter pipe. For the helium diffusion experiment, the straight inlet section of pipe was 26 ft long. The heat diffusion results were obtained with a 35-ft inlet. In both cases, the mean velocity profiles were essentially flat in the transverse region of interest along the 3- to 4-ft-long test section of pipe. The velocity at ± 2 in. was within 90 percent of the centerline value in the worst case ($U_{\phi} = 50$ ft/sec).

The mean flow velocity was the primary variable. Since the turbulent intensity $\sqrt{\overline{u^2}}/U_{\phi}$ was essentially independent of U_{ϕ} in the experimental range ($9.6 \times 10^5 < Re < 3.2 \times 10^6$), this variation of Reynolds' number gave a range of turbulent velocities plus a slight variation in the Eulerian scale of turbulence.

Hot-wire anemometry equipment was used to measure the turbulent intensities and the Eulerian correlation coefficients. The hot-wire anemometer amplifier was the constant-temperature type.¹⁵ The auxiliary

equipment includes a true root-mean-square voltmeter and/or an average square computer, a dual-channel tape recorder, and an autocorrelation computer.^{16,17} The actual data-reduction procedures are described by Mickelsen¹⁸ and Baldwin.¹⁹

Two different types of diffusion measurements were made. In the first, a 0.05-in. streamlined tube was used to inject a stream of helium gas into the flow at the local mean velocity. The mean helium concentration profiles downstream of this simulated point source were obtained with a movable sampling probe connected to a mass-spectrometer type of leak detector. The mean diffusion wake was mapped at $U_c = 50, 75, 100, 122, \text{ and } 164$ ft/sec. Surveying of the pipe core flow was also performed at these flow conditions with the hot-wire anemometer. The second set of diffusion data was obtained using a simulated line source of heat. For this work, an electrically heated wire was strung vertically across the test section inlet, and mean temperature profiles downstream were mapped with a thermopile. These data were obtained with a series of decreasing source diameters (0.065 to 0.010 in.) so an ideal, nondisturbing source could be estimated by extrapolating to "zero" source diameter. The thermal wake data and more complete anemometer surveys were obtained at $U_c = 72.6, 106, 135, \text{ and } 160$ ft/sec.

The two-dimensionality of the central diffusion wake simplifies the choice of coordinate systems. A rectangular Cartesian system is used herein with the origin at the intersection of the pipe's axial

centerline and the vertical source of heat or mass, which was located in the test-section inlet. The x-direction is measured from the origin in the mean flow direction; the y-direction is the lateral distance from the axial centerline in the horizontal plane.

Primary Data Results

The homogeneity of the axial core was established by radial surveys using hot-wire anemometers. These surveys showed that the longitudinal intensity $\sqrt{u^2}/U_\infty$ along the centerline was independent of axial station for all flow velocities. Using the calibration procedures described by Baldwin et al.²⁰ (rather than King's equation), $\sqrt{u^2}/U_\infty$ along the centerline was measured to be 0.035 at all flow velocities. In the transverse direction, $\sqrt{u^2}/U_\infty$ rises only about 15 percent (above the centerline value) at the extremes of the 2-in. core. Somewhat similar results were found for $\sqrt{v^2}/U_\infty$ using X-wires¹⁸ and single wires operated at three yaw angles to the flow.¹⁹ An exception to homogeneity was found in the first few inches downstream of the diffusion sources. At the extreme, the turbulent intensities were roughly doubled in this region, but this source distribution decayed completely within 6 in. downstream.

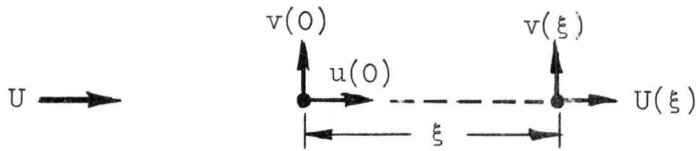
A necessary condition for isotropy would be equal values of $\overline{v^2}$ and $\overline{u^2}$. Using an X-wire anemometer in the manner described by Schubauer and Klebanoff,²¹ the ratio of $\sqrt{\overline{v^2}}/\sqrt{\overline{u^2}}$ was found to be between 1.1 and 1.0 in the helium diffusion experiment,¹⁸. Using a single yawed wire technique discussed by Baldwin et al.,²² this

intensity ratio was calculated to be between 0.8 and 0.7 in the later work on heat dispersion.¹⁹ The latter results compared favorably with measurements in isotropic turbulent flow produced by grids recently reported by Grant and Nisbet.²³ Here, they found $\sqrt{v^2}/\sqrt{u^2}$ was about 0.85.

In the diffusion experiment the lateral dispersion is measured, but the axial dispersion is essentially neglected. Therefore, a slight anisotropy is not serious. The primary requirement is homogeneity of $\sqrt{v^2}$.

The other important statistical properties obtained from the analysis of anemometer signals are the Eulerian correlation coefficients. Three different forms of these correlations were measured. These data are presented here and discussed later, along with the empirical relations for which they form the basis.

1. An X-wire anemometer signal may be regarded as being directly proportional to the instantaneous lateral turbulent velocity,²¹ although this contention can be debated. Furthermore, it may be assumed that the structure of an average eddy changes little during the time necessary for the eddy to pass over a single wire ("Taylor's hypothesis"). Then, the autocorrelation of this X-wire signal $g(t)$ can be transformed into an Eulerian space correlation $g(\xi)$ using $\xi = U_c t$, where ξ is measured along the pipe centerline. If the turbulence were isotropic, then $g(\xi) = \overline{v(0)v(\xi)}/\overline{v^2}$ is simply related to $f(\xi) = \overline{u(0)u(\xi)}/\overline{u^2}$ by continuity using the nomenclature and formula derived by Karman and Howarth²⁴:



$$f = \frac{2}{\xi^2} \int_0^{\xi} \xi g \, d\xi \quad (11)$$

The correlations derived in this manner are shown in Fig. 1. These curves will be used in interpreting the helium diffusion data.

2. A single transverse hot-wire anemometer has a signal proportional to the instantaneous longitudinal turbulent velocity. Again, using $\xi = U_{\xi}t$, the autocorrelation $f(t)$ of this signal can be transformed into the Eulerian space correlation $f(\xi)$. These results are shown in Fig. 2.

3. Finally, the signals of two transverse hot wires separated by a distance ξ along the pipe centerline can be recorded on magnetic tape. When these signals are correlated as a function of the delay time t introduced at the correlation computer, the result is a mixed Eulerian correlation coefficient $R_u(\xi, t)$ (as shown in the sketch in the preceding REVIEW section). By repeating this procedure for many values of ξ , it is possible to map this function in the ξ, t plane. These general Eulerian space-time correlations are plotted in Figs. 3a to 3d for the mean velocities used in the heat wake experiment. Complete correlation curves were obtained from 0 to 40 millisecond time delay for each wire spacing shown; but, to simplify the figures, only a few complete curves are shown. The portion of negative correlation is

shown only for extreme spacings to avoid excessive overlapping of curves. Incidentally, these curves have enough information to make a crude check of Taylor's hypothesis in the usual manner, by comparing the autocorrelation $R_u(0,t)$ at $t = \xi/U_\xi$ with $R_u(\xi,0)$. The results of this comparison are given in Table I; the approximation is certainly adequate for engineering purposes.

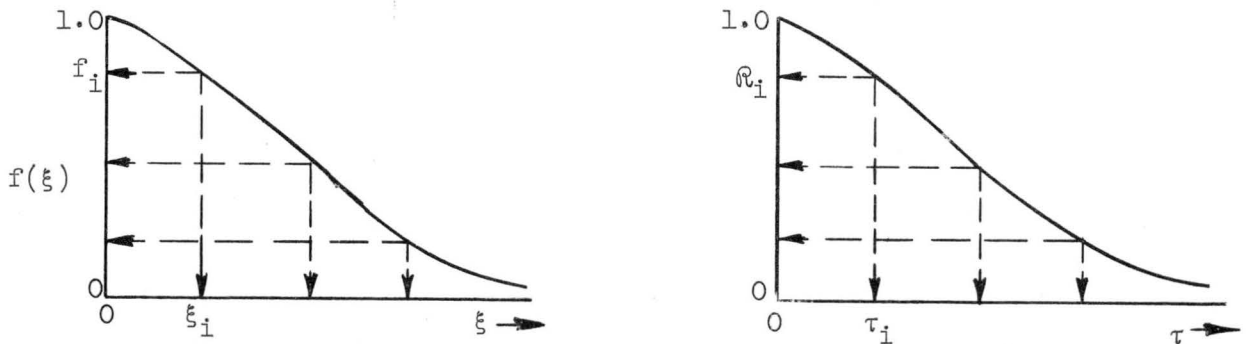
The primary diffusion data are a series of lateral concentration (He) and temperature profiles for various distances downstream of the source. For both sets of data, these profiles were essentially Gaussian and could therefore be described by a variance. Since $\sqrt{v^2}/U_\xi \ll 1$, the diffusion proceeds slowly, so that axial concentration gradients are small. Therefore, axial diffusion can be neglected and the variance of the measured profile at x set equal to $\overline{D^2}$ of Eq. (7), taking $t = X/U_\xi$.^{4,5} Using Eq. (7), a correction was made for molecular diffusivity in order to calculate $\overline{Y^2}$. The corrections were significant (but less than 10 percent) for the first profiles downstream of the source, but rapidly dropped to less than 4 percent. The helium data are summarized in Fig. 4. A sample of the primary heat wake data is given as Fig. 5, where the curve is drawn through the extrapolated "zero diameter" source initially and by best guess at larger times. A summary of these heat wake curves is given as Fig. 6.²⁵

EMPIRICAL RELATIONS BETWEEN EULERIAN AND LAGRANGIAN
STATISTICAL PROPERTIES

Perhaps the simplest form (and therefore potentially the most useful) of an empirical relation that might be found is a similarity of the Eulerian correlation $f(\xi)$ and the Lagrangian $\mathcal{R}(\tau)$. (Since the Eulerian correlation $g(\xi)$ becomes negative for a substantial range of ξ , a simple relation between $g(\xi)$ and $\mathcal{R}(\tau)$ could not be expected. To test the data for this possibility, the following coordinate transformation may be tried:

$$\xi = A \sqrt{v_{La}^2} \tau \quad (12)$$

The correlations would be similar if the following direct comparison could be made:



Where f_i equals \mathcal{R}_i , the factor $A_i = \frac{\xi_i}{\sqrt{v_{La}^2} \tau_i}$ may be calculated.

For all values of space and time, if $A_i = \text{constant} = A$, then the two correlations would be similar because $\sqrt{v^2}$, and presumably $\sqrt{v_{La}^2}$, is

not a function of ξ or τ in the flow field. It would follow that the Eulerian L_f and Lagrangian \mathcal{L} scales of turbulence are proportional:

$$L_f \equiv \int_0^{\xi_n} f(\xi) d\xi \quad (13)$$

and

$$\mathcal{L} \equiv \sqrt{\frac{v^2}{La}} \int_0^{\tau_n} R(\tau) d\tau \quad (14)$$

Assuming $\sqrt{v^2} = \sqrt{\frac{v^2}{La}}$ where necessary throughout this development and substituting Eq. (12) into the above expressions yields

$$\frac{L_f}{\mathcal{L}} = A \quad (15)$$

A similar relation would hold for the ratio of the microscales.

Rather than perform a double differentiation of the $\overline{Y^2}$ curves to obtain $R(\tau)$ for this comparison (see Eq. (5)), the similarity idea may be tested in the following manner. A double integration of the $f(\xi)$ curves can be related to the diffusion data, since $\tau = \xi/A\sqrt{v^2}$ is assumed:

$$\int_0^{\xi} \int_0^{\xi'} f(\xi'') d\xi'' d\xi' = A^2 \overline{\frac{1}{v^2}} \int_0^t \int_0^{t'} R(\tau) d\tau dt' \quad (16)$$

For convenience, the Eulerian double integral may be designated by the symbol ω_f which is the nomenclature of Ref. 18. Then, substituting Eq. (5) gives

$$\omega_f(\xi) = A^2 \left[\frac{1}{2} \overline{Y^2}(\tau) \right] \quad (17)$$

A direct comparison can be made by dividing by ξ^2 :

$$\frac{1}{\xi^2} \cdot \omega_f(\xi) = \frac{1}{v^2 \tau^2} \cdot \frac{1}{2} \overline{Y^2}(\tau) \quad (18)$$

As a consequence of similarity (i.e., $A = \text{constant}$), where the left-hand Eulerian function of ξ equals the right-hand Lagrangian function at τ , then these values, say ξ_i and τ_i , must be related by

$$\xi_i = A_i \sqrt{v^2 t_i}.$$

The Eulerian correlations of Fig. 1 (X-wire data) were used to calculate the curves of ω_f/ξ^2 in Fig. 7. The helium diffusion data of Fig. 4 were used along with the same X-wire anemometer measurements of $\overline{v^2}$ to calculate the curves of $\overline{Y^2}/2v^2t^2$ in Fig. 8. The results of the comparison of these functions (as outlined above) are summarized in Fig. 9. From this figure, it is seen that the hypothesis of simple similarity is not well supported by the data; if it were, the curves in Fig. 9 would be straight lines passing through the origin. Note that deviation is greatest at very short times and very long times, but that there is an appreciable range of ξ and τ where the curves are approximately linear in Fig. 9. However, since an integral technique has been used in this comparison, all that can be safely said of the critical test for similarity is that the data are inconsistent with the assumption $A = \text{constant}$ if $\xi = A \sqrt{v^2 \tau}$. The same conclusion would be drawn from the heat wake data of Fig. 6 and the single-wire correlation data of Fig. 2, although the final comparison plot would involve somewhat different absolute values.

If the condition that the similarity be exact is relaxed, an empirical relation between the two correlations may be found. To distinguish this second try from the first, let

$$K\xi = \sqrt{v^2\tau} \quad (19)$$

where K is varied in such a way that

$$\frac{1}{2} \overline{Y^2}(\tau) = \int_0^{K\xi} \left[\int_0^{K\xi'} f(K\xi'') d(K\xi'') \right] d(K\xi') \quad (20)$$

The heat wake data of Fig. 6 and the Eulerian correlations in Fig. 2 were first used by Baldwin²⁵ to find the functional form of K . The trial and error process for finding K that was used to satisfy Eq. (20) was restricted to the positive portion of the $f(\xi)$ curves because the constancy of the $\overline{Y^2}$ curves far from the source implies that $R(\tau)$ has approached a zero asymptote monotonically from +1.0. The K -results given earlier in Ref. 25 are shown as solid curves in Fig. 10. Repeating this analysis for the helium data and using the $f(\xi)$ curves of Fig. 1 gave results shown as the dashed curves.

The empirical factor K in Fig. 10 has been found to relate hot-wire anemometer correlations to the Lagrangian autocorrelation coefficients. Two limitations should be stressed. At very long times, the Lagrangian coefficient approaches zero monotonically, and Eulerian correlation $f(\xi)$ dips below zero to slightly negative values before approaching a zero value asymptote. Thus, the empirical correlation has been restricted to the positive portion of the $f(\xi)$ curves. On Fig. 10, this shows as an abrupt terminus of the K -curves. In the

microscale region of small times, the empirical factor varies considerably. This finding is consistent with the first test for similarity. However, there is an appreciable range of ξ and τ where K is constant, so the idea that similarity might exist was not too bad.

A criticism of the empirical relation found above is that the factor K varied appreciably over a fairly narrow range of turbulent flows. The K factor varied from about 1.2 to 0.14 as the turbulent velocity $\sqrt{u^2}$ varied from 1.8 to 4.8 ft/sec. How, then, might laboratory results apply to far different conditions, say in atmospheric turbulence? A recent review related to this question has been published by Hay and Pasquill,²⁶ so the present results may be compared with the data of that review. Hay and Pasquill compare Eulerian autocorrelations $f(t)$ with the Lagrangian $R(\tau)$ by using the relation $\beta t = \tau$. In the present work, "Taylor's hypothesis" has been used to transform the measured autocorrelations into spacial correlations to emphasize their Eulerian nature. To compare the present results with those of Hay and Pasquill, the following relations are required:

$$K\xi = \sqrt{v^2}\tau \quad (21)$$

and

$$KU_{\xi}t = \sqrt{v^2}\tau \quad (22)$$

For the present work, $\sqrt{v^2}/U_{\xi} \approx 0.03$ so that

$$\frac{K}{0.03} t = \tau \quad (23)$$

Therefore, Hay and Pasquill's β is approximately $K/0.03$. For their survey purposes, it was convenient to note, but to disregard, the variation of K . So the present results yield rough values of β varying from 18 to 4 depending on the mean flow rate. The summary of their atmospheric diffusion tests gave an average β of 4 with a "scatter range" from 1.1 to 8.5. Considering the difficulty in running controlled parameter experiments in the atmosphere, this comparison of wind tunnel data to atmospheric is a remarkable result, which hopefully will encourage more experiments of a similar kind.

An alternate method for predicting turbulent diffusion from hot-wire autocorrelations was proposed six years ago by Mickelsen.¹⁸ The double integral of the Eulerian correlation ω_f was discussed earlier; it has the units of square feet as does $\frac{1}{2} \overline{Y^2}$. If the value of the ω_f curve at a value ξ_1 is compared with an equal value of the diffusional variance $\frac{1}{2} \overline{Y^2}$ at τ_1 , it was found that a simple empirical relation exists between the ξ_1 and τ_1 values. Figure 11 gives the calculated ω_f curves, and Fig. 12 summarizes the empirical comparison. Note that the space and time coordinates are directly proportional so that, if $\xi = B\sqrt{v^2\tau}$, it was found that $B \approx 0.7$ fits all of the data fairly well. This simple relation could have utility if the objective were to predict the diffusional variance $\frac{1}{2} \overline{Y^2}$ from hot-wire measurements. However, it is difficult to relate this empirical factor B to the Eulerian and Lagrangian correlation coefficients or to the similarity of their space and time coordinates.

The final experimental relation between turbulent diffusion and hot-wire anemometer measurements that will be discussed herein involves the mixed Eulerian space-time correlations of Fig. 3. Favre et al.²⁷ were the first to report extensive measurements of two-point, two-time velocity correlations. In his analysis of their results, Bass²⁸ set up the space-time equivalents of the Karman-Howarth equation, but naturally no solutions were obtained. Recently, Deissler²⁸ has extended his analysis of turbulent dynamics to these mixed correlations. So, although correlations of this type played almost no role in the initial development of homogeneous turbulence theory,² discussions of these general Eulerian functions are now available.

J. M. Burgers³⁰ suggested briefly (in fact, almost parenthetically) that, in a flowing homogeneous turbulence, the function $R_u(\xi, \tau)$ evaluated along $\xi = U\tau$ would be expected to be approximately equal to the Lagrangian single particle correlation. Reference 25 discusses the physical significance of this idea and demonstrates that two principle assumptions are necessary: (1) The Lagrangian derivative is assumed to be:

$$\frac{Dv}{Dt} \approx \frac{\partial v}{\partial t} + U \frac{\partial v}{\partial x} \quad (24)$$

That is, the products of fluctuation terms are neglected:

$$u \frac{\partial v}{\partial x} + v \frac{\partial v}{\partial y} + w \frac{\partial v}{\partial z} \approx 0$$

(2) The interchange of particle averaging is assumed to be the same as in the assumption that $\overline{v_{La}^2}$ equals $\overline{v^2}$. After presenting some

experimental results, this discussion will be continued, but the motivation for this comparison should be clear at the outset. If successful, this experimental relation would be ideal because it is not only easily measured but also easily interpreted in the theory. If one thinks of a nearly stationary (on the diffusion time scale) "box of turbulence" moving at a velocity U , then the comparison to be made is between the Eulerian time-autocorrelation at a fixed point in this box to the Lagrangian single-particle correlation.

The comparison of $R_u(\xi, \tau)$ to $R(\tau)$ should be made for that slice of the general Eulerian correlation which occurs along $\xi = U\tau$. In the theoretical development,^{30,25} it is implicitly assumed that the peak correlation value will occur along this line for all values of ξ and τ . An isometric sketch is given in Fig. 13 to demonstrate this point. However, all the data in Fig. 3 show that the peak correlation occurs along $\xi = 0.93U_c\tau$. That is, the apparent convective velocity is 93 percent of the local centerline velocity. A possible explanation might be that the axial turbulent core receives some large-scale contributions from adjacent lower velocity flows, since the surrounding mean flow is always less than the centerline velocity. However, in all probability there is more to it than that. Laurence³¹ found the convective velocity was about 0.89 local stream velocity in the mixing region of a free jet. Bass²⁸ has noted a similar trend in the grid turbulence data of Favre, where the influence of shear should be negligible. In that work, the convective velocity of the peak correlation was consistently 0.985 percent of the mean flow. Bass used this fact,

together with the inconsistency of the two other u-correlations measured by Favre, to conclude that "the scheme (isotropy) utilized for studying the space-time correlations is not satisfactory for representing the turbulence in a wind tunnel. Now this scheme reduces, for $\tau = 0$, to the scheme generally adopted, which is in good agreement with experiment (like our Table I). The divergence between theory and experiment, small for $\tau = 0$, becomes much more apparent when τ is not zero.²⁸

Having pointed out this problem of approximate theory versus experiment, it now remains to find the experimental relation between $R_u(\xi, \tau)$ and $\mathcal{R}(\tau)$, using both of the mean velocities that were determined by experiment to be important. That is, what has been called the convective velocity $U_c = 0.93 U_{\xi}$ and the centerline velocity U_{ξ} will both be used in $\xi = U\tau$ for a specific evaluation of $R_u(\xi, \tau)$. Figure 14 shows the values read from Fig. 3 for the convective velocity case, and Fig. 15 gives the centerline velocity evaluation. With the exception of data from Fig. 3a, which is the lowest flow velocity, the values of these Eulerian curves $R_u(\xi, \tau)|_{\xi=U\tau}$ cannot be distinguished at different flow rates. So a single curve and scatter band have been shown of Figs. 14 and 15 for $U_{\xi} = 106, 135$ and 160 ft/sec. The results of Figs. 14 and 15 were next used to predict the diffusion variance, assuming that $R_u(\xi, \tau)|_{\xi=U\tau} = \mathcal{R}(\tau)$. That is,

$$\frac{1}{2} \overline{Y_P^2} \equiv \overline{v^2} \int_0^t \left[\int_0^{t'} R_u(\xi, \tau) \Big|_{\xi=U\tau} d\tau \right] dt' \quad (25)$$

where the subscript p indicates "predicted." The results of these calculations are shown in Figs. 16 and 17 for the two cases. The values of $\overline{v^2}$ taken from Ref. 25 are listed on Fig. 15. In both figures, the initial portion of the $\frac{1}{2} \overline{Y_p^2}$ curves are in fair agreement with the diffusion data of Fig. 6. At longer times, the convective velocity curves in Fig. 16 become increasingly poor, overpredicting the asymptotic slopes of the $\frac{1}{2} \overline{Y^2}$ curves at large times by factors of 1.5 to 3.6. For the local velocity evaluation of $R_u(\xi, \tau)|_{\xi=U\tau}$ in Fig. 17, the $\frac{1}{2} \overline{Y_p^2}$ curves also overpredict the diffusion; but the long-time asymptotic slopes are too large by lesser factors, 1.03 to 2.3. In other words, the prediction of eddy diffusivity based on Taylor's theory of continuous movements^{e.g., 25} and the assumed equivalence of $R_u(\xi, \tau)|_{\xi=U\tau}$ to $R(\tau)$ was within a factor of 2.3 of the observed eddy diffusivity. Since the method involves no adjustable constants, this "agreement" is considered a useful result.

By now the assumptions have been "stacked rather high," but perhaps one parting comment will help make the foregoing more plausible. It has long been postulated that turbulent diffusion proceeds essentially apart from the small-scale, dissipative motions and that the energy-containing eddies are mainly responsible for dispersion (Ref. 7, p. 383; see also the early work of Brier³² and Gifford.³³). So it may be argued that an interpretation of the Eulerian function $R_u(\xi, \tau)|_{\xi=U\tau}$ is that it maps the average life history of these energy-containing eddies. Therefore, it may be the most likely candidate for experimental relations between hot-wire measurements and turbulent diffusion parameters. An improvement

might be realized if $R_v(\xi, \tau)$ were measured, but this would come only at the expense of considerable experimental complexity.

It would be interesting to have micrometeorological data, such as Hay and Pasquill reported, also evaluated in terms of simultaneously measured space-time correlations. Another critical test might be made in the laboratory. Deissler²⁹ has predicted diffusion results in grid turbulence before the final decay period, using the approximate equivalence of space-time correlations and Lagrangian single-particle correlations. Deissler obtained good agreement for small and intermediate diffusion times with two sets of diffusion data obtained by Uberoi and Corrsin.¹⁰ Although the additional complication of nonstationary turbulence is necessary to the analysis, the simultaneous evaluation of $R_u(\xi, \tau)$ and $R(\tau)$ in this type of flow might be fruitful. (A few years ago, this would have been considered a well-explored flow field.)

CONCLUDING REMARKS

Several forms of experimental relations have been presented that relate hot-wire anemometer measurements and turbulent diffusion in homogeneous flows. A simple similarity transformation was not adequate for relating the Eulerian correlations $f(\xi)$ and the Lagrangian single-particle correlation $R(\xi)$. However, empirical factors defined by Eqs. (19) and (20) were found which relate the space axis of $f(\xi)$ to the time axis of $R(\tau)$. These factor curves are summarized in Fig. 10. If one settles for only a rough fit of the diffusion data, these empirical factors are shown to be in accord with micrometeorological findings.

An alternate procedure for predicting turbulent diffusion wakes from the double integration of the $f(\xi)$ curves are summarized briefly. The procedure worked fairly well in the present experimental range (see Figs. 11 and 12), but it may be difficult to work back to the relation of $f(\xi)$ and $R(\tau)$.

Finally, an Eulerian space-time correlation $R_u(\xi, \tau)$ was mapped using the time correlation of two wires separated at various distances ξ along the axis of the mean flow. The special case of $R_u(\xi, \tau)$ evaluated along $\xi = U\tau$ (where U is the local mean flow velocity) was shown to be approximately equivalent to the Lagrangian single-particle correlation. The eddy diffusivities predicted from hot-wire data alone (i.e., $\overline{v^2}$ and $R_u(\xi, \tau)|_{\xi=U\tau}$) was found to be 1.05 to 2.3 times larger than that inferred from actual diffusion data.

REFERENCES

1. G. I. Taylor, Proc. Roy. Soc. (London), vol. 151, (1935), p. 421.
2. G. K. Batchelor, "Theory of Homogeneous Turbulence," Cambridge Univ. Press (England), 1956.
3. G. I. Taylor, Proc. London Math. Soc., vol. 20, 1922, p. 196.
4. F. N. Frenkiel, in "Advances in Applied Mechanics," Vol. III, p. 61, Academic Press (New York), 1953.
5. W. R. Mickelsen, NACA, Report 1300, 1957.
6. A. A. Townsend, Proc. Roy. Soc. (London), vol. 224, 1954, p. 417.
7. G. K. Batchelor and A. A. Townsend, "Turbulent Diffusion Surveys in Mechanics," Cambridge Univ. Press (England), 1956.
8. G. K. Batchelor, A. M. Binnie and O. M. Phillips, Proc. Roy. Soc., Series A, 1957 or 1958.

9. G. B. Schubauer, NACA, Report 524, 1935.
10. M. S. Uberoi, and S. Corrsin, NACA, Report 1142, 1953.
11. W. R. Mickelsen, J. Fluid Mech., vol. 7, 1960, p. 397.
12. P. G. Saffman, J. Fluid Mech., vol. 8, 1960, pp. 273-283.
13. L. F. Richardson, Proc. Roy. Soc., Series A, vol. 110, 1926, p. 709
14. G. I. Taylor, "Advances in Geophysics," Vol. 6, p. 105, Academic Press (New York), 1959.
15. J. C. Laurence, and L. G. Landes, NACA TN 2843, 1952.
16. V. A. Sandborn, NACA TN 3266, 1955.
17. E. R. Carlson, C. C. Conger, J. C. Laurence, E. H. Meyn and R. A. Yocke, Proc. Inst. Radio Engrs., vol. 47, 1959.
18. W. R. Mickelsen, NACA TN 3570, 1955.
19. L. V. Baldwin, Ph.D. thesis, Case Inst. Tech. (Cleveland, Ohio), 1959.
20. L. V. Baldwin, V. A. Sandborn and J. C. Laurence, "Heat Transfer," Trans. A.S.M.E., Series C., vol. 82, no. 2, 1960, p. 77.
21. G. B. Schubauer, and P. S. Klebanoff, NACA WR W-86, 1946.
22. L. V. Baldwin, V. A. Sandborn and J. C. Laurence, Am. Soc. Mech Engrs., Paper No. 59-HT-5.
23. H. L. Grant and J. C. T. Nisbet, J. Fluid Mechanics, vol. 263, 1957.
24. T. von Karman and L. Howarth, Proc. Roy. Soc. (London), Series A, vol. 164, 1938, p. 192.
25. L. V. Baldwin and T. J. Walsh, A.I.Ch.E. Journal, vol. 7, no. 1, March 1961, pp. 53-61.
26. J. S. Hay and F. Pasquill, "Adv. in Geophysics," Vol. 6, pp. 345-366, Academic Press, 1959.

27. A. Favre, J. Gaviglio, and R. Dumas, NACA TM 1370, 1955.
28. J. Bass, "Space and Time Correlations in a Turbulent Fluid, I and II," Vol. II, p. 55, Univ. of Calif. Public. in Statistics, 1954.
29. R. G. Deissler, NASA TR R-96, 1961.
30. J. M. Burgers, Rep. No. E-34.1, Calif. Inst. Tech., July 1951.
31. J. C. Laurence, NASA TN D-294, 1960.
32. G. W. Brier, Meteorol. Monographs, vol. 1, 1951, p. 15.
33. F. Gifford, Monthly Weather Review, vol. 83, no. 12, March 1956, pp. 293-301.

TABLE I. - A LIMITED EXPERIMENTAL EVALUATION
OF TAYLOR'S HYPOTHESIS

$R_u(\xi, 0)$ MEASURED SPACE CORRELATIONS			$R_u(0, t)$ MEASURED AUTOCORRELATIONS	
U_{ξ} FT/SEC	$f(\xi)$ (NONE)	ξ (IN.)	$t = \frac{\xi}{U_{\xi}}$ (MILLISECONDS)	$f(t)$ (NONE)
160	$\left\{ \begin{array}{l} 1.0 \\ 0.39 \\ \text{----} \\ 0.0 \end{array} \right.$	$\left\{ \begin{array}{l} 0. \\ 2.0 \\ 4.0 \\ 6.0 \end{array} \right.$	$\left\{ \begin{array}{l} 0. \\ 1.04 \\ 2.08 \\ 3.12 \end{array} \right.$	$\left\{ \begin{array}{l} 1.0 \\ 0.44 \\ 0.11 \\ 0.01 \end{array} \right.$
135	$\left\{ \begin{array}{l} 1.0 \\ 0.28 \\ 0.05 \\ -0.04 \end{array} \right.$	$\left\{ \begin{array}{l} 0. \\ 2.0 \\ 4.0 \\ 6.0 \end{array} \right.$	$\left\{ \begin{array}{l} 0. \\ 1.24 \\ 2.48 \\ 3.72 \end{array} \right.$	$\left\{ \begin{array}{l} 1.0 \\ 0.34 \\ 0.05 \\ -0.01 \end{array} \right.$
106	$\left\{ \begin{array}{l} 1.0 \\ 0.28 \\ 0.02 \\ -0.06 \end{array} \right.$	$\left\{ \begin{array}{l} 0. \\ 2.0 \\ 4.0 \\ 6.0 \end{array} \right.$	$\left\{ \begin{array}{l} 0. \\ 1.60 \\ 3.20 \\ 4.80 \end{array} \right.$	$\left\{ \begin{array}{l} 1.0 \\ 0.34 \\ 0.07 \\ -0.02 \end{array} \right.$
72.6	$\left\{ \begin{array}{l} 1.0 \\ 0.21 \\ 0.0 \\ -0.10 \end{array} \right.$	$\left\{ \begin{array}{l} 0. \\ 2.0 \\ 4.0 \\ 6.0 \end{array} \right.$	$\left\{ \begin{array}{l} 0. \\ 2.31 \\ 4.62 \\ 6.93 \end{array} \right.$	$\left\{ \begin{array}{l} 1.0 \\ 0.24 \\ 0.01 \\ -0.10 \end{array} \right.$

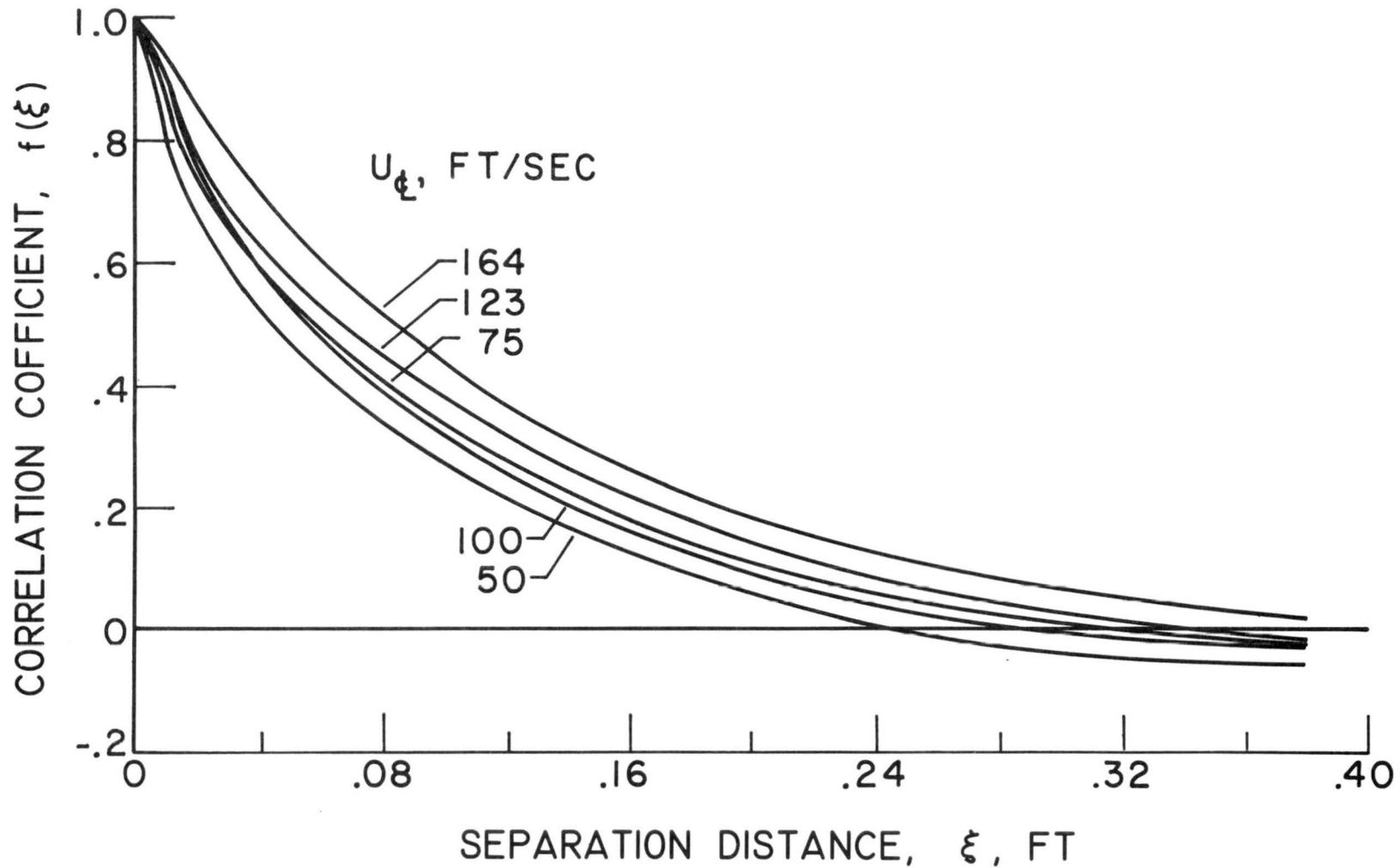


Fig. 1. Summary of correlation coefficients $f(\xi)$ calculated from measured correlation coefficients $g(\xi)$.

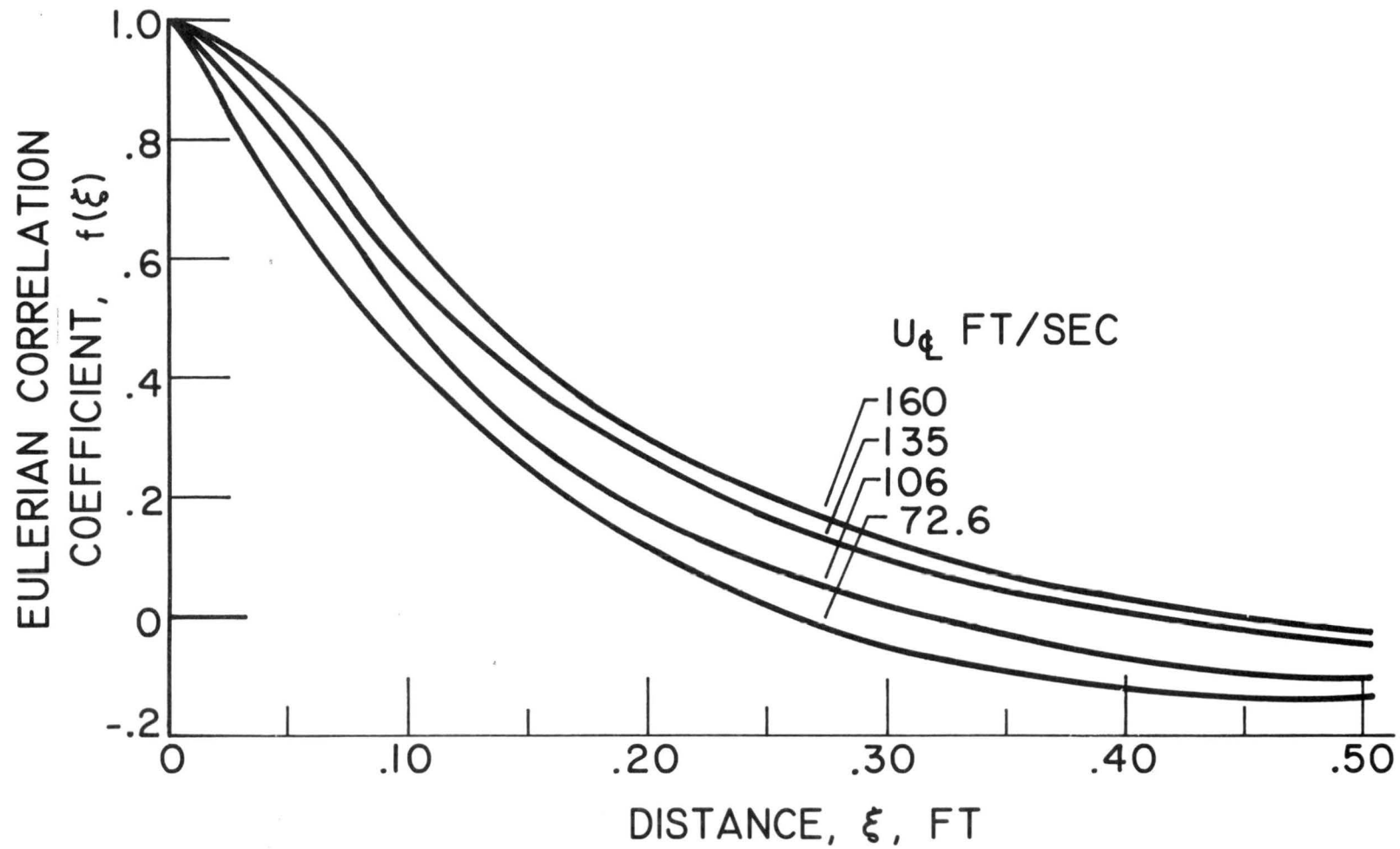


Fig. 2. Typical Eulerian correlation coefficients at each mean flow velocity.

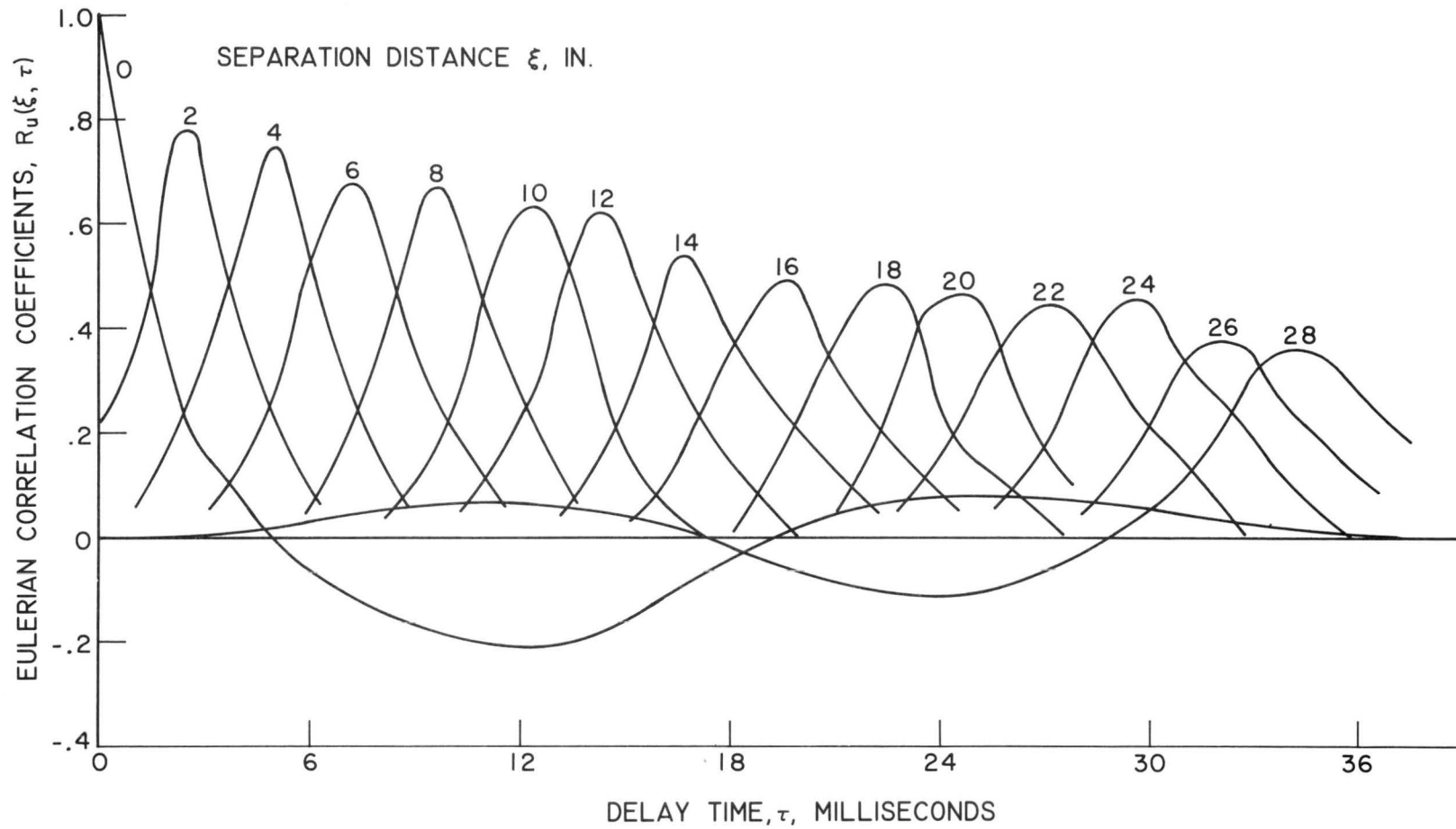


Fig. 3a. General Eulerian space-time correlation coefficient at mean flow velocity; $U_c = 73$ ft/sec.

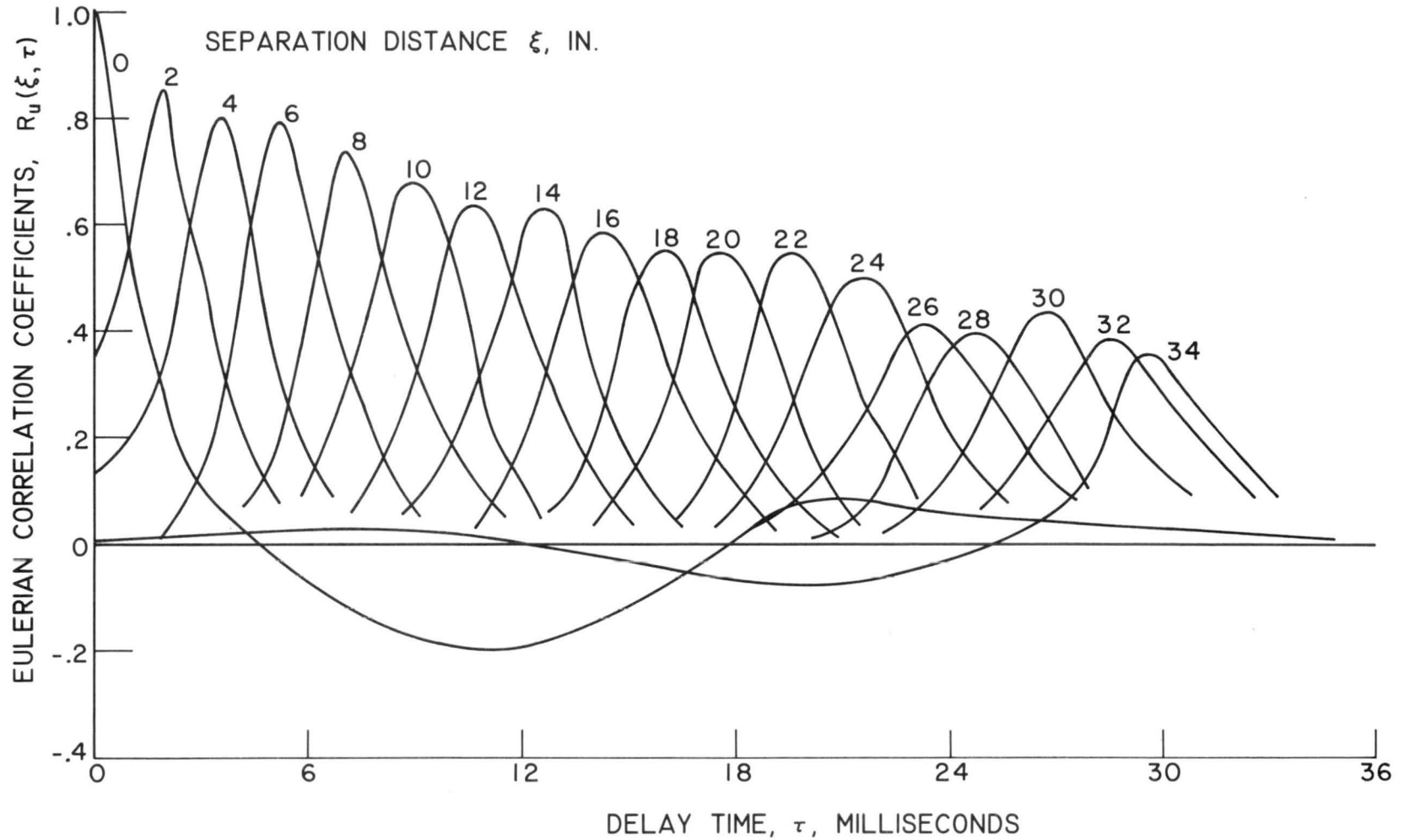


Fig. 3b. General Eulerian space-time correlation coefficient at mean flow velocity; $U_{\bar{t}} = 106$ ft/sec.

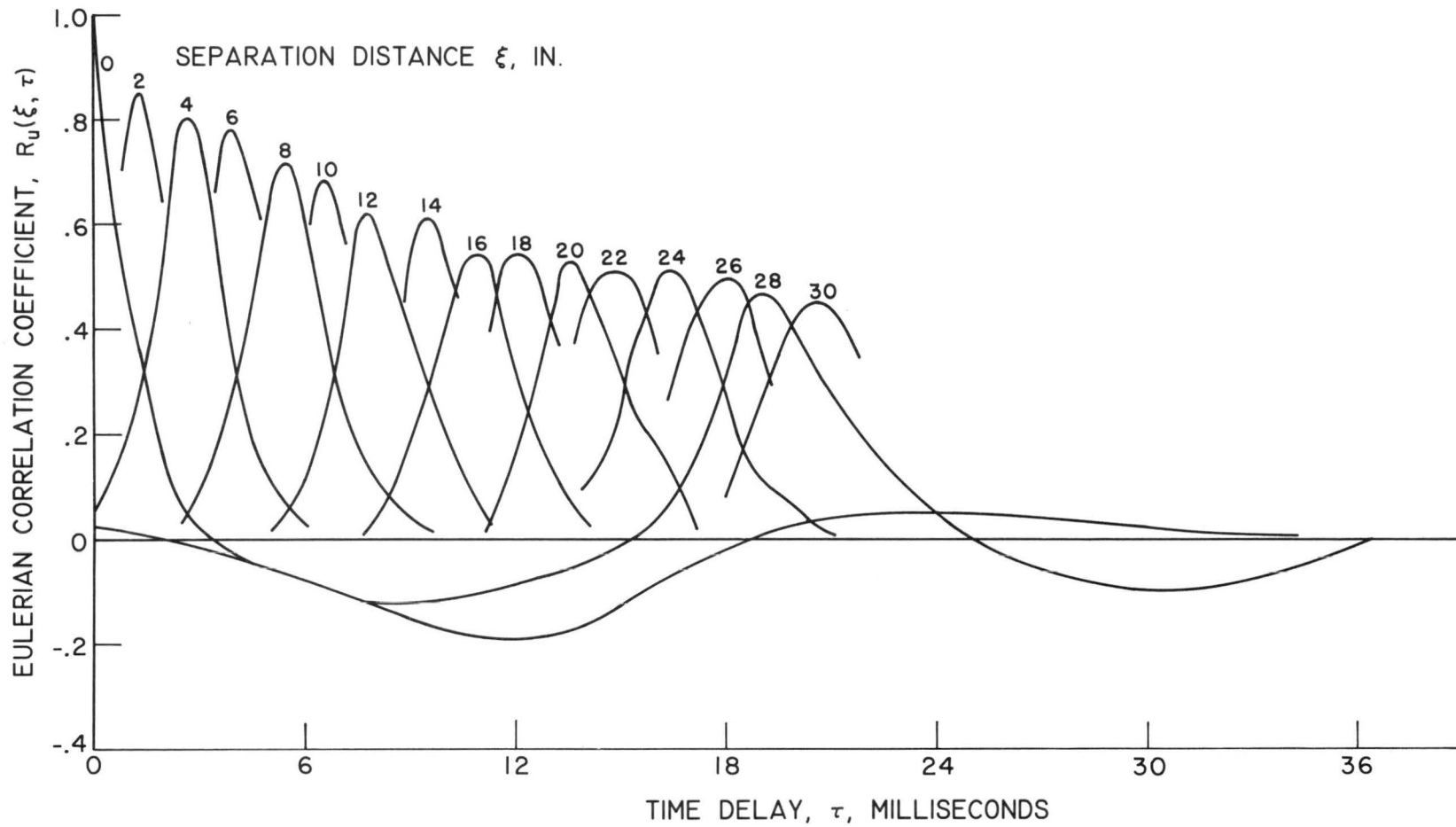


Fig. 3c. General Eulerian space-time correlation coefficient at mean flow velocity; $U_c = 135$ ft/sec.

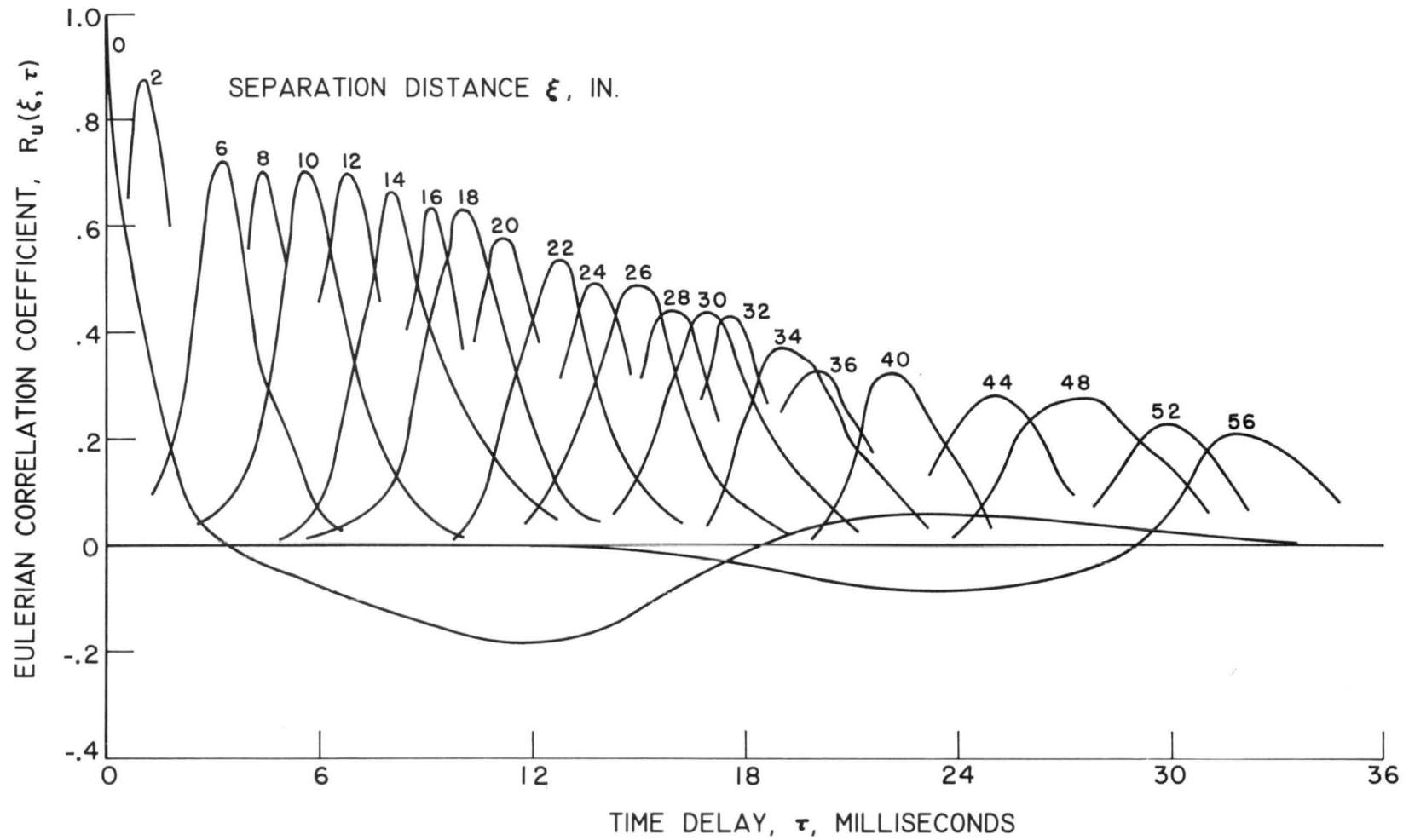


Fig. 3d. General Eulerian space-time correlation coefficient at mean flow velocity; $U_{\bar{c}} = 160$ ft/sec.

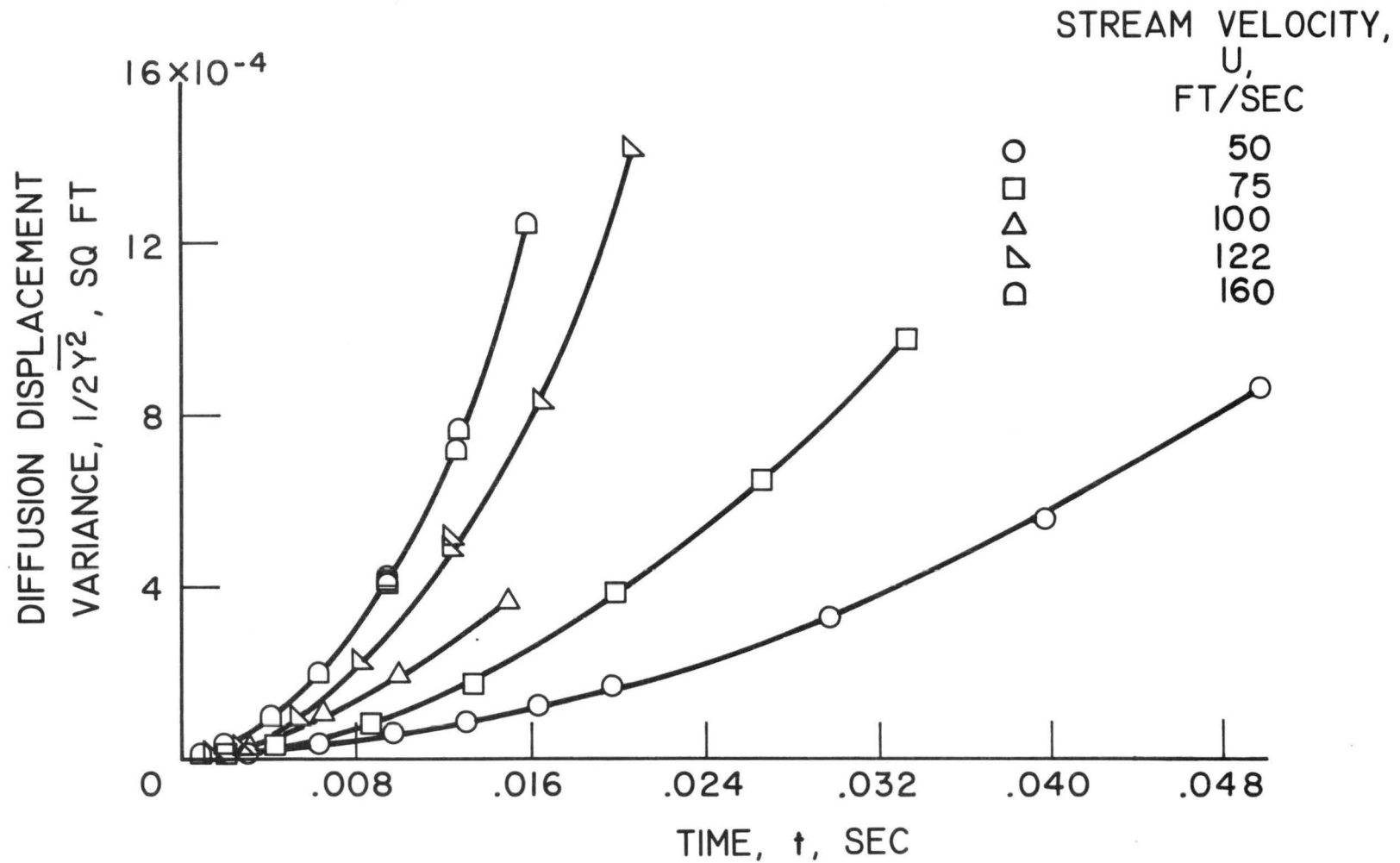


Fig. 4. Summary of helium diffusion data.

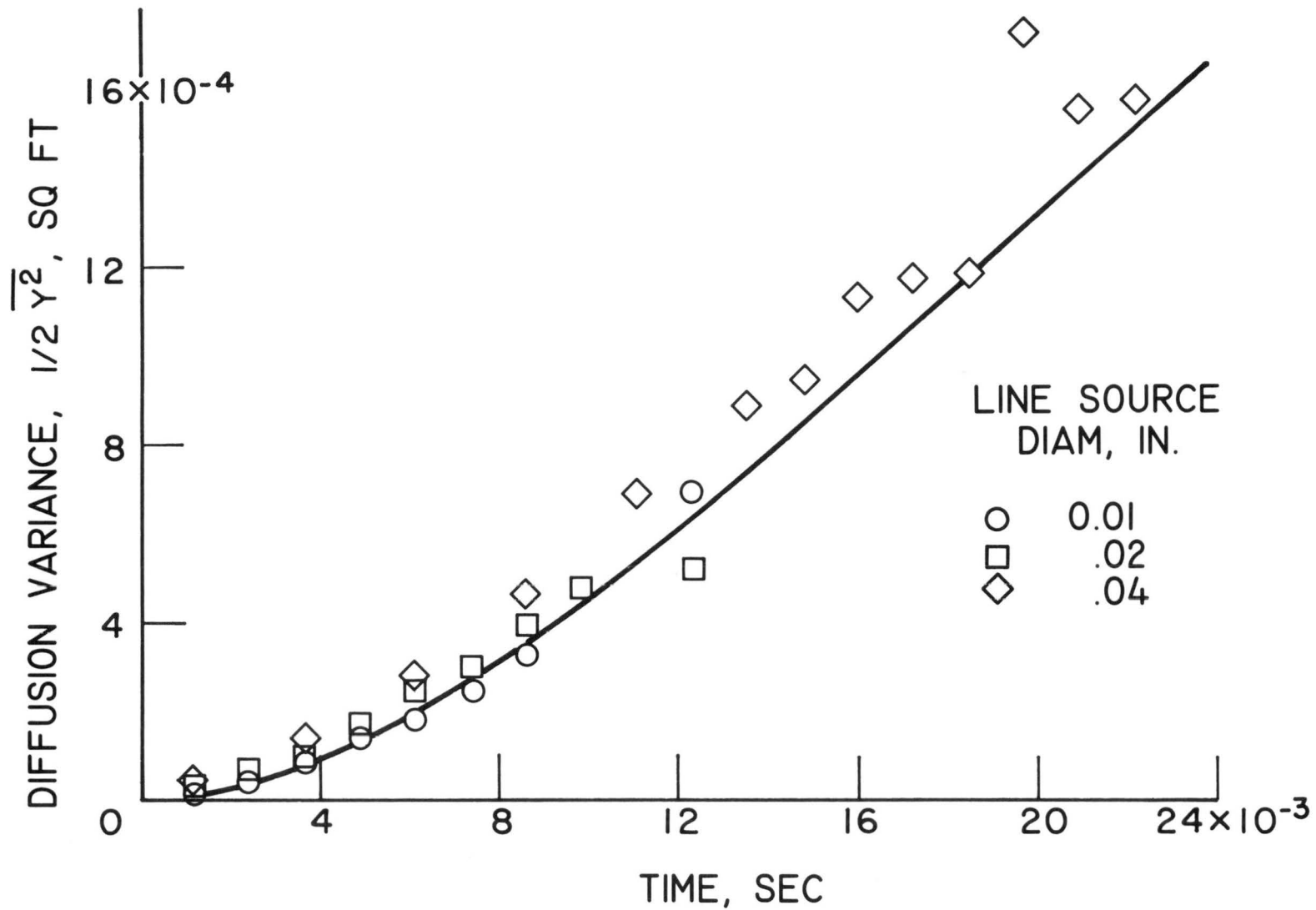


Fig. 5. Example of turbulent diffusion data at $U = 135$ ft/sec.

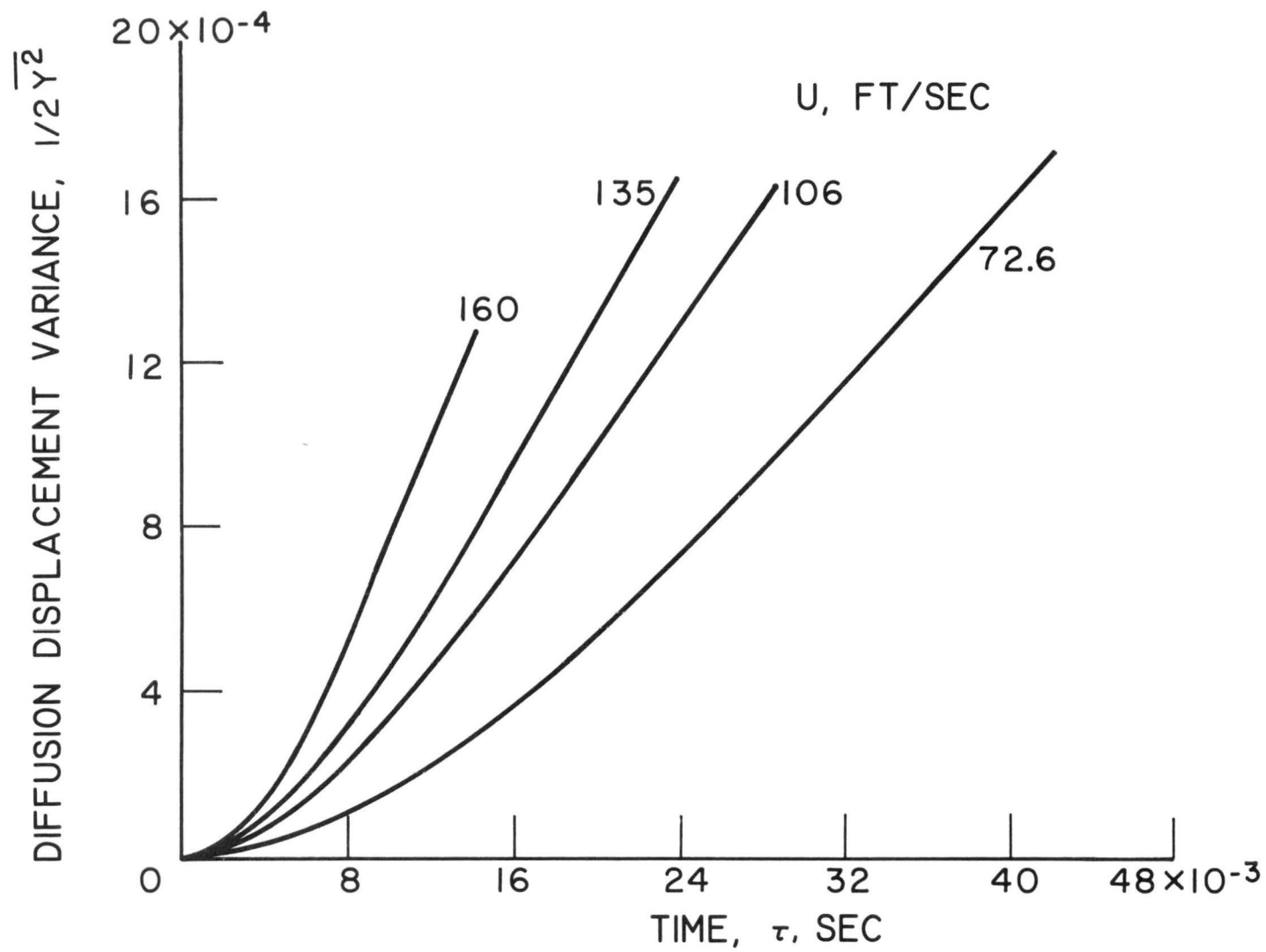


Fig. 6. Summary of heat diffusion data.

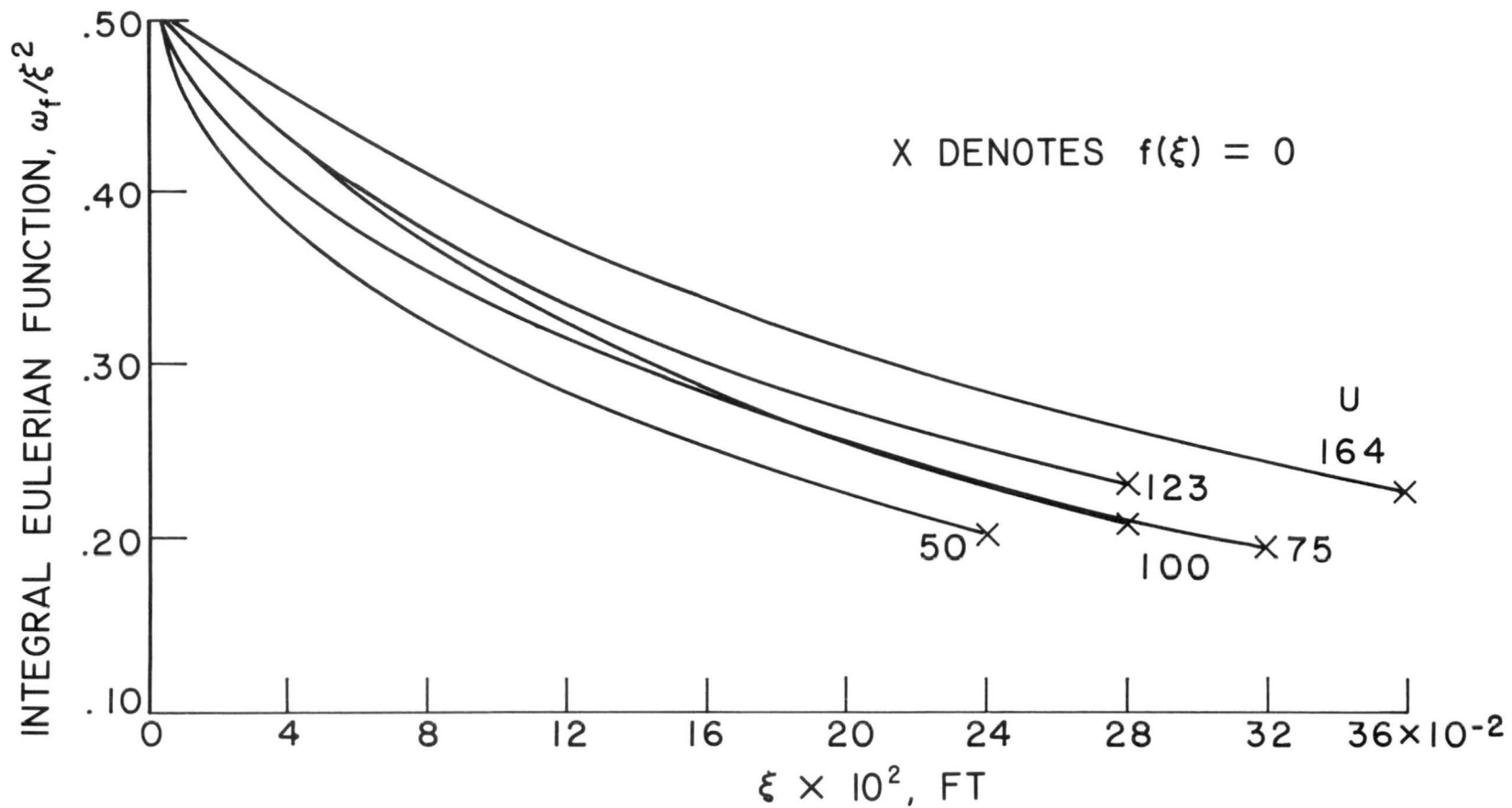


Fig. 7. Integral Eulerian function for similarity comparison of correlation coefficients. Calculated from Fig. 1. (Identical with ω_f of Fig. 11a within range of Fig. 11; i.e., $\xi > 0.06$ ft).

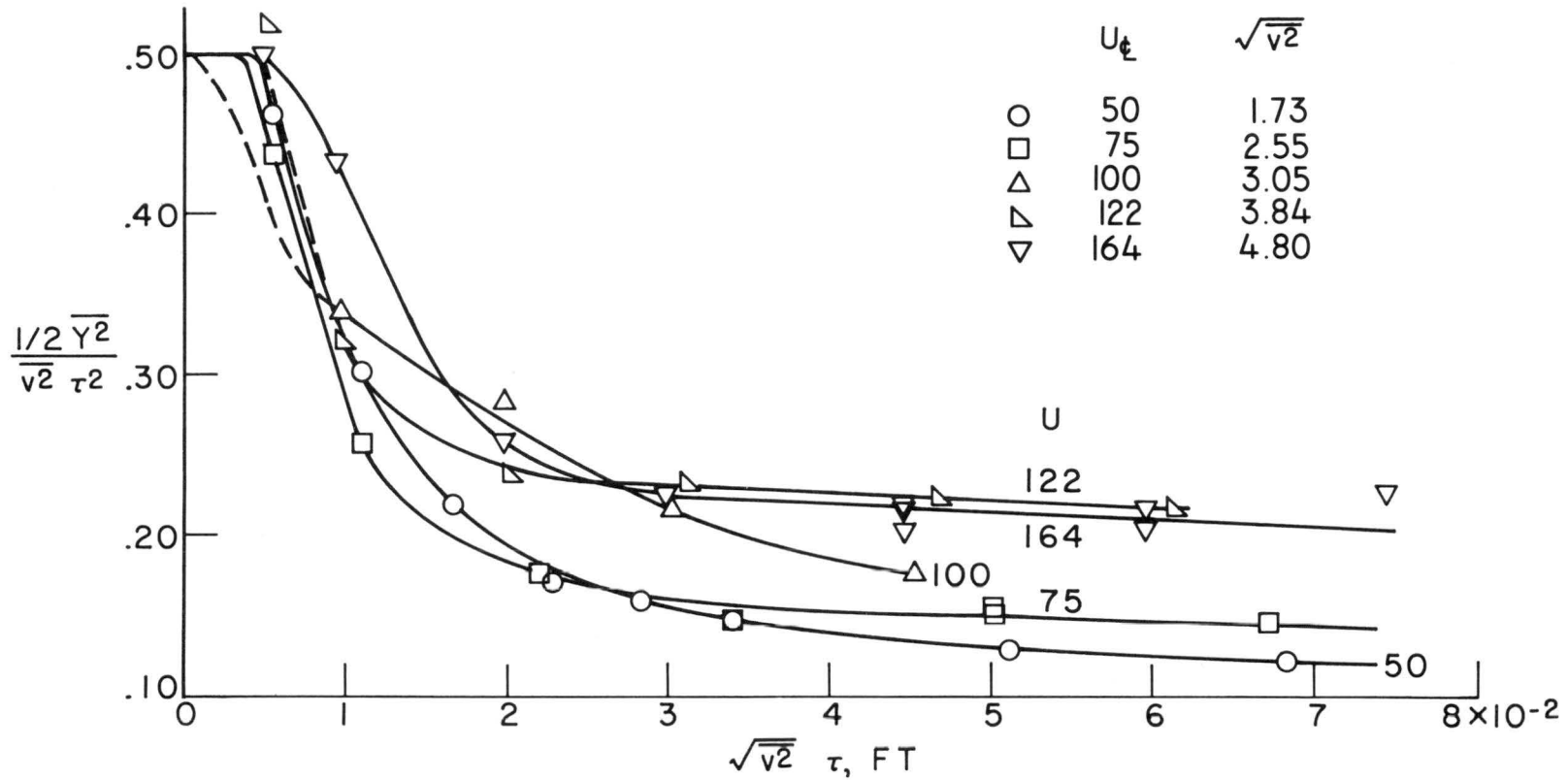


Fig. 8. Integral Lagrangian function for similarity comparison of correlation coefficients. Calculated from Fig. 12, TN3570. Note: Data points at lowest t for each curve was taken from table on p. 16, TN3570 (except $U = 100$).

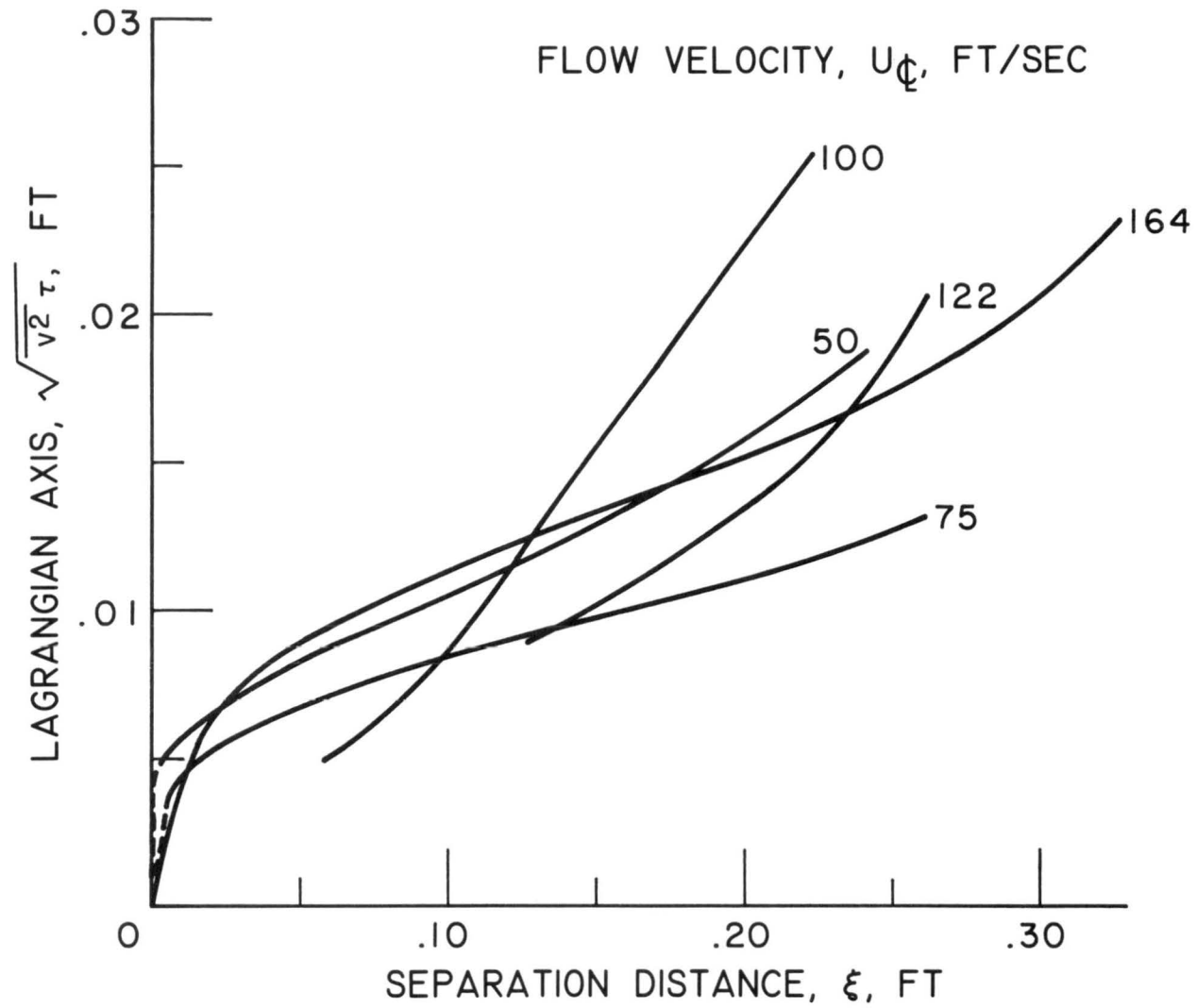


Fig. 9. Test for similarity of Eulerian correlation coefficient $f(\xi)$ and transformed Lagrangian correlation coefficient $R(A\tau)$.

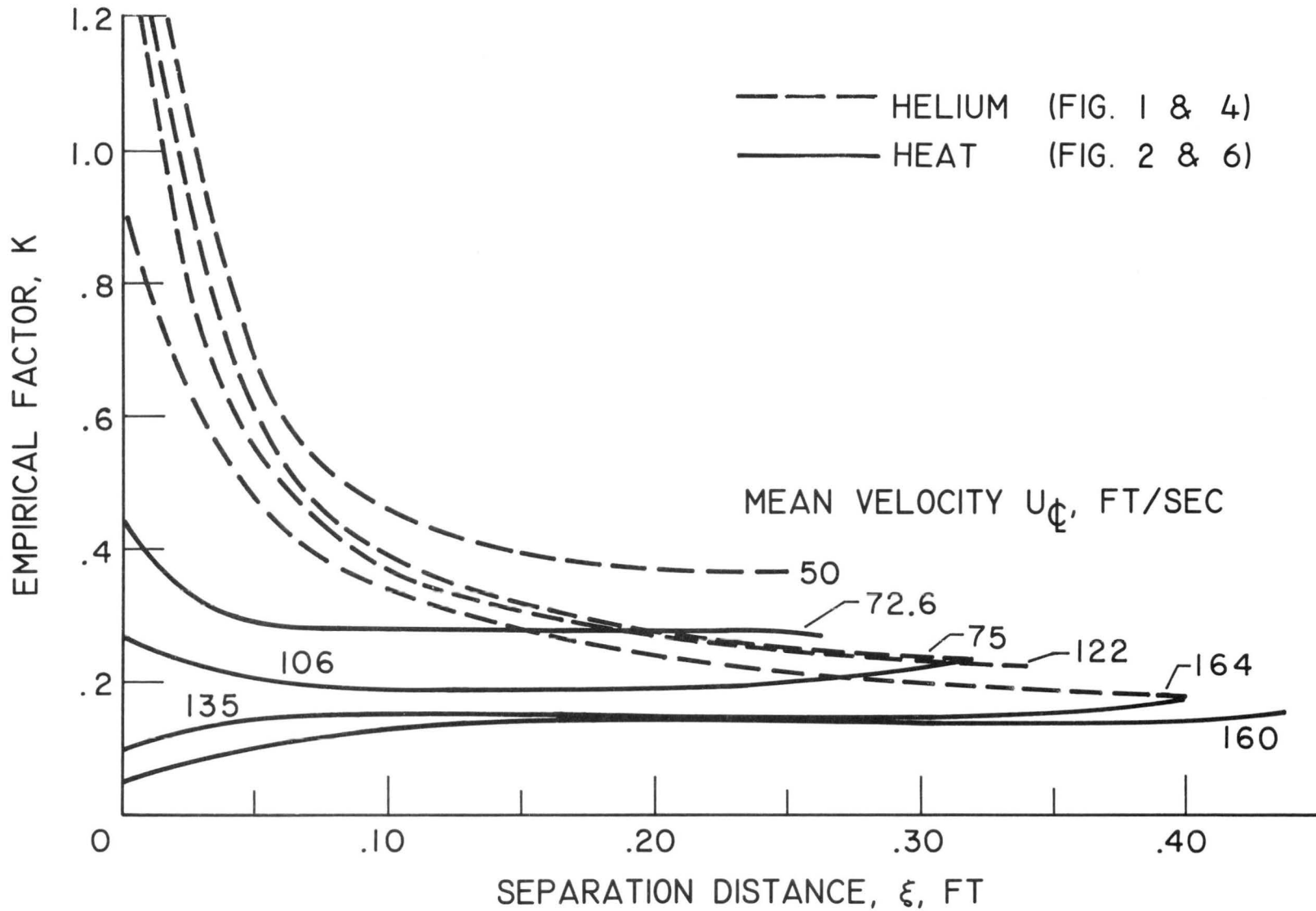


Fig. 10. Empirical factor Eulerian and Lagrangian correlation coefficients.

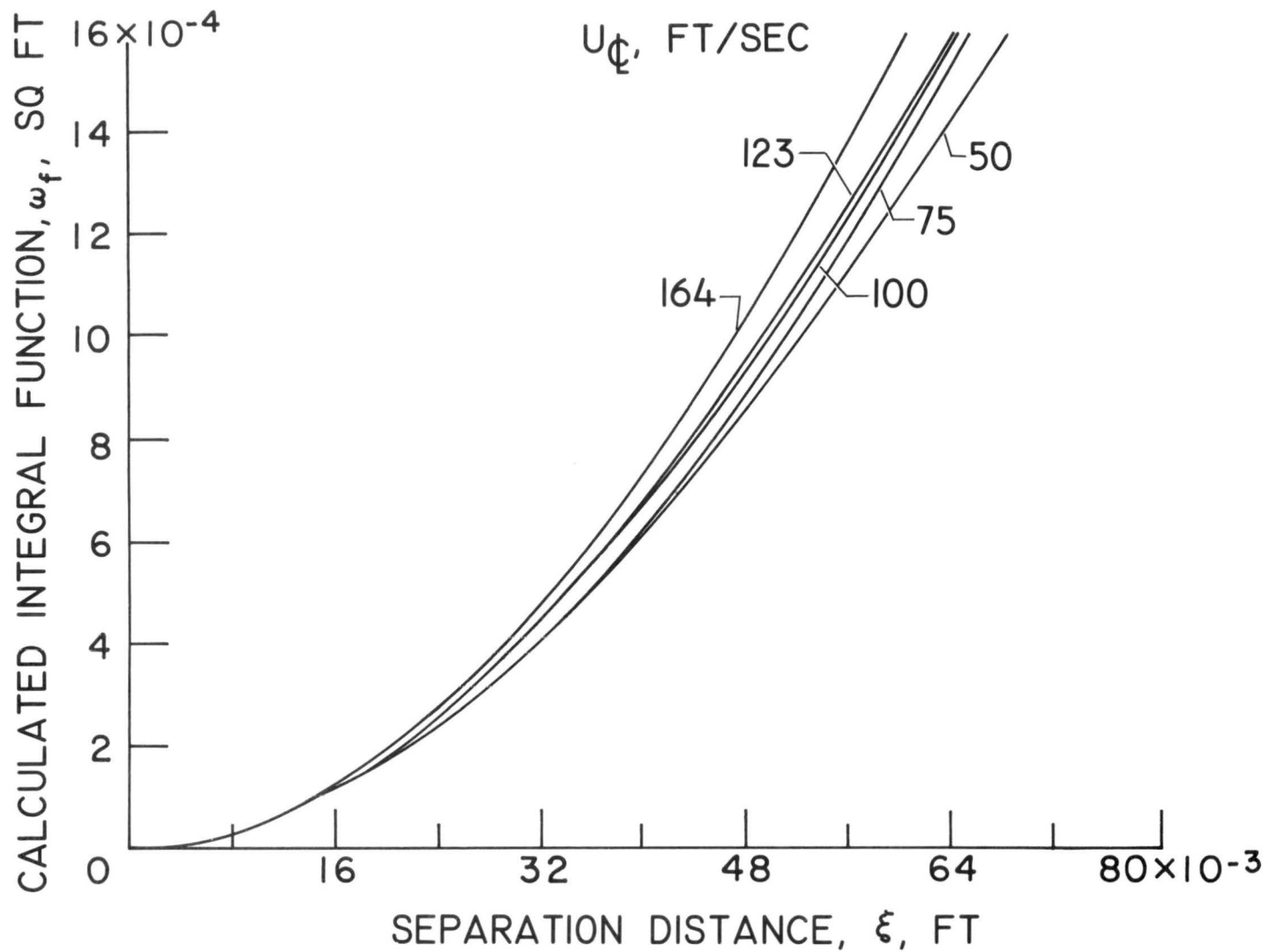


Fig. 11a. Summary of integral function ω_f calculated from Eulerian correlation coefficients $f(\xi)$ in Fig. 1.

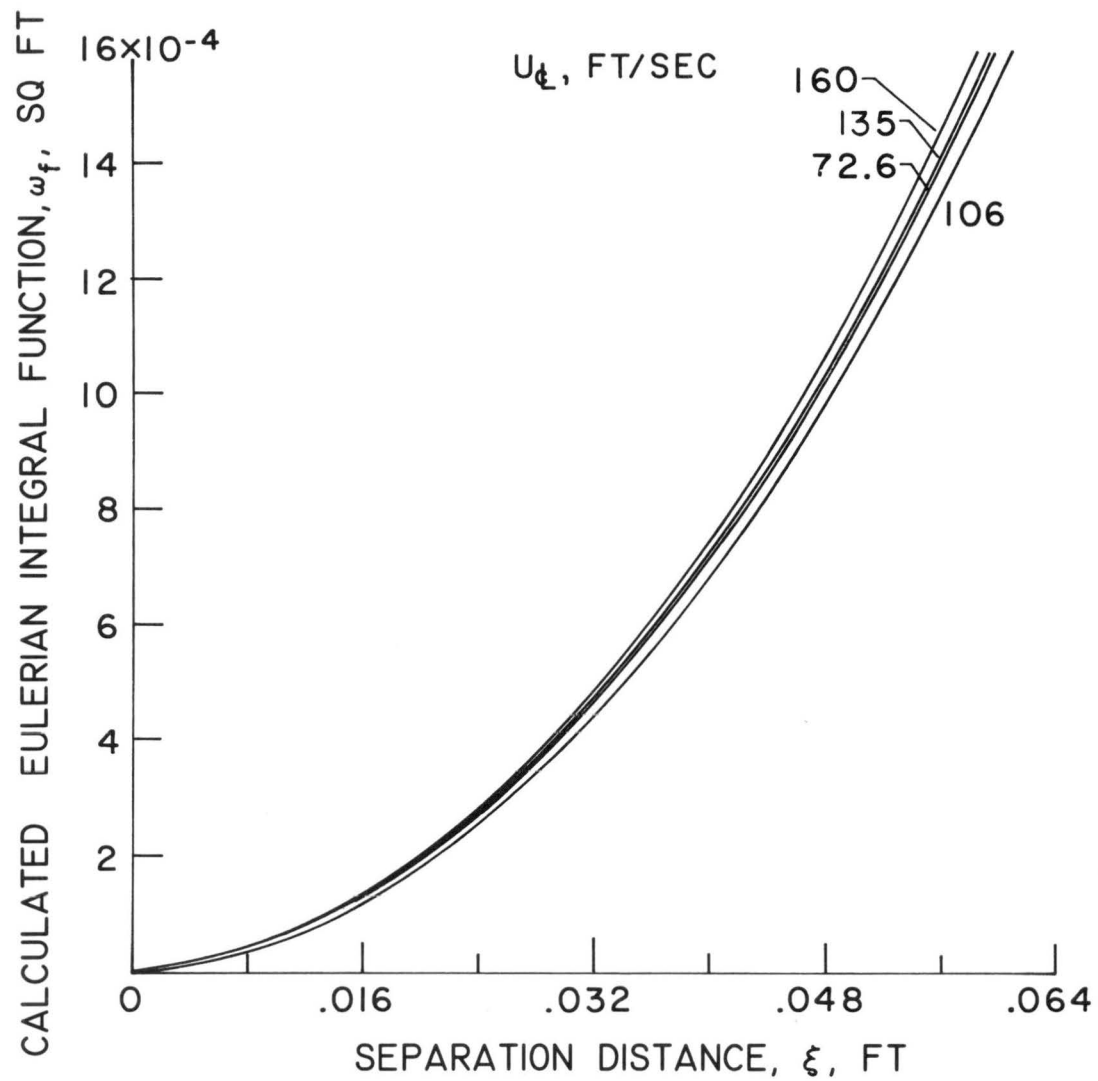


Fig. 11b. Summary of Eulerian integral functions calculated from Eulerian correlation coefficients $f(\xi)$ in Fig.2.

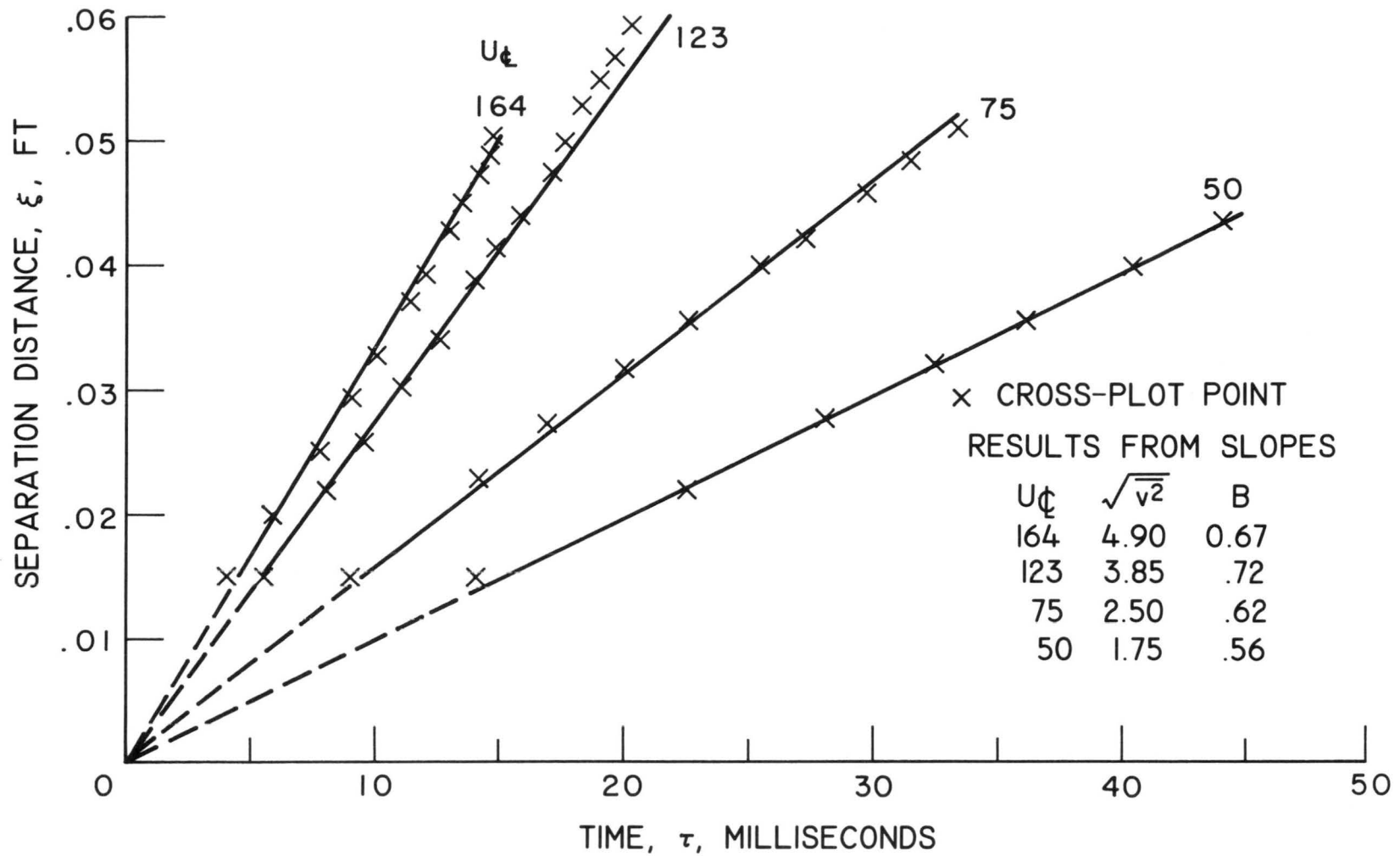


Fig. 12a. Crossplot of Figs. 11a and 4 showing relation between ω_f and $\frac{1}{2}Y^2$.

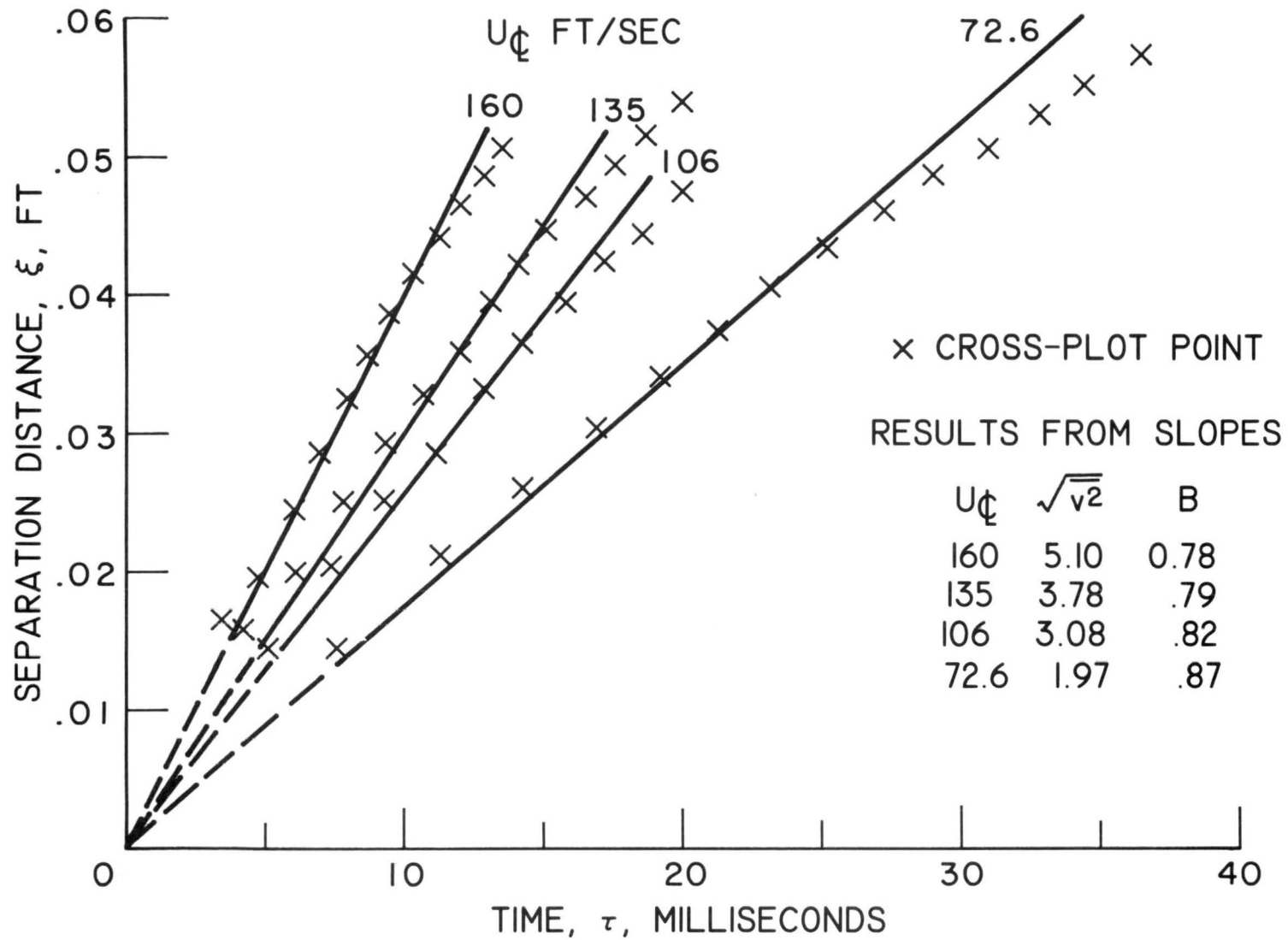


Fig. 12b. Crossplot of Figs. 11b and 6 showing relation between ω_F and $\frac{1}{2}\bar{Y}^2$.

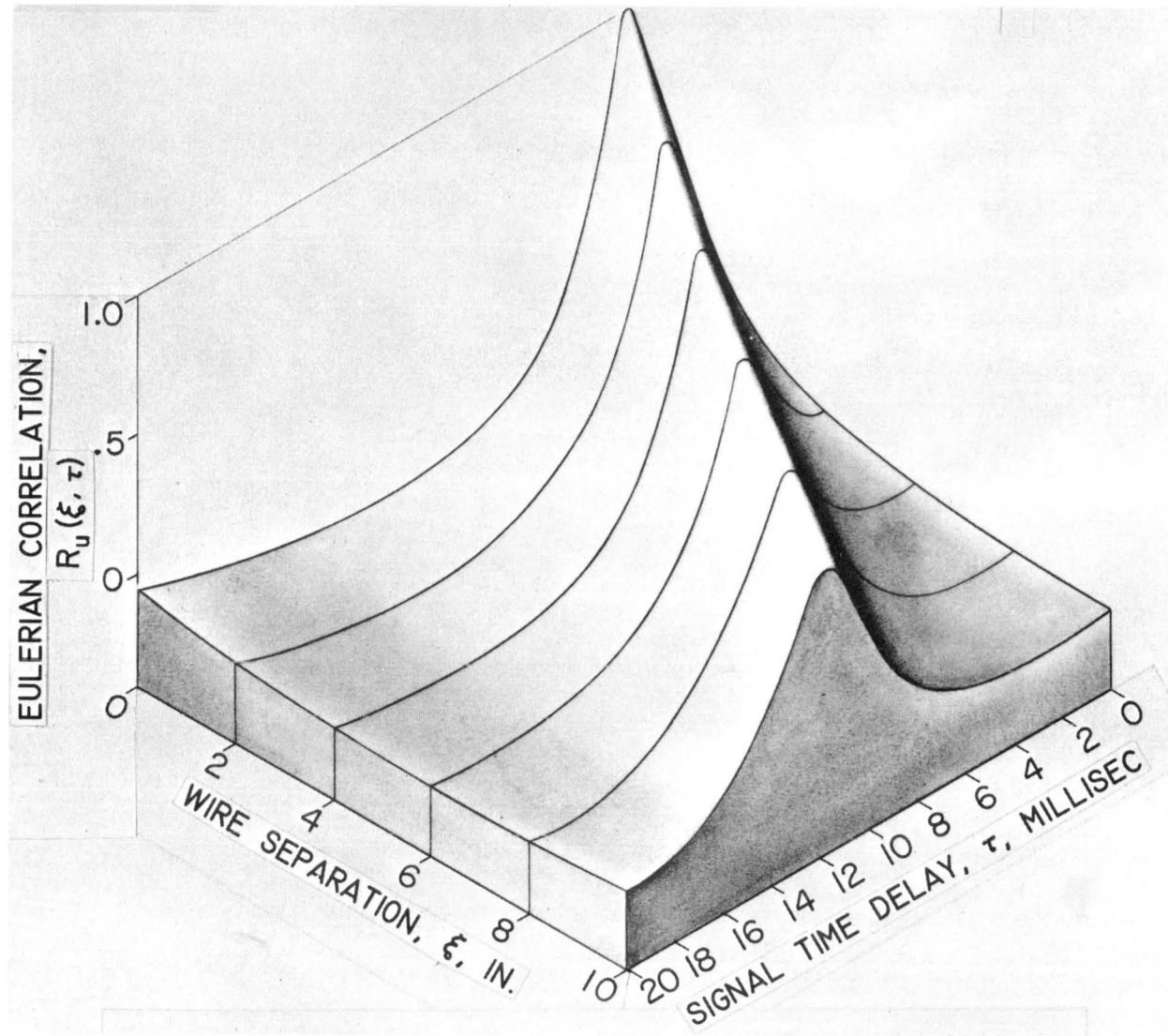


Fig. 13. Isometric sketch of example general Eulerian correlation coefficient.

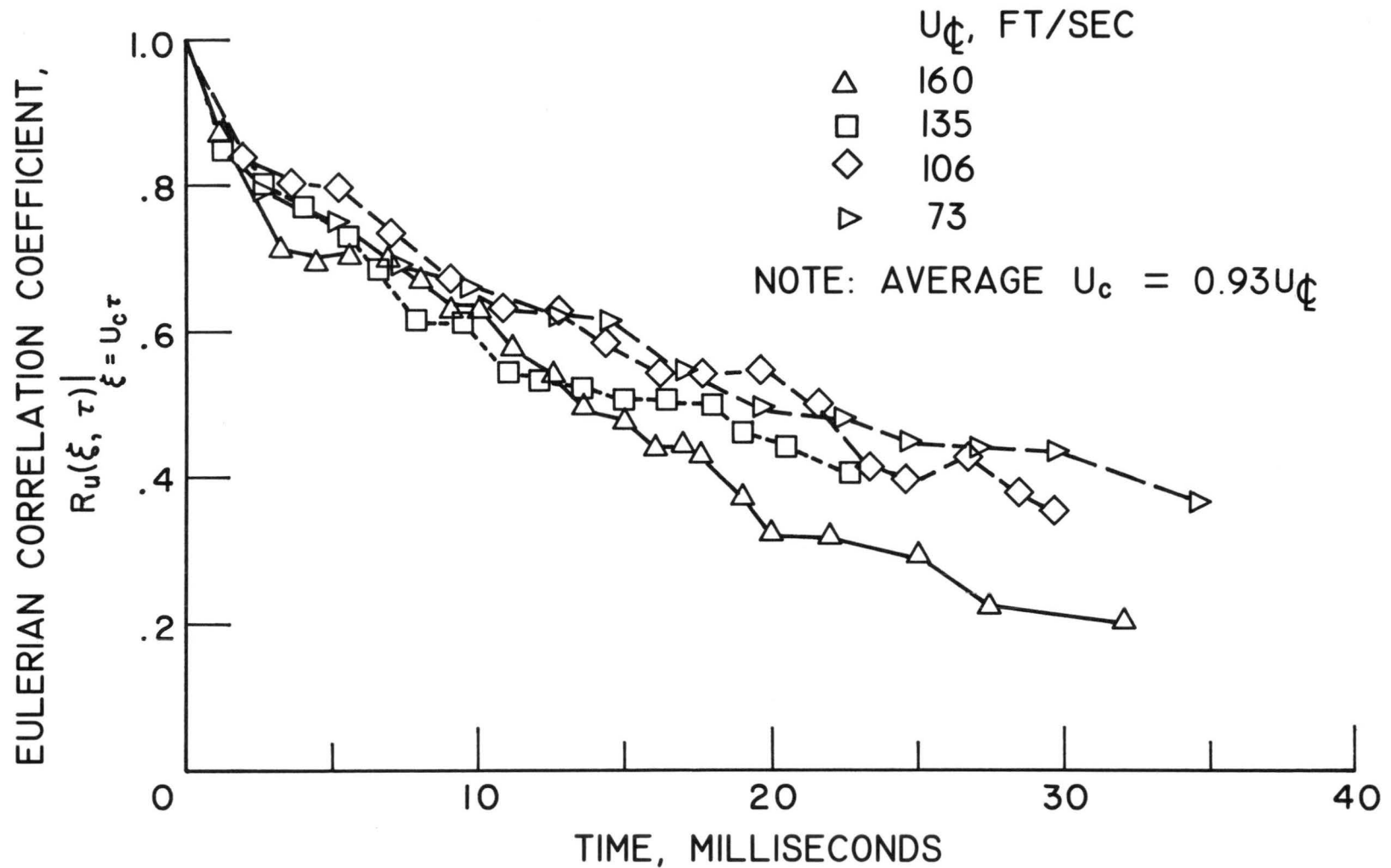


Fig. 14. Evaluation of Eulerian space-time correlation along $\xi = U_c \tau$ where U_c is convective velocity of peak correlation.

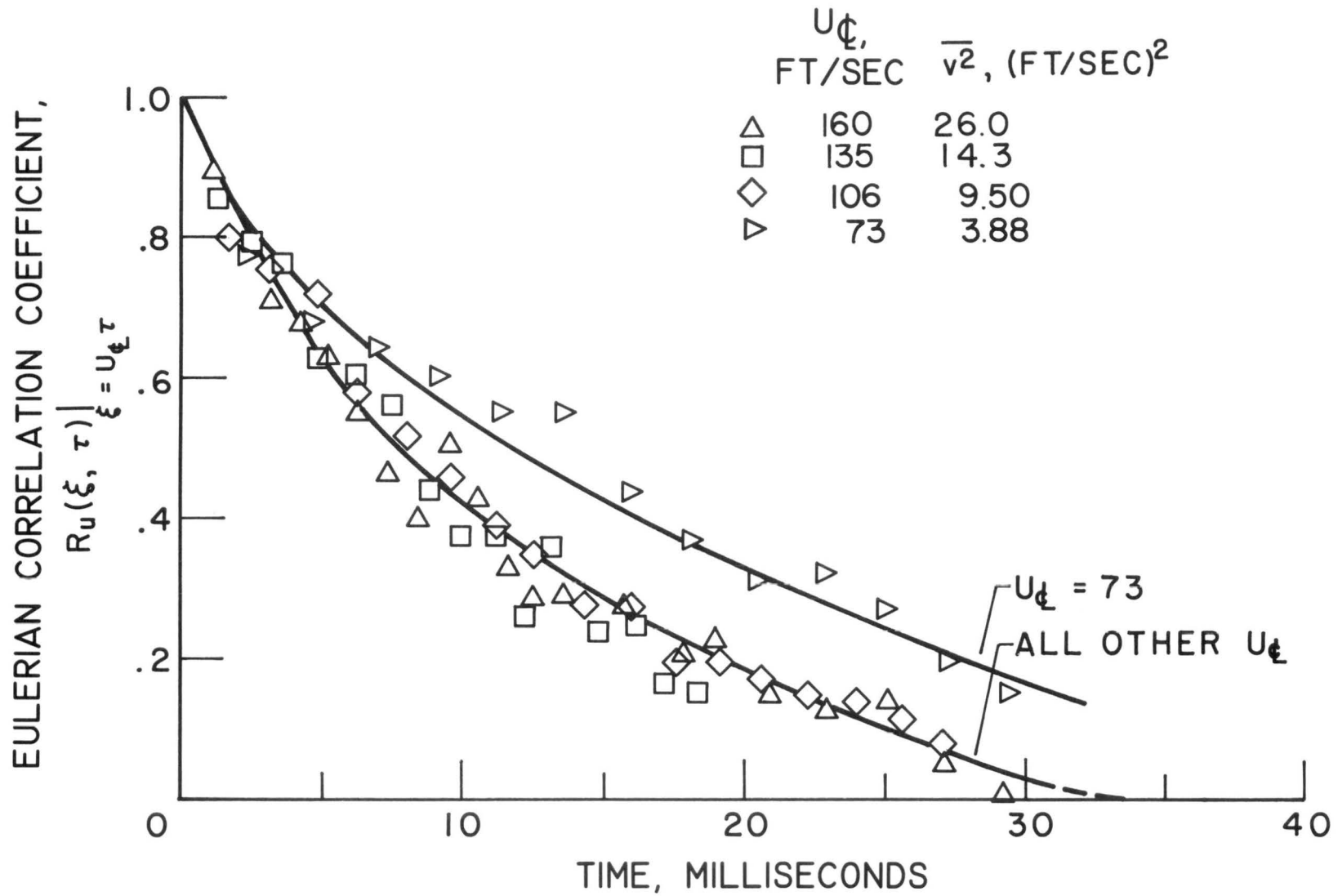


Fig. 15. Evaluation of Eulerian space-time correlation along $\xi = U_{\xi} \tau$ where U_{ξ} is local flow velocity.

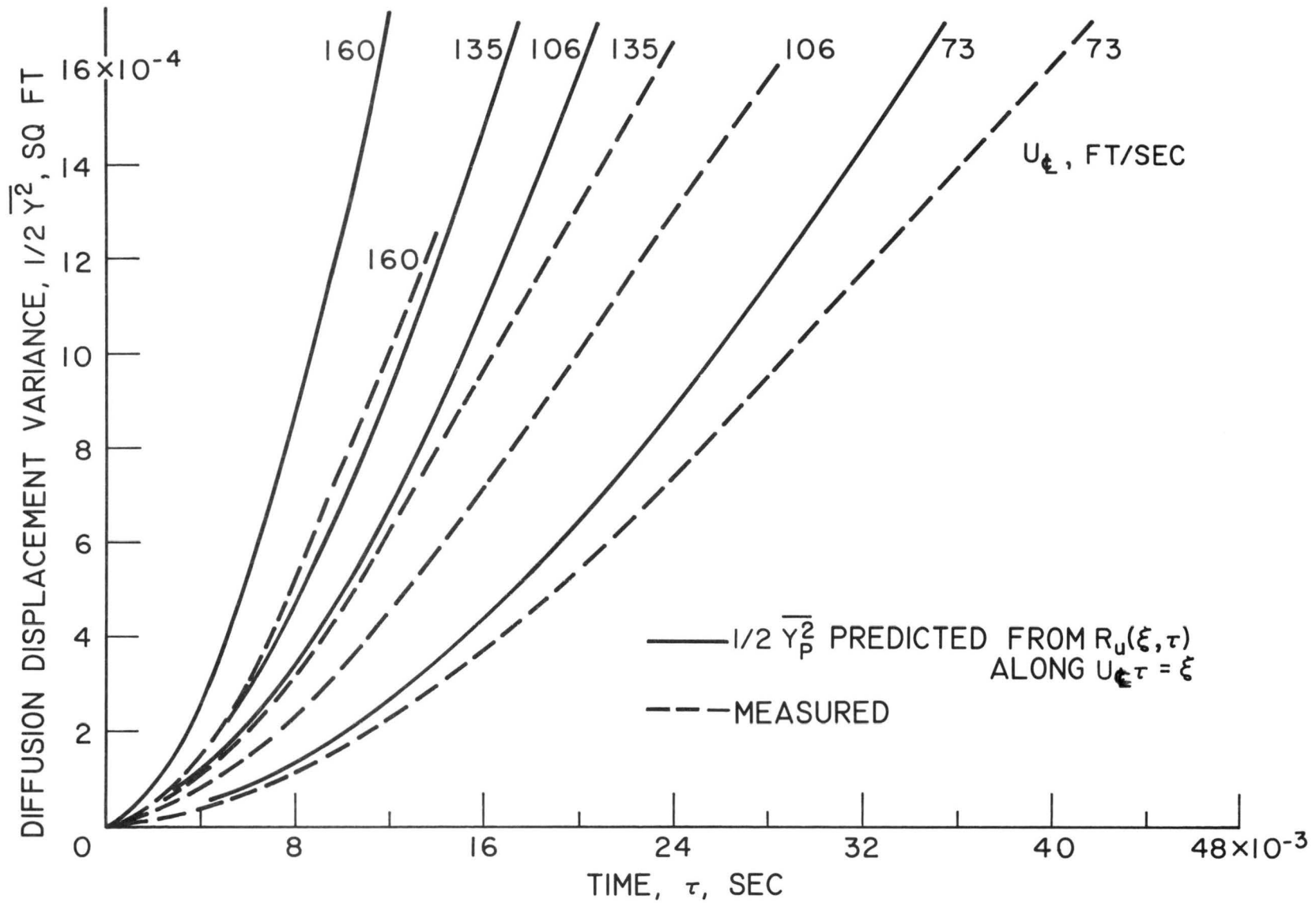


Fig. 16. Comparison of measured diffusion wake with prediction from $R_u(\xi, \tau) \Big|_{\xi = U_c \tau}$.

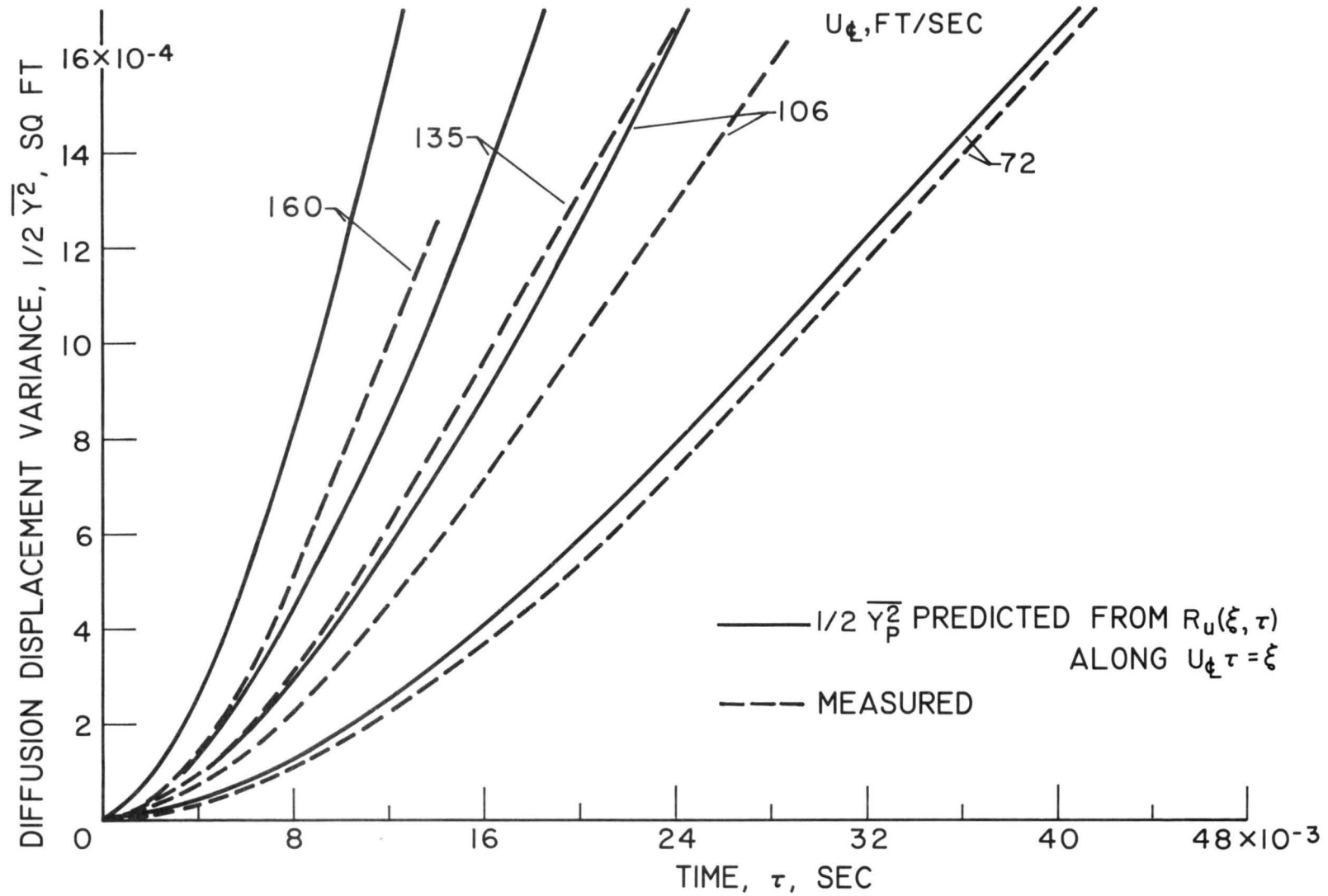


Fig. 17. Comparison of measured diffusion wake with prediction from $R_u(\xi, \tau) \Big|_{\xi = U_{\xi} \tau}$.